

# **Vortex Condensation and Confinement in Centre-Projected Lattice Yang–Mills Theory**

**Dissertation**

zur Erlangung des Grades eines  
Doktors der Naturwissenschaften

der Fakultät für Physik  
der Eberhard-Karls-Universität Tübingen

vorgelegt von  
**Oliver Tennert**  
aus Stuttgart

2000

Tag der mündlichen Prüfung: 16. Juni 2000

Dekan: Prof. Dr. K. Werner

1. Berichterstatter: Prof. Dr. H. Reinhardt

2. Berichterstatter: Prof. Dr. M. Müller-Preussker

*Meinen Eltern*



# Danksagung

Ich möchte zunächst meinen großen Dank an Herrn Professor Dr. Hugo Reinhardt aussprechen, meinen Doktorvater, der sich dem Thema dieser Dissertation stets mit sehr großem Interesse gewidmet hat und mir durch seine fortlaufende Unterstützung außerordentlich geholfen hat, diese Arbeit zustandezubringen.

Mein ganz besonderer Dank gilt Herrn Priv.-Doz. Dr. Kurt Langfeld. Seine ungeheure Begeisterungsfähigkeit, sein Ideenreichtum und sein unermüdliches Interesse an diesem Thema haben mir über die ganze Zeit hinweg als Unterstützung gedient. Mein freundschaftliches Verhältnis zu ihm hat sicher viel, auch über manche Durststrecke hinweg, zu einer fruchtbaren Zusammenarbeit beigetragen.

Herrn Dr. Michael Engelhardt möchte ich für die vielen Möglichkeiten danken, die ich zu Diskussionen mit ihm hatte. Sie haben mir stets weitergeholfen, und sicherlich habe ich während der Zusammenarbeit mit ihm viel von seinem physikalischen Gespür profitiert.

Meinem Bürokollegen Dipl.-Phys. Jochen Gattnar möchte ich für die Kollegialität und die äußerst angenehme Atmosphäre in unserem gemeinsamen, ständig von surrenden Festplatten und Ventilatoren beschallten Zimmer danken.

Von unschätzbarem Wert waren die nicht in Zahlen zu nennenden und in Zeiten zu messenden Diskussionen mit Dr. Holger Gies, die uns entweder von Beginn des Tages an oder auch zu später Stunde hin fortlaufend in neue interessante Gebiete der Physik vorstoßen ließen. Ich habe die büroliche und auch die private Nähe zu ihm sehr genossen.

Ich möchte der gesamten Arbeitsgruppe von Professor Dr. Reinhardt sehr für die angenehme Atmosphäre danken, in der ich mich über die Zeit der Promotion ausgesprochen wohlgeföhlt habe. In diesem Sinne möchte ich vor allem Herrn Priv.-Doz. Dr. Herbert Weigel hervorheben, der mir während seiner Anwesenheit am Institut oft bei physikalischen Problemen weiterhalf. Ebenso dankbar bin ich Herrn Dr. Markus Quandt für die zahlreichen Diskussionen mit ihm.

Meiner Mutter möchte ich für all die Unterstützung danken, die sie mir zeit meines Lebens und insbesondere während meines gesamten Studiums zukommen ließ. Ohne sie hätte ich es nie geschafft. Meiner Freundin Ilka danke ich für das viele Verständnis, das sie aufbrachte, als ich unzählige Abende hinter meinem Schreibtisch verbrachte und schrieb.

Allen Komponenten der informationstechnischen Infrastruktur, insbesondere

den Rechnern Pion01 bis Pion20 danke ich dafür, daß sie mir während der Zeit ihrer Betreuung durch mich keine allzugroßen Sorgenkinder waren. Unserem ehemaligen Server Alpha1 bin ich zu tiefstem Dank verpflichtet, daß sie im Zuge ihrer spontanen Festplattenbereinigungsanfänge niemals auch nur eine Datei von mir gelöscht hat.

Einen Teil meiner Promotionszeit wurde ich vom Graduiertenkolleg *Struktur und Wechselwirkung von Hadronen und Kernen* durch ein Stipendium unterstützt. Ich möchte in diesem Zusammenhang Herrn Professor Dr. Herbert Müther für sein Engagement danken.

# Zusammenfassung

Mit der Formulierung der Quantenchromodynamik (QCD) als fundamentale Theorie der starken Wechselwirkung zwischen den elementaren Bausteinen der hadronischen Materie war die Hoffnung verbunden, eines der herausragenden Probleme in der Physik zu lösen, das *Confinement-Problem*. Die Störungstheorie, welche sich in anderen Teilen der Physik als höchst erfolgreich bewährt hat, erwies sich jedoch in dem diesbezüglich interessanten physikalischen Bereich schnell als unanwendbar.

Die Gittereichtheorie ist ein nichtperturbativer Zugang zur Untersuchung der Grundzustandseigenschaften quantisierter Eichtheorien. Hinsichtlich des Confinement-Problems besteht die Vermutung, daß der gluonische Teil der QCD allein den grundlegenden Mechanismus für die Nichtexistenz freier farbgeladener physikalischer Zustände in sich birgt, weswegen eine reine Yang–Mills-Theorie auf dem Gitter betrachtet wird.

In dieser Arbeit wird ein möglicher Confinement-Mechanismus durch die Kondensation von Vortizes in *zentrumprojizierter Yang–Mills-Theorie* beleuchtet — basierend auf einer Idee aus den späten Siebziger-Jahren, welcher durch die Formulierung einer wohldefinierten Vorschrift, den Vortexgehalt einer Yang–Mills-Konfiguration zu extrahieren, in den späten Neunziger-Jahren zu erneutem Interesse verholfen wurde. Frühere Versuche, auf dem Gitter formulierte Vortex-Modelle im Kontinuumslimit zu betrachten, scheiterten am mangelnden Skalenverhalten der Vortizes. Die zentrumprojizierte Yang–Mills-Theorie gibt jedoch Anlaß zur Hoffnung, daß die in ihr definierten *dünnen Vortizes*, welche per Definition eine Dicke von einem Gitterabstand besitzen, lediglich die Relikte physikalischer, *dicker Vortizes* sind. Diese werden durch die *Zentrumsprojektion* dann auf die dünnen Vortizes, auch *Zentrumsvortizes* genannt, abgebildet. Die Zentrumsprojektion bildet eine Yang–Mills-Konfiguration auf eine Konfiguration ab, deren Basisvariablen Elemente aus dem Zentrum der Eichgruppe sind. Das relevante Infrarotverhalten der Theorie wird dabei beibehalten. Die Zentrumsvortizes als die resultierenden Freiheitsgrade nach der Projektion zeigen weiterhin ein konsistentes Skalenverhalten im Sinne der Renormierungsgruppe, welches eine notwendige Bedingung für die Existenz eines Kontinuumslimites der effektiven Vortextheorie ist.

Darüberhinaus wird in der zentrumprojizierten Theorie ein *Deconfinement-*

*Phasenübergang* reproduziert. Dieser erscheint bei einer Temperatur, welche identisch ist zur kritischen Temperatur in der vollen, unprojizierten Theorie. Die räumliche und die temporale String-Tension werden mit hoher Genauigkeit reproduziert, wenn man den drastischen Einschnitt betrachtet, welche die Zentrumsprojektion für die volle Theorie darstellt.

Nach einer kurzen Einführung beginnt das erste Kapitel mit einer Darstellung der geometrischen Begriffe, welche der Gitterformulierung von Eichtheorien zugrundeliegen. Ein kurzer Abriß über Gittereichtheorien im allgemeinen mitsamt des zentralen Themenkreises der Renormierung wird gegeben.

Kapitel zwei beginnt mit einem kurzen Rückblick auf einige  $\mathbb{Z}_N$ -Gittermodelle. Insbesondere wird das *Wegner-Modell* vorgestellt, da dessen Eigenschaften im Hinblick auf die zentrumsprojizierte Yang–Mills-Theorie von großem Interesse sind und das Modell einige Analogien aufweist. Die Bedeutung eines nicht-trivialen Zentrums der Eichgruppe wird durchweg betont. Der Hauptteil des zweiten Kapitels ist der Frage gewidmet, inwiefern Zentrumsvortizes physikalische Größen widerspiegeln und keine Gitterartefakte darstellen. Es werden daher Gitterrechnungen vorgestellt, welche sowohl zeigen, daß die durch die Zentrumsprojektion entstandenen Vortizes die relevanten Freiheitsgrade im Infrarotsektor der Theorie sind — zumindest hinsichtlich des Confinement-Phänomens — als auch das perturbative Skalenverhalten einer definierten Vortex-Flächendichte belegen. Diese als *Vortex-Dominanz* bezeichnete Eigenschaft wird als starker Hinweis dafür angesehen, daß die Zentrumsvortizes physikalischer Natur sind.

Im dritten Kapitel wird das Verhalten der zentrumsprojizierten Yang–Mills-Theorie bei endlichen Temperaturen untersucht. Nach einer kurzen, allgemeinen Einführung in die Formulierung von Quantenfeldtheorien bei endlichen Temperaturen werden einige topologische Eigenschaften von Eichtheorien auf dem Torus diskutiert. Ziel dieser Betrachtungen ist es, die in der Gittereichtheorie so wichtige *Zentrumssymmetrie* aus dem Transformationsverhalten von Eichfeldern auf dem Torus in der Kontinuumstheorie mit verallgemeinerter Eichsymmetrie abzuleiten. Diese Zentrumssymmetrie muß in der Natur nicht realisiert sein, sondern kann auch in der spontan gebrochenen Phase vorliegen. Der *Polyakov-Loop-Operator* als Ordnungsparameter für das Vorliegen dieser Symmetrie ist gleichzeitig auch Ordnungsparameter für das Vorliegen einer Confinement-Phase oder einer Deconfinement-Phase. Der Großteil des dritten Kapitels stellt dann die Messungen vor, welche zur Untersuchung des Verhaltens der zentrumsprojizierten Yang–Mills-Theorie bei endlichen Temperaturen durchgeführt wurden. Die Existenz eines Deconfinement-Phasenübergangs und damit die Gültigkeit der Vortex-Dominanz auch über den Phasenübergang hinaus wird gezeigt.



# Abstract

Ever since the conception of quantum chromodynamics (QCD) as the fundamental theory for the strong interaction between the basic matter constituents of the hadronic world, the hope has been to explain one of the most challenging phenomena in physics, the *confinement problem*. Due to the very nature of QCD as a non-abelian gauge theory, calculational methods which are successful in other parts of physics fail in the domain of interest.

Lattice gauge theory is a non-perturbative approach to the investigation of the ground state properties of quantum gauge theories. With respect to the confinement problem, the hypothesis is that the gluonic part of the theory alone contains the basic mechanism for disallowing coloured physical states, which is why pure Yang–Mills theory on the lattice is regarded.

In this work, a possible confinement mechanism due to the condensation of vortices in Yang–Mills theory is illuminated, an idea dating back to the late seventies but having experienced renewed interest in the late nineties due to an advanced proposal to give a prescription to extract the vortex content of a Yang–Mills configuration. Whereas earlier attempts to tackle the problem of translating vortex models defined in a discretized space-time to the continuum theory were not crowned with success, *centre-projected Yang–Mills theory* gives some promising indications that the vortices defined in the theory caricature vortices of finite thickness in the continuum limit. In lattice theory, these hypothetical *thick vortices* are mapped onto *centre vortices*, which by definition have the thickness of one lattice spacing, by the method of *centre-projection*. This projection onto centre degrees of freedom seems to retain the relevant low-energy properties of lattice Yang–Mills theory. Moreover, the *centre vortices*, which are the result of the projection, show the right scaling behaviour necessary for the centre-projected theory to be taken to the continuum limit.

Furthermore, centre-projected Yang–Mills theory reproduces a deconfinement phase at a critical temperature identical to the one obtained in the full, unprojected theory. The spatial as well as the temporal string tension is reproduced to a very high degree of accuracy concerning the drastic intervention centre projection constitutes for the full theory.

After a short introduction, the first chapter begins with giving gauge theory its due geometric foundation, as the lattice formulation, which is given a basic

introduction after that, is based heavily on the geometric origin of gauge theories.

Chapter two begins with a short review of some lattice  $\mathbb{Z}_N$  models. In especial, the *Wegner model* is shortly presented as the results obtained there bear some analogies to centre-projected Yang–Mills theory, which is then explained in detail. The relevance of the *centre* of a unitary gauge group in the confinement mechanism is emphasized throughout. The main part of the second chapter is then devoted to the issue of the physicality contained within the centre vortices. Therefore, lattice measurements are presented which indicate that centre projection singles out vortices as degrees of freedom relevant in the infrared sector of Yang–Mills theory, exhibiting perturbative scaling behaviour in the weak coupling limit. This property is called *vortex dominance*. A model based on randomly distributed vortices is taken to show that correlations between the centre vortices are important for the behaviour of the theory.

The third chapter is wholly devoted to the investigation of the finite temperature properties of centre-projected Yang–Mills theory. Therefore, a short introduction to general quantum field theory at finite temperatures is given, before the topological properties of Yang–Mills theory on the torus are discussed. This is done to explain the occurrence of *centre symmetry* as part of a generalized gauge symmetry, which is not necessarily realized in nature, but may be broken spontaneously at a certain set of parameters. The *Polyakov loop operator* as an order parameter distinguishing whether this symmetry is realized or not also distinguishes a confinement phase from a deconfinement phase of a gauge theory. The better part of the third chapter then presents the measurements performed to investigate the finite temperature properties of centre-projected Yang–Mills theory. It is shown that a deconfinement phase transition is realized, and vortex dominance is retained throughout the whole temperature range from  $T = 0$  to temperatures high above  $T_c$ .

# Contents

<b>Danksagung</b>	<b>v</b>
<b>Zusammenfassung</b>	<b>vii</b>
<b>Abstract</b>	<b>ix</b>
<b>1 Yang–Mills Theory on the Lattice</b>	<b>1</b>
1.1 The Need for a Non-Perturbative Treatment . . . . .	1
1.2 A Brief Résumé of Lattice Gauge Theory . . . . .	4
1.2.1 The Geometrical Setting of a Gauge Theory . . . . .	5
1.2.2 The Transition to the Lattice . . . . .	14
1.2.3 Wilson Criterion and Confinement on the Lattice . . . . .	19
1.2.4 Renormalization and Extraction of Physical Quantities . . . . .	22
1.3 Definitions and Conventions . . . . .	27
<b>2 Centre Dominance and Vortex Condensation</b>	<b>29</b>
2.1 Gauge Groups and Their Topology . . . . .	30
2.2 Vortex Condensation in $\mathbb{Z}_N$ models . . . . .	32
2.3 The Emergence of Vortices in Yang–Mills Theory . . . . .	36
2.4 Perturbative Scaling and the Continuum Limit . . . . .	39
2.5 Random Vortex Model and Correlations . . . . .	45
<b>3 Centre Dominance at Finite Temperature</b>	<b>51</b>
3.1 Finite Temperature in Field Theory . . . . .	52
3.2 The Topology of Gauge Fields on the Torus . . . . .	54
3.3 The Deconfinement Phase Transition . . . . .	60
3.4 Centre Dominance at Finite Temperature . . . . .	63
3.4.1 Centre Projection and the Deconfinement Phase Transition . . . . .	63
3.4.2 The String Tension at Finite Temperature . . . . .	66
3.5 Vortex Polarisation and Percolation . . . . .	68
3.5.1 Anisotropy of Vortices . . . . .	68
3.5.2 Vortex Clustering and Percolation . . . . .	71

3.5.3 Winding Vortices in the Deconfinement Phase . . . . .	77
<b>4 Conclusions and Outlook</b>	<b>81</b>
<b>A Useful Formulae for <math>SU(N)</math> Gauge Groups</b>	<b>85</b>
<b>Curriculum Vitae</b>	<b>93</b>

# Chapter 1

## Yang–Mills Theory on the Lattice

*After a motivation of the objectives aimed for in this work, the basic ingredients of the lattice formulation of Yang–Mills theory are introduced. Crucial terms and connections are presented, which recur on various occasions and need a clarified treatment. The geometrical setting of gauge theories is shown, as the basic variables of lattice gauge theories are of a deep geometric origin. Their formulation on a discretized space-time as well as renormalization, which is a necessary ingredient in quantized field theories, are explained. Eventually, some conventions are given.*

### 1.1 The Need for a Non-Perturbative Treatment

It is difficult not to keep regurgitating the phrases which are virtually the same again and again. But it is simply the case that to our knowledge, *quantum field theory* is the most fundamental theory available in the world of nature, at least from the viewpoint of theoretical predictability. Of course, it may well be that it eventually is proven to be an effective theory, with string theory being a promising candidate for the underlying framework. But, should this be the case, it nevertheless has justified its domain of applicability down to the smallest distances available in present-day physical experiments. Its true impact is disclosed in the microscopic world of atoms or even elementary particles, where “everyday concepts” stemming from the perception of physical events available to us in normal life must at least be thought over from an epistemological point of view and reformulated, or eventually lose their meaning. These include classical notions of the space-time point of an event or the presence of a particle, as well as the change in time thereof, its *trajectory*. Eventually, the notion of a particle itself must be recreated. We say that the microscopic world is dominated by the *quantum principle*. In a way, quantum field theory is but an application of the quantum principle to a certain model class, that of  $(3 + 1)$ -dimensional fields. In

$(0 + 1)$  dimensions, we get ordinary *quantum mechanics*, and it is but fair to say that especially non-relativistic quantum mechanics is mathematically one of the most consistent and powerful theories ever conceived. Never has there been any experimental result not being in accordance with its predictions.

Of course, it is incorrect to deduce from that, that the validity is lost in the macroscopic world, but the *correspondence principle* tells us that the larger the scale, the less dominant are the quantum effects, and classical physics reaches its domain of applicability. On even larger, cosmological scales, however, where the only interaction playing a role is *gravitation*, corrections of a different kind are necessary due to another prevailing principle in physics, the *equivalence principle*, which identifies two seemingly so different concepts like gravitation and acceleration. This identification of a dynamical and a kinetic quantity led to a total geometrization of gravitation theory, terminating in the formulation of a theory of space-time itself, the *general theory of relativity*, which finds its expression within the realm of differential geometry.

It shall now not be recapitulated how and why merging the two theories residing at the two most extreme endpoints of the length scale ends in a variety of insurmountable problems. Every physicist knows that, and it would take us too far astray. Quantum field theory, which is the general framework we will be dealing with here, too, has its own problems, but they are not so much of a conceptual nature. Rather, they are calculational in kind, as it is as yet not known how to solve the two most important models in quantum field theory exactly, namely *quantum electrodynamics (QED)*, which is the jubilated quantum theory for electrodynamics, and *quantum chromodynamics (QCD)*, which supposedly seems to be the fundamental quantum theory for the strong interaction in the hadronic world. Disregarding the whole problem of renormalization for the moment, by an exact solution we define a closed exact expression for the *correlation functions* or *Green functions*, because it is they who constitute the solution to the characteristic equations which mathematically are of a functional kind. For QED, matters are not so bad, since nature gives us an instrument at hand for finding approximate solutions to the problem by means of *perturbation theory*, at least within our domain of interest. This domain is characterized by a small value for the (renormalized) coupling constant  $e$ , identified with the electric elementary charge, and within the framework of perturbation theory, quantities interesting to us like the above-mentioned Green functions or the corresponding *generating functional* itself, are expressed by a series expansion in  $e$ , and the calculational results are in accordance with the experimental data to a degree of precision unprecedented by any other theory in physics. In the end, this lucky circumstance is due to the characteristic behaviour of the so-called *beta function* of the theory, which, within the issue of renormalization, gives the advantageous opportunity of defining a numerical value for the renormalized electric charge in an asymptotic sense, i.e. for very large distances in space. Moreover, the renormalizational analysis reveals that the larger the distance, the more applicable

and precise perturbation theory becomes.

In contrast, the conditions are not so lucky with the other fundamental model quantum field theory, QCD: the theory for the interaction between quarks and gluons, the hypothetical elementary components of the hadrons. The renormalizational analysis, as far as it is possible anyway, shows that perturbation theory is getting better and better as the distances between interacting particles become smaller and smaller. The reason is that the renormalized *running coupling constant* (a contradiction in terms, of course, but it has found its way into the language) tends to zero when the momentum transfer is increased. This behaviour is termed *asymptotic freedom*, and it expresses the fact that in the limit of infinite momenta, QCD is in fact a theory of free quarks and gluons without any interaction.

The issue interesting to us, namely when the two elementary particles are separated by a fair distance, e.g. of the radius of an atom, is impossible to treat perturbatively, so that even the beta function constituting a critical quantity in the renormalizational analysis cannot be calculated any more with the means at hand. Thus, in a way, perturbation theory yields its own limit of applicability. Moreover, an asymptotic state for a quark or a gluon does not seem to exist; they are confined within the hadrons, which are classified either as *baryons*, when three valence quarks give the hadrons their quantum numbers including the spin, or as *mesons*, when the quantum numbers are borrowed from a quark and an antiquark. The gluons do not contribute anything to the internal quantum numbers but provide the mechanism for binding all the valence quarks and the pairs of virtually produced quarks and antiquarks together to hadrons, and most probably contribute a significant part to the spin. But here we arrive at our main problem: the idea of virtual pairs of particles and antiparticles stems from perturbation theory, and we know that perturbation theory loses its validity at distances comparable to the diameter of a nucleon, which is about 1 fm. Taking also into account that quarks or gluons simply do not appear as free particles possessing a definite mass, or anything like the equivalent of a charge, we are forced to find a solution to the problem how a theory, which is composed of fundamental fermions (quarks), massless vector mesons (gluons) responsible for the interaction between them and even themselves, and an internal degree of freedom with a local symmetry, the  $SU(3)$  *gauge symmetry*, is transformed, when quantized, into an effective theory of hadrons. What is desired is something like baryons as effective matter particles interacting with each other by an exchange of mesons as effective intermediate particles in a first approximation, only much more detailed and elaborated. This is the *confinement* problem, and it appears to be one of the most intriguing problem in whole physics.

Therefore, analogues are looked for in similar model theories, which by construction are simpler to solve, be it because the number of space-time dimensions is reduced (many  $(1+1)$ -dimensional quantum field theories are exactly solvable, for example), or because the degree of symmetry is increased. Thus, in supersym-

metric models, attempts to tackle the problem of finding a solution have recently been crowned with success, as it has been possible to calculate just the effective theory in various models, although the similarity in structure between the supersymmetric models of the *Seiberg–Witten* type and QCD with fundamental fermions is not overly distinct and overemphasized sometimes.

For the time being, theoretical physicists have buried their hope to find an exact solution to the confinement problem soon. An exact solution would deliver a closed form of all Green functions, propagators as well as vertex functions for the whole range of the renormalized coupling constant  $g$ . Whereas perturbation theory is only applicable for small  $g$ , which in turn applies in non-abelian gauge theories like QCD for large momentum transfers or, equivalently, for small distances, in the opposite domain, i.e. large distances, a perturbative analysis breaks down and no predictions are available. Therefore, it is self-evident to look for *non-perturbative methods* to tackle the problem of solving for the Green functions or the effective theory, which is expressed in the *effective potential*, for the case of low momentum transfers, at least approximately. One of the most important of these is the approach via *lattice gauge theory*, which on the one hand admits a regularized formulation of a gauge theory, the regularization method being a momentum cut-off, and therefore is free from any infinities. This does not mean, however, that there is not any renormalization. Renormalization automatically enters the game when dimensionful quantities are related with measurable observables on the lattice, which acquire their canonical dimension only by the *lattice spacing*  $a$  with an initially undefined value. On the other hand, the discretization of a continuum theory, which makes the mathematical vicinity of quantum field theory and statistical physics even more obvious, opens up the powerful approximative methods of statistical physics to the treatment, one of the most important being the *Monte Carlo method*. By means of this method, the high-dimensional integrals occurring in expectation values are numerically evaluated by *importance sampling*, i.e. dominant contributions are preferred in a random sampling of configurations.

In this work, Monte Carlo calculations will constitute the main tool for extracting physical statements. This is why the next section is devoted to a brief review of the theoretical framework the following work is based upon.

## 1.2 A Brief Résumé of Lattice Gauge Theory

This section is intended to serve as a concise overview of the basic ingredients of lattice gauge theories. In order to fully grasp the meaning of the quantities inherent to the lattice formulation of a gauge theory, it is helpful to have a sound grip on the geometrical setting of a continuum gauge theory, the lattice being nothing else than a discretized version of space-time.

The concepts introduced below will recur many times in this work in various



contexts, so the following is intended to lay the ground in a precise though enlightening way. Nothing new is presented, but the technical foundations are laid on which the physical discussion starting in chapter 2 can be built up. Therefore, the reader already familiar with the necessary concepts of lattice gauge theory, its origin in the geometrical formulation of gauge theory, and its statistical treatment, including renormalization on the lattice, may without loss of information skip the chapter and perhaps just throw a glance upon section 1.3, where some conventions are introduced.

### 1.2.1 The Geometrical Setting of a Gauge Theory

The notion of fibre bundles, and the topological considerations being made about them is the natural framework for the mathematical formulation of a gauge theory, although, historically, these two theories — fibre bundles and gauge theory — have evolved separately for a long time until the early 1970s. A systematic study of these aspects can be found in [Nak90, MM92] or [Nab97]. To be concrete, a *fibre bundle*  $B$  is a differentiable manifold that is locally isomorphic to the direct product of two differentiable manifolds  $M \times F$ ,  $M$  being called the *base space* and  $F$  being the *standard fibre*. Also the case of a discrete fibre like  $\mathbb{Z}$  or  $\mathbb{Z}_N$  may be considered. In this case the fibre bundle is called a *covering manifold* of the base space.

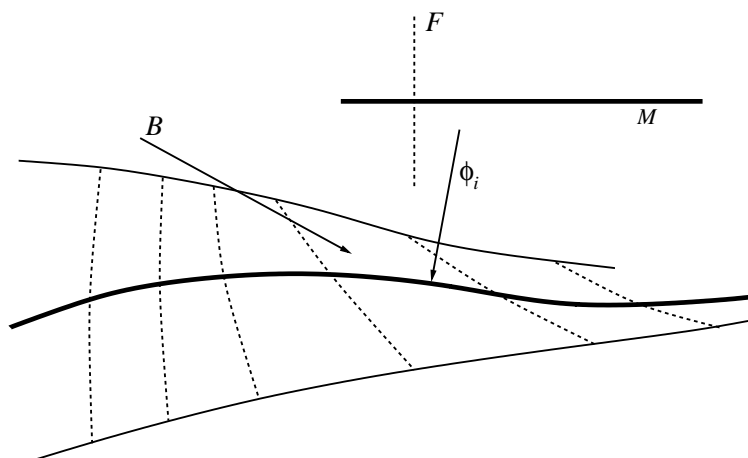


**Figure 1:** A fibre bundle  $B$  is locally the product of two manifolds  $M$  and  $F$ ,  $M$  being called the base space, and  $F$  the standard fibre.  $\phi_i$  is the local trivialization, which maps the product space  $M \times F$  to the bundle space  $B$  locally.

There must also exist a *projection*  $\pi : B \rightarrow M$ , which is surjective. The fibre is thus nothing but the inverse image of  $\pi$ . Moreover, a *structure group*  $G$  must be given, acting on  $F$  from the left. Being a manifold, the base space must also admit an open covering  $\{\mathcal{U}_i\}$ . Together with the so-called local trivializations

$\phi_i : \mathcal{U}_i \times F \rightarrow \pi^{-1}(\mathcal{U}_i)$  a very special structure is given to the bundle by demanding that in the overlap region of two open subsets  $\mathcal{U}_i, \mathcal{U}_j$  the *transition functions*  $t_{ij} = \phi_i^{-1}\phi_j$  be  $G$ -valued. For the transition functions  $t_{ij}$  the following consistency conditions must hold:

$$t_{ii} \equiv \mathbb{1} \tag{1.1}$$

$$t_{ij} = t_{ji}^{-1} \tag{1.2}$$

$$t_{ij}t_{jk} = t_{ik}. \tag{1.3}$$

The last relation is called the *cocycle condition*. These relations are not independent, since the first and third relation imply the second. If the bundle is *trivial*, i.e. if it has the *global* structure  $B = M \times F$ , the structure group can be reduced to the trivial group  $\{\mathbb{1}\}$ .

If a different local trivialization  $\phi'$  is given, we can define a *gauge transformation*  $f \in G$  by  $f = \phi^{-1}\phi'$ . For later use, we denote the function space of all continuous gauge transformations  $f : \pi^{-1}(\mathcal{U}_i) \rightarrow \pi^{-1}(\mathcal{U}_i)$  as  $\mathcal{G}$ .

A *local section* is defined to be a smooth map  $\sigma_i : \mathcal{U}_i \rightarrow F$ . For example, in the case that  $F$  is a vector space, it can be recognized to constitute nothing but a *vector field* on  $\mathcal{U}_i$ .

It now turns out that the topological properties of bundles may all be found out by considering the so-called *principal bundle*  $P$ , which as its standard fibre has the structure group  $G$  itself. Other bundles like, e.g., vector bundles may then be constructed as *associated bundles*  $B_{\text{ass}} = P \times V/G$ , with  $V$  a vector space, in that case.

The connection to physics is achieved when we identify the base space  $M$  with space-time or a suitable subspace of it. The structure group  $G$  then is nothing but the gauge group like  $U(1)$  or  $SU(N)$ . The gauge group, therefore, plays a double role: being the standard fibre, it represents the set of gauge transformations possible at each space-time point (gauge freedom). On the other hand, as the structure group of the principal bundle, it encodes the topological structure of the physical configuration, which, e.g., stem from certain boundary conditions on the gauge fields, as explained below. The choice of a local trivialization is referred to in physics as the choice of a *local gauge*. The topological non-triviality can be extracted from defining overlap regions  $\mathcal{U}_i \cap \mathcal{U}_j$  of an open covering  $\{\mathcal{U}_i\}$  of the base manifold and determining the transition functions  $t_{ij}$  [WY75a].<sup>1</sup>

In order to give a precise mathematical meaning to the physical gauge field, the notion of a connection must now be introduced. The idea is to separate the

---

<sup>1</sup>In the case of a *Dirac monopole*, e.g., the overlap region can be chosen to be homotopically equivalent to  $S^1$ . The maps  $S^1 \rightarrow U(1)$  are classified according to which *first homotopy class* they belong. The set of all first homotopy classes form the *first homotopy group*  $\pi_1(U(1)) \cong \mathbb{Z}$  and can be labelled by an integer  $m \in \mathbb{Z}$ , which is the magnetic charge of the monopole. If  $m = 0$ , the resulting principal bundle is trivial. For  $m = 1$  the resulting bundle is  $S^3$ , and the projection  $\pi : S^3 \rightarrow S^2$  is the well-known *Hopf map*.

tangent space of the bundle  $T_uP$  at a point  $u \in P$  into a so-called *vertical* part  $V_uP$  and a *horizontal* part  $H_uP$  in a systematic and unique way:  $T_uP = V_uP \oplus H_uP$ . The vertical subspace is naturally given as the subspace of  $T_uP$  tangent to the fibre  $G$ , thus being isomorphic to the Lie algebra  $\mathfrak{g}$  of the structure group  $G$ . This leaves open the residual freedom to define the complement of  $V_uP$ . This is exactly where the idea of a connection comes in: a *connection one-form*  $\omega$  is a *projection* of  $T_uP$  onto the vertical component  $V_uP \cong \mathfrak{g}$ , for every  $u \in P$ , and in a continuous way. According to the choice of  $\omega$ , a different component of  $T_uP$  is projected out. Then the horizontal part  $H_uP$  is just the kernel of  $\omega$ :

$$\ker \omega = \{v \in T_uP | \omega(v) = 0\} = H_uP. \quad (1.4)$$

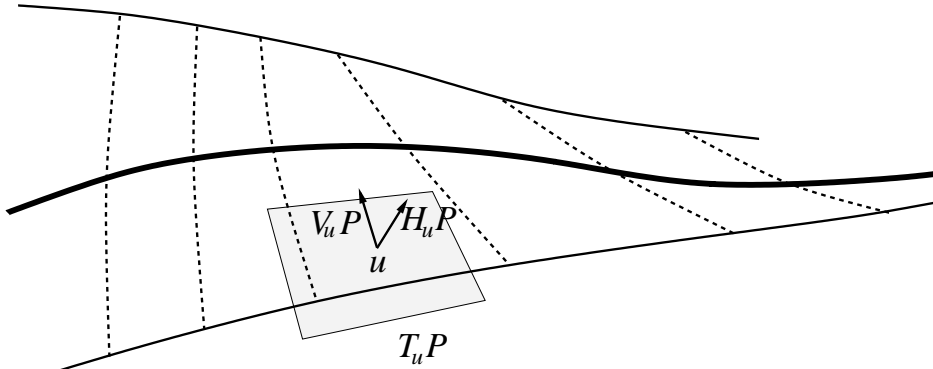


**Figure 2:** At each point  $u \in P$ , the tangent space to  $P$  is split into the canonically defined vertical part  $V_uP$  and the horizontal part  $H_uP$  defined by the connection.

Now let  $\sigma_i$  be a local section defined on each  $\mathcal{U}_i$ . The pulled-back<sup>2</sup> one-form  $A_i \equiv \sigma_i^* \omega$  is then called a *local connection form* and exactly represents what we know from physics as a gauge potential. Note that  $\omega$  and  $A_i$  are Lie-algebra-valued. Although we know from physical situations where it is not possible to define a smooth gauge potential  $A$  over the whole base space  $M$  as in the case of a Dirac monopole, the connection one-form  $\omega$ , also called the *Ehresmann connection*, is *per definitionem* everywhere continuous on  $M$ . The reason for the difference of behaviour lies in the fact that the pull-back  $\sigma^*$  is in general not well-defined over the whole of  $M$ , because a global section  $\sigma$  exists if and only if the bundle  $P$  is trivial.

Having introduced a connection one-form, we are now in a position to define quantities like covariant derivative, curvature, and parallel transport. Let  $\phi : TP \otimes \dots \otimes TP \rightarrow \mathfrak{g}$  a Lie-algebra-valued  $r$ -form.  $\phi$  is called *vertical* if  $\ker \phi = HP$  and *horizontal* if  $\ker \phi = VP$ . Similarly,  $Hv$  denotes the horizontal component

<sup>2</sup>Remember: If  $f : M \rightarrow N$  is a mapping from one space to another, the *pull-back*  $f^*$  denotes the induced reverse mapping between the respective dual tangent spaces  $f^* : T^*N \rightarrow T^*M$ .

of a vector  $v \in T_u P$  and  $Vv$  its vertical component. Let  $v_1, \dots, v_{r+1} \in T_u P$ . The *covariant derivative*  $D\phi$  of  $\phi$  is defined as

$$D\phi(v_1, \dots, v_{r+1}) \equiv d\phi(Hv_1, \dots, Hv_{r+1}). \quad (1.5)$$

We will come back to the covariant derivative if we encounter associated bundles.

The *curvature two-form*  $\Omega$  is defined as the covariant derivative of the connection one-form  $\omega$ , i.e.  $\Omega \equiv D\omega$ . It satisfies the *Bianchi identity*

$$D\Omega \equiv 0. \quad (1.6)$$

Just as the connection one-form also has a local form, the same is true for the curvature: When  $\sigma$  is a local section, the pulled-back two-form  $F \equiv \sigma^*\Omega$  is called the *local curvature form*, and it is the same  $F$  that is known from physics as the field strength tensor.<sup>3</sup> Its expression in terms of the above defined local connection is

$$F = dA + A \wedge A. \quad (1.7)$$

Note that  $\Omega$  and  $F$ , too, are Lie-algebra-valued. The Bianchi identity in its local expressions reads

$$DF := dF + A \wedge F \equiv 0, \quad (1.8)$$

where  $D$  is the covariant derivative operator in its local form, acting on a  $\mathfrak{g}$ -valued  $p$ -form on  $M$  in the above way.

It must be understood, however, that the above-defined curvature generalizes the intuitive notion of curvature that is known from Riemannian geometry in so far as the *Riemann* curvature is the curvature form belonging to the *frame bundle* of a Riemannian manifold, where the fibres are the set of local  $SO(N)$  transformations,  $N$  being the dimension of the manifold. But in general, the curvature one-form  $\Omega$  *has nothing to do with the curvature of the bundle  $P$  seen as a Riemannian manifold!*

It shall briefly be shown how a gauge transformation translates into the mathematical language. For that reason, consider that the connection one-form  $\omega$  was introduced to *uniquely* separate the tangent space  $T_u P$  at a point  $u \in P$  into a horizontal and a vertical part. That means, given an open covering  $\{\mathcal{U}_i\}$  the condition

$$\omega_i = \omega_j \quad \text{on} \quad \mathcal{U}_i \cap \mathcal{U}_j \quad (1.9)$$

must hold. From that, a *compatibility condition* can be derived, which dictates how the local connection one-forms must behave if equation (1.9) for the Ehresmann connection is to hold. Remember that in the overlap region  $\mathcal{U}_i \cap \mathcal{U}_j$  there

---

<sup>3</sup>Although the same symbol  $F$  is used both for the local curvature form and the standard fibre, the respective meaning should be clear from the context.

may be a change of coordinates  $\phi_i \rightarrow \phi_j$ , with the transition functions  $t_{ij}$  elements of  $G$ . One arrives at [Nak90]:

$$\begin{aligned} A_j &= t_{ij}^{-1} A_i t_{ij} + t_{ij}^{-1} dt_{ij} \\ \iff A' &= g^{-1} A g + g^{-1} dg, \end{aligned} \tag{1.10}$$

if we regard the transition functions as operators giving rise to a gauge transformation. Analogously, it can be shown that a similar compatibility condition yields the transformation law for the local curvature two-form:

$$\begin{aligned} F_j &= t_{ij}^{-1} F_i t_{ij} \\ \iff F' &= g^{-1} F g, \end{aligned} \tag{1.11}$$

which shows that in a gauge theory, the field strength transforms with the adjoint representation of the gauge group. Note that this gauge transformation has nothing to do with choosing another gauge, but is necessary because the base space must be covered with more than one open patch and the bundle has non-trivial topology. On the other hand, choosing another gauge also results in determining new transition functions. In this case, the overlapping region is the whole base manifold itself. Therefore, the transformation law is exactly the same.

The important concept of parallel transport can now be provided by the horizontal lift of a curve  $\gamma$  lying in the base space  $M$ . Given that curve, a *horizontal lift* of  $\gamma$ , denoted by  $\tilde{\gamma}$ , is defined to be a curve in the bundle  $P$  with the starting point anywhere on the same fibre where  $\gamma$  begins, but the tangent vector of which is horizontal everywhere.

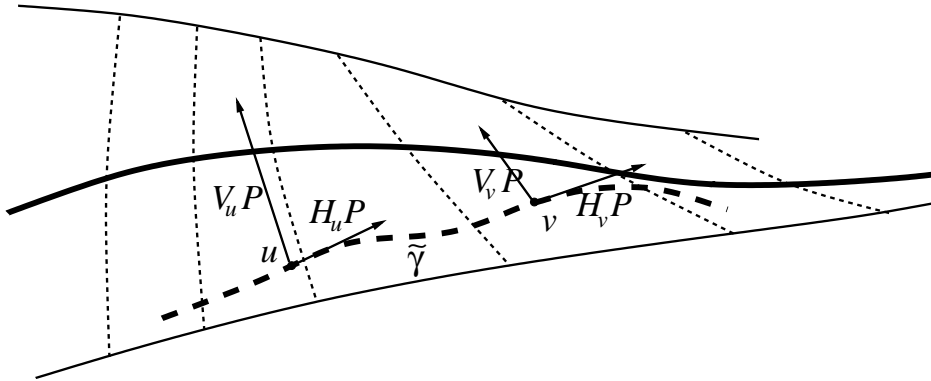


**Figure 3:** A horizontal lift  $\tilde{\gamma}$  of a curve  $\gamma \in M$  is horizontal everywhere.

Clearly,  $\pi\tilde{\gamma} = \gamma$ . If  $t \rightarrow \gamma(t)$  and  $t \rightarrow \tilde{\gamma}(t)$  are parametrizations of the original and lifted curve, respectively,  $\sigma_i$  is a local section, and  $g_i(t)$  is an element of  $G$  we can derive a differential equation connecting the two curves (once again, for a detailed derivation see [Nak90, GS87]):

$$\tilde{\gamma}(t) = \sigma_i(\gamma(t)) U_i(\gamma(t)). \tag{1.12}$$

If the tangent vectors at  $\sigma_i(\gamma(t))$  were horizontal everywhere,  $U_i(t)$  would always be the identity element  $\mathbb{1}$ . From that, one gets

$$\begin{aligned} \frac{dU_i(t)}{dt} &= -A_i(\dot{\gamma}(t))U_i(\gamma(t)) \\ \iff U_i[\gamma] &= \mathcal{P} \exp \left( - \int_{\gamma(0)}^{\gamma(t)} \langle A_i(\gamma(t)), dx \rangle \right), \end{aligned} \quad (1.13)$$

where  $\mathcal{P}$  is the so-called *path-ordering operator*, reflecting the fact that the integrand has, in general, non-abelian group elements, so that a naive line integration is not possible. Thus, the exponential form of equation (1.13) is to be taken only formally.  $U_i[\gamma]$  is called the *parallel transport operator*, reflecting the fact that the lifted curve is everywhere “parallel” to the horizontal direction on  $P$ , which in turn is defined by the connection one-form  $\omega$ .

For two concatenated curves  $\gamma_1, \gamma_2$ , the following property holds:

$$U_i[\gamma_2 \circ \gamma_1] = U_i[\gamma_2]U_i[\gamma_1], \quad (1.14)$$

where  $\circ$  denotes the concatenation, and the product on the right hand side is the group product.

Although the stress is put on principal fibre bundles, associated bundles naturally emerge if matter fields are included. As explained above, a vector field  $\phi : M \rightarrow V$  on a manifold  $M$  can be considered as a section of a vector bundle  $B_{\text{vec}} = P \times V/G$ . The structure group  $G$  then acts on  $\phi$  from the left, the same as we have it in physics: if we perform a gauge transformation, the matter field transforms like  $\phi \rightarrow R(G)\phi$ , with  $R$  being a representation into the set of linear operators acting on  $V$ , denoted as  $R : G \rightarrow GL(V)$ . The covariant derivative is also defined in a natural way, with the connection one-form now replaced by a representation  $R : \mathfrak{g} \rightarrow GL(V)$ . Let  $s$  be a local section of a vector bundle  $V$ ,  $\gamma(t)$  a curve on  $M$  going through  $p_0$ , and  $X$  the tangent vector of  $\gamma$  at  $p_0$ . This defines a vector field along the curve  $\gamma$  according to  $s(t) = s(\gamma(t))$ . In the principal bundle  $B$ ,  $\tilde{\gamma}(t)$  would be the lifted curve to  $\gamma(t)$ , connected to  $\gamma(t)$  by equation (1.12). It is horizontal everywhere. In the associated vector bundle  $B_{\text{vec}}$ , we define horizontality of a vector field  $s$  along the curve  $\gamma$  according to

$$s(t) = R(U_i(\dot{\gamma}(t)))s_0, \quad (1.15)$$

where  $R$  is the above-defined representation of  $G$ ,  $s_0 = s(\gamma(0))$ , and  $U_i$  is the path-ordering operator (1.13). Therefore, if  $s$  is horizontal (or, parallel), it solves the differential equation

$$\frac{ds(t)}{dt} = -r(A_i(\dot{\gamma}(t)))s(\gamma(t)) \quad (1.16)$$

$$\text{or } D_X s := \frac{ds(t)}{dt} + r(A_i(\dot{\gamma}(t)))s(\gamma(t)) = 0, \quad (1.17)$$

where  $D_X$  is the covariant derivative operator along  $X$  acting on  $s$ , and  $r$  is the induced representation of  $\mathfrak{g}$ .

The whole concept of covariant derivative stresses the fact that there is not any notion of a preferred local trivialization of the bundle. Without a local trivialization, an ordinary derivative does not have an intrinsic meaning. The reader may perhaps be reminded of ordinary Riemannian geometry, where Christoffel symbols must be added to the ordinary derivative to get a geometrically meaningful quantity, the Christoffel symbols and the ordinary derivative by themselves being not tensorial quantities, but coordinate-dependent entities. The Christoffel symbols in Riemannian geometry are the coefficients of the local connection one-form of the *frame bundle*, where the structure group  $SO(N)$  is isomorphic to the set of all possible orthonormal frames at a point  $p \in M$ . The covariant derivative therefore takes into account that, dependent on the trivialization chosen, the tangent spaces to the bundle are assigned a different orientation towards each other. One can understand the parallel transport as “turning around” any vector field, tensor field,  $p$ -form etc. until the change of relative orientation of the tangent spaces is compensated, and the real change of the field can be measured.

Let us now return to the principal bundles and the notion of lifted curves. One might ask what happens if the curve  $\gamma$  on the base manifold is closed? It turns out, of course, that the lifted curve  $\tilde{\gamma}$  need not be so. Instead, the initial and final points  $\tilde{\gamma}_i, \tilde{\gamma}_f$  will generally differ by a group element  $W \in G$ . The set of all such group elements can be shown to form a subgroup of the structure group  $G$  called the *holonomy group*  $\mathcal{H}$ . Clearly, a non-trivial holonomy group is due to the curvature of the bundle, as is formulated in the *Ambrose–Singer theorem*: the Lie algebra  $\mathfrak{h}$  of the holonomy group  $\mathcal{H}_u$  at a point  $u \in P$  is identical to the subalgebra of  $\mathfrak{g}$  spanned by the elements of the form  $\Omega_u(v, w)$ , where  $\Omega_u$  is the curvature two-form at  $u$  and  $v, w \in H_u P$ . The group element  $W$  itself is then (formally) given by

$$W[\gamma] = \mathcal{P} \exp \left( - \int_{\gamma} \langle A, dx \rangle \right), \quad (1.18)$$

where the index  $i$  is suppressed. Later on, when going to lattice gauge theory, a discretized version of  $W$  will be identified with the *Wilson loop*, or, if the curve closes in a non-trivial way<sup>4</sup>, the *Polyakov loop*. It can be shown that the knowledge of all elements  $W[\gamma]$  of the holonomy group  $\mathcal{H}_u$  at a point  $u \in P$  contains the complete physical information of a gauge configuration, whereas it is known that the gauge potential  $A$  has spurious degrees of freedom, and the field strength  $F$  has too few.<sup>5</sup> This understanding can be taken as a starting

<sup>4</sup>e.g. due to some periodic boundary conditions on the base space  $M$

<sup>5</sup>In an abelian gauge theory, the field strength  $F$  contains at least all the *local* information of the physical configuration, the *Aharonov–Bohm effect* being a global phenomenon. In a Yang–Mills theory  $F$  does not even locally specify the physical situation uniquely, a fact sometimes referred to as the *Wu–Yang ambiguity* [WY75b].

point for a reformulation of Yang–Mills theory in terms of gauge invariant *loop variables* (see e.g. [GP96]), and indeed, when investigating lattice gauge theory in the next section, the above-mentioned Wilson loops take on a prominent role.

In the case of an infinitesimal loop, the path-ordering operator may be dropped, and the relation between holonomy group and curvature can be made manifest [GS87]:

$$W[\gamma_{\text{inf}}] = \exp\left(-\int_{\gamma_{\text{inf}}=\partial\mathcal{A}_{\text{inf}}} \langle A, dx \rangle\right) \quad (1.19)$$

$$= \mathbb{1} - \int_{\mathcal{A}_{\text{inf}}} \langle dx, F dx \rangle + \mathcal{O}(l^3), \quad (1.20)$$

where  $\mathcal{A}$  is the infinitesimal area in the base space bounded by  $\gamma$ , and  $l$  is the infinitesimal length of  $\gamma$ .

The problem of *Gribov ambiguities* shall also shortly be touched upon in its geometrical context (see [MM92]). Until now we have concentrated on bundles  $P$  which describe the geometrical situation of a space-time  $M$  as base manifold and a structure group  $G$  as the set of gauge transformations possible along any fibre. Each possible bundle corresponds to a definite physical situation of different topological type, such as magnetic monopoles with different magnetic charge, or different  $k$ -instanton configurations. The topological sector is encoded in the topological properties of  $P$ . We will now deal with  $\mathcal{A}(P)$ , the set of all possible connection one-forms on  $P$ . We say that  $\omega_1, \omega_2 \in \mathcal{A}$  are *gauge equivalent* if there exists a gauge transformation  $f \in \mathcal{G}$  such that  $\omega_2 = f^*\omega_1$ . This way,  $\mathcal{G}$  defines an action on  $\mathcal{A}$ , and we denote the orbit space  $\mathcal{M} = \mathcal{A}/\mathcal{G}$  as the *moduli space* of gauge potentials on  $P$ . The moduli space is thus isomorphic to the physical configuration space, each point in  $\mathcal{M}$  corresponding to a different physical configuration residing in the same topological sector.  $\mathcal{A}$  can be given the structure of an infinite-dimensional principal fibre bundle over  $\mathcal{M}$ . We know that the choice of a gauge connection is defined by a *gauge fixing functional*  $F[\omega]$  in the way that  $F[\omega] \equiv 0$  picks out a certain  $\omega$ , or, as is usually said, fixes the gauge. Thus, a local section  $s$  is defined on  $\mathcal{A}$  by  $F$ . This section  $s$  can locally be equipped with a Riemannian structure by defining a metric on it. The determinant of this metric can in turn be shown to be proportional to the *Faddeev–Popov determinant* [BV79]

$$\Delta[\omega] = \left. \frac{\delta F[f^*\omega]}{\delta f} \right|_{F[\omega]=0}. \quad (1.21)$$

But as we know, the Faddeev–Popov determinant has zeroes, so at these points  $p \in s$  where this is the case we have a coordinate singularity similar to the situation of the hedgehog theorem<sup>6</sup> on the sphere. And similar to the case of

---

<sup>6</sup>“You cannot comb a hedgehog!”



the sphere, it can be shown that no global section exists on  $\mathcal{A}$  whenever certain boundary conditions on  $\omega$  are imposed which imply the compactification of  $M = \mathbb{R}^4$  to  $S^4$  [Sin78]. From a different view, with  $\Delta[\omega]$  acquiring a zero value, the gauge-fixing functional  $F$  does not change under an infinitesimal change in  $\omega$  under the action of  $f_0 \in \mathcal{G}_0$ , the set of *small gauge transformations*, which belong to the component connected to the identity element  $\mathbb{1}$ . Therefore, the tangent space to  $s$  is getting tangent to the fibre given by the orbit of  $\mathcal{G}_0$ , too, and the gauge orbits are not transversal any more.

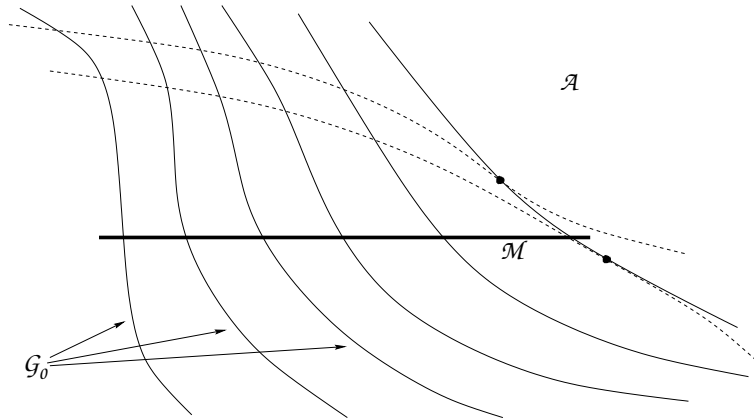


**Figure 4:** A simplified illustration of the Gribov problem. The solid lines constitute the gauge orbits of  $\mathcal{G}_0$ . The dashed lines constitute local sections of  $\mathcal{A}$ . At the marked points, the gauge orbits are not transversal any more, and a Gribov horizon is reached.

The region of the configuration space where the degeneracy of  $\Delta[\omega]$  takes place the first time when starting from a regular point in  $s$  is called a *Gribov horizon*. It encloses a region  $\Omega$  where the Faddeev–Popov determinant has a definite sign, called a *Gribov region*. If  $\Delta[\omega]$  is positive,  $\Omega$  is called the *first Gribov region*, and  $\partial\Omega$  the *first Gribov horizon*. As figure 4 illustrates, in a somewhat simplified viewing, the Gribov horizon constitutes the set of fixed points under the action of  $\mathcal{G}_0$ . These fixed points, however, are nevertheless connected by a set of gauge transformations, called the *fundamental modular group*  $\Gamma(M)$  of  $M$ . These are the *large gauge transformations*.  $\Gamma(M)$ , in almost all interesting cases, is a discrete group, which eventually is responsible for  $\mathcal{M}$  not possessing the structure of a manifold, but that of an *orbifold*. The action of  $\Gamma$  on  $\mathcal{A}$  leads to a multiplication of gauge potentials all satisfying the functional condition  $F[\omega] \equiv 0$ , but nevertheless are connected by a gauge transformation. These are the *Gribov copies* omnipresent in non-abelian gauge theories [Gri78].

The reason why we dwell upon Gribov copies so much at this early point is that later on, we will encounter them again when the issue of fixing the maximal centre gauge on the lattice is treated.

## 1.2.2 The Transition to the Lattice

Now that a concise review of the mathematical framework of gauge theories has been given, the stage is set for the formulation of the lattice version of it. As we are dealing with static, external charges only, pure Yang–Mills theory is regarded. A detailed treatment of quantum fields on the lattice can be found in [MM94, Rot97] or, of course, [Cre83].

As mentioned earlier, what in our sense is denoted by a lattice is nothing else but a discretized version of space-time. Nevertheless, throughout this work, though being mathematically rather sloppy, the term *space* will be used for denoting the lattice, and when considering certain global aspects like gauge-fixing, for example, we treat our lattice like a differentiable manifold.

There are, in principle, two advocated ways to formulate a lattice field theory. On the one hand, there is the *Euclidean formulation*, where space-time is taken to be locally isomorphic to  $\mathbb{R}^4$ , and is discretized in all four dimensions. On the other hand, there is the *Hamiltonian formulation*, where a continuous time variable is kept and only three-dimensional space is discretized [KS75]. Here we will only consider a four-dimensional Euclidean lattice.

Then the universe consists of single points denoted by  $x$ , called *sites*. Its topology is usually given by specifying certain boundary conditions. Throughout this work, *periodic* boundary conditions are used, i.e.,

$$x + N_{(\mu)}a_{\mu} = x, \quad (1.22)$$

where  $a_{\mu}$  is a unit vector pointing in one of the four directions ( $\mu = 1 \dots 4$ ), and  $N_{(\nu)}a$  is the lattice size in this direction,  $a$  being the lattice constant. This results in the space-time lattice being topologically equivalent (homeomorphic) to a 4-torus  $T^4$ .<sup>7</sup> It is important to stress, however, that periodic boundary conditions on the space-time manifold do not necessarily imply periodic boundary conditions on the quantum fields defined on the manifold. Indeed, as will be commented upon in chapter 3, apart from the usual *anti-periodic* boundary conditions on spinor fields on a torus (when fermions are included), there is a certain freedom in fixing the behaviour of gauge fields in overlapping regions of local charts when pure Yang–Mills theory is considered.

A gauge theory on the lattice is not defined by the gauge field  $A_{\mu}(x)$  itself, but by the bilocal quantity

$$U(y, x) = \mathcal{P} \exp \left( \int_{\mathcal{C}} -gA_{\mu}(x)dx^{\mu} \right) \quad (1.23)$$

defined in the previous section as the parallel transport operator from  $x$  to  $y$  along the curve  $\mathcal{C}$ . On the lattice, the smallest unit is called a *link*, as pictorially

<sup>7</sup>Note, however, that the metric used in our lattice is *flat (Euclidean)*, so that it is still a space with zero curvature. Topology does not *dictate* local geometry, but it *allows* us to use a flat metric, because a torus is a *parallelizable* manifold, with its *Euler characteristic*  $\chi = 0$  as a necessary condition.

it links two adjacent points  $x$  and  $x + \mu := x + a_\mu$ , and is denoted by  $U_\mu(x)$ . A lattice definition of the gauge field  $A_\mu(x)$ , which is by no means unique, can then be given by:

$$U_\mu(x) = \exp(-agA_\mu(x)). \quad (1.24)$$

As before,  $U_\mu(x)$  is an element of the gauge group.

All properties shown in the previous section to hold for the parallel transport operators now also hold in the discretized case, e.g. those concerning the concatenation of curves: if  $\mathcal{C}_1$  and  $\mathcal{C}_2$  are curves, with  $U(\mathcal{C}_1), U(\mathcal{C}_2)$  the corresponding parallel transport operators, then  $U(\mathcal{C}) = U(\mathcal{C}_2)U(\mathcal{C}_1)$  is the operator corresponding to the concatenated curve  $\mathcal{C} = \mathcal{C}_2 \circ \mathcal{C}_1$ , the product being the group product.

If the curves are closed in a trivial way (see the previous section), the operators are called *Wilson loops*. The smallest Wilson loop constructable is called a *plaquette*, and is denoted by

$$P_{\mu\nu}(x) = U_\nu^\dagger(x)U_\mu^\dagger(x + \nu)U_\nu(x + \mu)U_\mu(x). \quad (1.25)$$

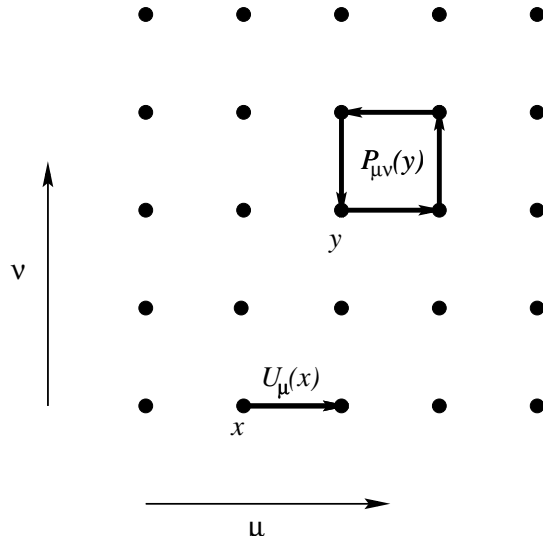


**Figure 5:** The lattice as a discretized universe.

The use of the bilocal operators  $U_\mu(x)$  allows the construction of gauge invariant quantities on the lattice. Consider a gauge transformation  $\Omega(x)$  acting on the link variables according to

$$U_\mu(x) \mapsto U_\mu^\Omega(x) = \Omega(x + \mu)U_\mu(x)\Omega^\dagger(x). \quad (1.26)$$

As can be seen, the elementary gauge invariant quantity is the plaquette, because the transformed links are along a closed line, and the transformation matrices cancel against each other. In general, Wilson loops are gauge invariant operators.<sup>8</sup>

<sup>8</sup>Loops along topologically non-trivial cycles, *Polyakov loops*, need not be so. More about that in chapter 3.

With the basic gauge invariant variables at hand, it is now easy to find a gauge invariant action necessary for formulating the gauge theory. In principle, as Wilson loops of any size are gauge invariant objects, a variety of actions are conceivable. The simplest choice is the *Wilson action* [Wil74]

$$S[U_\mu] = \beta \sum_{P_{\mu\nu}} \left( 1 - \frac{1}{2N} (\text{Tr} P_{\mu\nu} + \text{Tr} P_{\mu\nu}^{-1}) \right) \quad (1.27)$$

$$= \beta \sum_{P_{\mu\nu}} \left( 1 - \frac{1}{N} \text{Re} \text{Tr} P_{\mu\nu} \right) \quad (1.28)$$

for an  $SU(N)$  gauge theory.  $\beta$  is a parameter to be determined from the demand for the correct continuum limit. Here the sum over plaquettes  $P_{\mu\nu}$  is meant to include every plaquette only with one orientation:

$$\sum_{P_{\mu\nu}} = \sum_x \sum_{1 \leq \mu < \nu \leq 4} \quad (1.29)$$

$$= \frac{1}{2} \sum_{x, \mu, \nu}. \quad (1.30)$$

Apart from being gauge invariant, the action functional (1.28) is easily seen to be real and positive.

It is to be checked that the Wilson action really reduces to the Yang–Mills action in the *naive* or *classical continuum limit* where the lattice spacing goes to zero:  $a \rightarrow 0$ . Using (1.24) for the link variable and definition (1.25) for the plaquette, together with the Baker–Campbell–Hausdorff formula, an expression can be derived establishing the connection between the plaquette and the field strength at  $x$  (see also equation (1.20)):

$$P_{\mu\nu}(x) = \exp(-a^2 g F_{\mu\nu}(x) + \dots) \quad (1.31)$$

$$= \mathbb{1} - a^2 g F_{\mu\nu} + \frac{1}{2} a^4 g^2 F_{\mu\nu}^a F_{\mu\nu}^b T^a T^b + \dots, \quad (1.32)$$

where  $a$  is the colour index. Therefore

$$\text{tr} P_{\mu\nu} = N + \frac{1}{4} a^4 g^2 F_{\mu\nu}^a F_{\mu\nu}^a + \dots, \quad (1.33)$$

$$\implies \frac{\beta}{2} \sum_{x, \mu, \nu} \left( 1 - \frac{1}{N} \text{tr} P_{\mu\nu} \right) \xrightarrow{a \rightarrow 0} - \int d^4x \beta \left( \frac{g^2}{8N} F_{\mu\nu}^a F_{\mu\nu}^a \right), \quad (1.34)$$

which, if  $\beta = \frac{2N}{g^2}$ , reduces to the usual Yang–Mills action.

For the plaquette variables  $P_{\mu\nu}$ , the Bianchi identity introduced in 1.2.1 delivers the following important relation:

$$\prod_{P_{\mu\nu} \in C} P_{\mu\nu}(x) = 1, \quad (1.35)$$

where  $C$  is a three-dimensional cube.

After having defined the field variables and an action the next step is quantizing the theory, which means specifying the functional integral.

In the continuum we would write down the formal expression

$$\langle O \rangle = \frac{1}{Z} \int \mathcal{D}\mu[A_\mu] O(A_\mu) e^{-S_{\text{YM}}[A_\mu]} \quad (1.36)$$

$$\text{with } Z = \int \mathcal{D}\mu[A_\mu] e^{-S_{\text{YM}}[A_\mu]} \quad (1.37)$$

for the expectation value of some observable  $O(A_\mu)$ , where  $S_{\text{YM}}[A_\mu]$  is the Yang–Mills action, and the integration measure  $\mathcal{D}\mu[A_\mu] = \mathcal{D}A_\mu \Delta_{\text{FP}} f(F[A_\mu])$  includes the Faddeev–Popov determinant  $\Delta_{\text{FP}}$  and a weight function  $f$  of the gauge-fixing functional  $F$ . The integral is meant to be a functional integral over all configurations of the gauge field.

Let us now consider the case of lattice gauge fields. On a lattice the expectation value of an observable  $O(U_\mu)$  is analogously written as

$$\langle O \rangle = \frac{1}{Z} \int \mathcal{D}\mu[U_\mu] O(U_\mu) e^{-S[U_\mu]} \quad (1.38)$$

$$\text{with } Z = \int \mathcal{D}\mu[U_\mu] e^{-S[U_\mu]}, \quad (1.39)$$

where  $Z$  is the *partition function* of the theory, and  $\mathcal{D}\mu[U_\mu]$  is an appropriately chosen integration measure.

As each link variable  $U_\mu(x)$  is an element of the gauge group  $G = SU(N)$ , the domain of integration is the set  $\{\text{conf}\} = \{U_\mu | \mathbb{R}^4 \rightarrow G\}$ . Accordingly, the preferable integration measure is the *functional Haar measure*:

$$\mathcal{D}\mu[U_\mu] = \mathcal{D}U_\mu \quad (1.40)$$

$$= \prod_{x,\mu} dU_\mu(x) \quad (1.41)$$

with  $dU_\mu(x)$  being the *invariant group measure* or *Haar measure*, which is uniquely defined by the following properties:<sup>9</sup>

$$\text{right invariance: } \int_G f(U) dU = \int_G f(UU') dU \quad \text{for all } U' \in G \quad (1.42)$$

$$\text{left invariance: } \int_G f(U) dU = \int_G f(U'U) dU \quad \text{for all } U' \in G \quad (1.43)$$

$$\text{normalization: } \int_G dU = 1. \quad (1.44)$$

---

<sup>9</sup>In general, there is a left-invariant group measure and a right-invariant group measure. But for all groups of interest here these two are equivalent [Gil74].

Some important properties of the functional integral are worth mentioning here: first of all, in a strict sense, it is not a functional integral any more. The discretization of space-time has turned it from a nondenumerably infinite dimensional functional integral to a denumerably infinite dimensional Riemann integral. Furthermore, virtually all calculations assume a finite volume, so that eventually one ends up with a finite dimensional Riemann integral, which, at least in principle, is exactly solvable. Nevertheless, even for numerical computations, the dimension of the integral is too high — typically of the order of  $10^4$  to  $10^6$  — which means that specially adapted methods have to be called on. Analytically, some few techniques like the *strong coupling expansion* or the *weak coupling expansion* exist to calculate expectation values like (1.38), each with their distinct domain of applicability, depending on the value of the parameter  $\beta$  in (1.28).<sup>10</sup> The method used throughout this work, is the *Monte Carlo method*, an introduction of which is given in [MM94], for example.

Yet another consequence arises due to the possibility of using the Haar measure as integration measure. As mentioned before, this can be done because each domain of integration is the group itself and thus compact. In calculations of expectation values according to (1.38) the volume of the gauge group factors out and is irrelevant as long as it is finite. Because of the normalization (1.44) the infinite volume limit does not pose any new problems. Therefore the expressions (1.38,1.39) are formally still valid in the continuum limit even without including a gauge-fixing factor like in (1.36,1.37), where the domain of integration even in the lattice regularized form is the non-compact set of gauge potentials.

Nevertheless, although gauge-fixing is not mandatory, it is allowed, and even advantageous sometimes. In this work, great importance will be attached to fixing the gauge in several ways, the possible choices of gauge being introduced in the next chapter. On the lattice, gauge-fixing is equivalent to changing the values of certain link variables in such a way that gauge invariant quantities do not change their values. This means that either link variables along a *tree*<sup>11</sup> have their values fixed, in which case it can be shown that there always exists a gauge transformation which exactly yields the prescribed configuration, or (as is done throughout the second chapter of this work) a gauge transformation is performed on the lattice sites to change the values of the link variables according to the prescription of a given gauge-fixing functional. For the former, the maximum of gauge fixing can be achieved if the link variables with prescribed values form a *maximal tree*, so that no additional gauge fixing is possible. In any case, fixing the gauge does not alter the values of gauge invariant quantities like the Wilson loop. A detailed calculation can be found in [MM94].

The third important property is known as *Elitzur theorem* [Eli75]. The statement is that on an infinite lattice — the finite lattice case being trivial to that

---

<sup>10</sup>See [Cre83] for details and references therein.

<sup>11</sup>A *tree* is a connected set of link variables not containing any closed loop.

respect — a gauge symmetry cannot be spontaneously broken. This has important consequences for the study of the phase structure of a gauge theory: any order parameter suitable for distinguishing different phases of a lattice gauge theory must be non-local. In especial, the expectation value of a single link vanishes identically in any phase:  $\langle U \rangle \equiv 0$ , and is therefore inappropriate. For reviews including proofs, see e.g. [Gro88, ID89].

### 1.2.3 Wilson Criterion and Confinement on the Lattice

The aim of using lattice calculations, either analytical or numerical, is to gain insight into the non-perturbative properties of gauge theories. In particular, the *QCD ground state* is of special interest for at least one reason: to explain quark confinement. In pursuit of an explanation of that effect with the means at hand, one is now led to formulate a lattice version of QCD, which means defining a fermion field on the lattice, in addition to the already defined gauge field, to which the fermions are to be coupled in a gauge covariant way.

However, it shall now not be dwelt any further on the implementation of quark fields on the lattice as the subject is somewhat outside the main line of reasoning in this work, and can be studied in depth in [MM94], for example. Moreover, the general belief is that for the issue of quark confinement, it is not necessary to define dynamical fermions on the lattice, and the information whether quarks are confined or not is entirely encoded in the ground state of the Yang–Mills gauge field in terms of the yet-to-be-defined *Wilson criterion*.

In the following we derive the relation between Wilson loops and the static quark potential. For the arguments to be formulated more easily, we temporarily turn to the Euclidean space continuum. The argument is usually given within the framework of the Hamiltonian picture and goes as follows (see e.g. [MM94, MO81]): the Hamiltonian  $H$  of our pure gauge system is given by

$$\hat{H} = \frac{1}{2} \int d^3x (\hat{E}_i^a \hat{E}_i^a + \hat{B}_i^a \hat{B}_i^a), \quad (1.45)$$

where  $\hat{E}_i^a, \hat{B}_i^a$  are the non-abelian electric and magnetic field strength, respectively.

A *static external charge* is defined to transform according to the fundamental representation of the gauge group  $G = SU(N)$ :<sup>12</sup>

$$[R(\Omega)\Psi]_\alpha = \Omega_{\alpha\beta}\Psi_\beta, \quad (1.46)$$

where  $\Omega \in G$  and  $\alpha, \beta = 1 \dots N$ . There is a superselection rule: owing to the gauge invariance of the Hamiltonian  $H$ , sectors with different distributions

---

<sup>12</sup>The given definition expresses the restriction to the consideration of fundamental quarks only.

of external static charges decouple completely. We consider a static external charge at  $\mathbf{x}$ , which is described by a state vector  $|\Psi\rangle \in \mathcal{H}_{\mathbf{x}}$ . In our functional representation, the basic variables are the parallel transport operators  $\{U(\mathbf{y}, \mathbf{x})\}$ , so let  $\Psi[U] = \langle U|\Psi\rangle$ .

Now let  $\mathcal{H}_{\mathbf{xy}}$  be the Hilbert space of states with a static external quark at  $\mathbf{x}$  and an antiquark at  $\mathbf{y}$ , and  $|\Psi\rangle \in \mathcal{H}_{\mathbf{xy}}$  be arbitrary. Accordingly,  $|\Psi\rangle$  transforms under a gauge transformation  $\Omega \in G$  as follows:

$$[R(\Omega)\Psi]_{\alpha\beta} = \Omega_{\alpha\gamma}(\mathbf{x})\Omega_{\beta\delta}^{-1}(\mathbf{y})\Psi_{\gamma\delta}. \quad (1.47)$$

Let  $\{|\Psi^{(n)}\rangle\}$  be a complete set of eigenvectors of the Hamiltonian  $\hat{H}$ :  $\hat{H}|\Psi^{(n)}\rangle = E_n|\Psi^{(n)}\rangle$ . We denote the distance between quark and antiquark by  $R = |\mathbf{y} - \mathbf{x}|$ . Due to rotational invariance, the energy  $E_0$  of the ground state  $|\Psi^{(0)}\rangle$  will only be a function of  $R$ , and is called the *static quark potential*:

$$V(R) := E_0(R) = \min_{\mathcal{H}_{\mathbf{xy}}} \hat{H}. \quad (1.48)$$

For an arbitrary state  $|\Psi\rangle \in \mathcal{H}_{\mathbf{xy}}$  the potential  $V(R)$  can be obtained by means of

$$\langle \Psi | e^{-T\hat{H}} | \Psi \rangle = \sum_n |\langle \Psi^{(n)} | \Psi \rangle|^2 e^{-TE_n} \quad (1.49)$$

$$\xrightarrow{T \rightarrow \infty} |\langle \Psi^{(0)} | \Psi \rangle|^2 e^{-TV(R)}, \quad (1.50)$$

if  $|\Psi\rangle$  has non-vanishing overlap with the ground state:  $\langle \Psi^{(0)} | \Psi \rangle \neq 0$ .  $T$  is the Euclidean time. As an arbitrary state  $|\Psi\rangle \in \mathcal{H}_{\mathbf{xy}}$  we take

$$\Psi[U]_{\alpha\beta} = U_{\alpha\beta}(\mathbf{y}, \mathbf{x})\Psi_{\text{vac}}, \quad (1.51)$$

where  $\Psi_{\text{vac}}$  is the gauge invariant vacuum wave functional, and  $U_{\alpha\beta}(\mathbf{y}, \mathbf{x})$  corresponds to a straight path between  $\mathbf{x}$  and  $\mathbf{y}$ . Now we silently switch back to the lattice formulation.

Then, we can calculate  $\langle \Psi | e^{-T\hat{H}} | \Psi \rangle$  directly as:

$$\langle \Psi | e^{-T\hat{H}} | \Psi \rangle = \frac{1}{Z} \int \mathcal{D}U \langle \Psi | U \rangle \langle U | e^{-T\hat{H}} | \Psi \rangle e^{-S[U]} \quad (1.52)$$

$$= \frac{1}{Z} \int \mathcal{D}U U_{\alpha\beta}^\dagger(\mathbf{x} + Ta_4, \mathbf{y} + Ta_4) U_{\alpha\beta}(\mathbf{x}, \mathbf{y}) e^{-S[U]} \quad (1.53)$$

With a little sleight-of-hand, we can convert this equation into the expectation value of the Wilson loop along a closed contour. Bearing in mind that we still have the gauge freedom to prescribe the value of a tree of link variables, we choose the axial gauge, in which all timelike links are defined to be unity:  $U_4(x) = \mathbb{1}$ . In a strict sense, this is not quite correct, as on a finite lattice, as we usually



consider, this implies the prescription of the value of a gauge invariant quantity, namely the Polyakov loop. However, on a large lattice, this only leads to some negligible error. Thus, we have

$$\langle \Psi | e^{-T\hat{H}} | \Psi \rangle = \frac{1}{Z} \int \mathcal{D}U \operatorname{tr} U(\mathcal{C}_{R,T}) e^{-S[U]} \quad (1.54)$$

$$= \langle \operatorname{tr} U(\mathcal{C}_{R,T}) \rangle =: W(R, T), \quad (1.55)$$

and, together with equation (1.50) we can derive

$$V(R) = - \lim_{T \rightarrow \infty} \frac{1}{T} \log W(R, T). \quad (1.56)$$

We now have a criterion at hand to decide whether external static quarks are confined or not, called the *Wilson criterion*: it is clear that the behaviour of  $V(R)$  at large  $R$  is the decisive factor. If  $V$  is linearly rising in  $R$  in the asymptotic regime  $R \rightarrow \infty$ , quarks can never be liberated. The condition for this is a leading order *area law* for the Wilson loop expectation value. Let  $A = RT$  be the area enclosed by the cycle belonging to the Wilson loop  $W(R, T)$ . Then an area law means

$$W(R, T) = e^{-\kappa A + (\text{subleading terms})} \quad (1.57)$$

$$\implies V(R) \xrightarrow{R \rightarrow \infty} \kappa R, \quad (1.58)$$

where  $\kappa$  is called the *string tension*. In the case of vanishing string tension, the subleading terms become important, and generally the Wilson loop expectation value then exhibits the so-called *perimeter law*. Let  $P = 2(R+T)$  be the perimeter of the above cycle. Then a perimeter law means

$$W(R, T) = e^{-\mu P + (\text{next-to-leading-order terms})} \quad (1.59)$$

$$\implies V(R) \xrightarrow{R \rightarrow \infty} \text{const}, \quad (1.60)$$

i.e. asymptotically  $V(R)$  approaches a constant value, which can be regarded as the self-energy of a free quark-antiquark pair.

It shall just be stated here that in a lattice gauge theory with any arbitrary gauge group  $V(R)$  cannot rise faster than linearly with  $R$  asymptotically [Sei78], but at least has to approach a constant value at infinity [SY82], so the Wilson loop expectation value always has an area law as an upper bound and a perimeter law as a lower bound.

In Monte Carlo calculations, where the investigation of the Yang–Mills ground state properties and the extraction of the string tension  $\kappa$  are among the foremost tasks, it is not the Wilson loop expectation value  $W(R, T)$  direct which is measured<sup>13</sup>. As we have just learned, apart from certain restrictions on the

<sup>13</sup>In fact, a Monte Carlo calculation is nothing else but a numerical measurement.

asymptotics, the general behaviour of  $W(R, T)$  can be quite complicated. In addition, as the bare coupling is reduced and the continuum limit approached, the perimeter piece actually diverges and dominates for any loop of fixed size in unrenormalized lattice units. To eliminate this distraction, it is convenient to consider ratios of loops with different area but same perimeter. In particular, in the *Creutz ratios*, defined by [Cre83]

$$\chi(R, T) = -\log \left( \frac{W(R, T)W(R-1, T-1)}{W(R, T-1)W(R-1, T)} \right), \quad (1.61)$$

the perimeter dependence and any constant factors in the Wilson loops cancel. Whenever  $W(R, T)$  is dominated by an area law,  $\chi(R, T)$  serves as an estimator<sup>14</sup> for the string tension, i.e.  $\chi \rightarrow a^2\kappa$  when  $RT$  large, or in the limit  $\beta \rightarrow 0$ .

### 1.2.4 Renormalization and Extraction of Physical Quantities

It shall now be explained how physical information can be extracted from treating the lattice as a statistical system. Renormalization is a necessary ingredient of performing calculations within a quantized field theory. Thus, in the following, it shall be briefly outlined how it is done within the framework of lattice gauge theory, where a certain familiarity with perturbative renormalization is assumed. For a more detailed treatment, the reader is referred to the literature [MM94, Cre83, Rot97]. The lattice is taken to be extended to infinity (*infinite volume limit*), in order to have a clear understanding of taking the continuum limit.

In view of equations (1.38,1.39) for the expectation value of an observable, and the partition function, respectively, it is clear that methods borrowed from statistical physics are appropriate instruments for exploiting the properties of a lattice gauge system. Eventually, however, what is actually the aim is investigating the properties of a continuum gauge theory, and we regard the lattice gauge system only as a regularized version of it.

The outline of reasoning is as follows: the lattice gauge theory is treated as a statistical system, the statistical fluctuations of which mimic the quantum fluctuations of the underlying quantum theory. The lattice spacing  $a$  serves as a coordinate space cut-off, so  $\Lambda = 1/a$  is the usual momentum cut-off. Initially, an observable  $O$  is a function of the lattice variables and of the undefined lattice spacing  $a$ .<sup>15</sup>

$$O = O(U_\mu; a). \quad (1.62)$$

Its expectation value is a functional of the lattice configuration  $\{U_\mu\}$ , and a function of the lattice spacing  $a$  and bare parameter  $\beta$ :

$$\langle O \rangle = \langle O \rangle(a, \beta), \quad (1.63)$$

<sup>14</sup>See the definition of an estimator in the next section.

<sup>15</sup>On a finite lattice, it would also depend on  $N_{(\mu)}$ , the lattice extension in the  $\mu$  direction.

$\beta$  entering through the partition function of the lattice system. Remember that  $\beta$  is essentially the inverse of the *bare* coupling constant:  $\beta = 2N/g^2$ .

This lattice observable, also called an *estimator*, should of course have a well-defined meaning in the *naive continuum limit* where  $a$  simply goes to zero:  $a \rightarrow 0$ . The prescription which estimator is to take to represent the lattice version of a continuum observable is not unique, as with the action itself. So-called *improved estimators*, and *improved actions*, are of great importance. They differ from the usual estimators by having an improved convergence behaviour in the limit  $a \rightarrow 0$ , as terms are included which cancel some of the next-to-leading-order terms in expansions like (1.32) [Sym83a, Sym83b]. A closer inspection, however, lies completely outside the scope of this work and the main line of reasoning.

As in the usual perturbative treatment of quantum field theory, when extracting physical information from the system, the bare quantities have to be replaced by *renormalized quantities* in a well-defined way, the prescription in which way this replacement is to be made is called a *renormalization scheme*. As the lattice spacing  $a$  can initially be taken to be of any size (there is no natural fundamental scale), its meaning is as unphysical as the meaning of any arbitrary scale  $\mu$  which enters a quantum theory through a regularization procedure. It is important that there is any scale at all. In the end,  $a$  will be assigned a physical value by renormalization.

The expectation value of any estimator  $O$  representing a physical observable with canonical dimension  $d$  is the product of a dimensionless function  $f(\beta)$ , as the  $\{U_\mu\}$  themselves are dimensionless, and as many powers of  $a$  as needed to build up the canonical dimension  $d$ :

$$\langle O \rangle(a, \beta) = f(\beta)a^{-d}, \quad (1.64)$$

with  $a$  essentially representing an inverse cut-off scale not having been assigned any value yet, and the bare inverse coupling  $\beta$  not having any physical meaning.

*Physical* quantities are identified with the above expectation values for any value of  $\beta$ , which in turn gives rise to a renormalization-scheme-dependent relation between  $a$  and  $\beta$ , but in an asymptotic sense, as will be explained in short:

$$\langle O \rangle(a, \beta) \xrightarrow{a \rightarrow 0} O_{\text{phys}}. \quad (1.65)$$

Depending on the renormalization scheme chosen,  $O_{\text{phys}}$  is defined to be a physically measurable quantity.

In general, there is an infinity of renormalization schemes. In QED, one usually fixes the physical electron mass and the coefficient of the long-range Coulomb force to acquire a certain value, e.g. the one which is measured in the laboratory at “infinity” — practically at a macroscopic distance from the source — which in turn means at a momentum  $p = 0$ .

In a confining theory such as QCD is hoped to be, the choice is less obvious. For pure Yang–Mills theory, a popular selection, and the one selected throughout this work, is the string tension, i.e. the coefficient of the Wilson loop area

law, which, as shown in the previous section, equals the coefficient of the asymptotically linear potential between static external sources with quark quantum numbers.<sup>16</sup> Experimentally it is gained from the study of the so-called *Regge trajectories*: it is observed that in a diagram where the angular momenta of the mesons are drawn against their masses, the values acquired lie approximately on straight lines, the slope of which is just the string tension. In a model where two quarks connected by a spinning string revolve around each other with the speed of light, this fact can be explained in a quite simple way (see e.g. [CL84]).

Formula (1.65) states that the lattice observable  $\langle O \rangle$  has a well-defined continuum limit, but not in the naive sense that on dimensional grounds, the lattice quantity tends to the continuum version if  $a \rightarrow 0$ .  $a$  is the lattice spacing, i.e. the minimum distance between two space-time points in the physical universe! It acquires a value only after renormalization of the observable  $\langle O \rangle$ . This requires a functional dependency between the bare coupling constant  $g$  and  $a$ . Such a relation is delivered by means of the *beta function*  $\tilde{\beta}(g_R)$  of the theory under consideration. Together with the renormalization of an arbitrary physical quantity, the physical scale  $a$  is uniquely determined.

In a mass-independent scheme like the MS scheme (see [IZ80, Ami84]), the beta function is defined by

$$\tilde{\beta}(g_R) = \lim_{a \rightarrow 0} a \frac{\partial}{\partial a} g_R(g, \mu_r, a), \quad (1.66)$$

where  $a$  is the inverse momentum cut-off, or, a space-time cut-off,  $\mu_r$  is some fixed renormalization point, the value of which determines the renormalization scheme, and  $g$  is the bare coupling constant. As can be seen, the beta function is defined in the limit where the cut-off is removed. The beta function has been perturbatively calculated for various theories, mostly up to two loops or more,<sup>17</sup> and the series is usually written as

$$\tilde{\beta}(g_R) = -(\beta_0 g_R^3 + \beta_1 g_R^5 + \beta_2 g_R^7 + \dots). \quad (1.67)$$

The coefficients in the MS scheme are:

$$\beta_0 = \frac{1}{(4\pi)^2} \frac{11C_2(A)}{3} \quad (1.68)$$

$$\beta_1 = \frac{1}{(4\pi)^4} \frac{34C_2(A)^2}{3} \quad (1.69)$$

$$\beta_2 = \frac{1}{(4\pi)^6} \frac{2857C_2(A)^3}{54}, \quad (1.70)$$

<sup>16</sup>Another possible choice would be the energy of the lowest excited state, the *mass gap*, identified with the glueball mass.

<sup>17</sup>The first successful two-loop calculations have been done in [Jon74, Cas74], the formidable three- and four-loop calculations are done in [TVZ80].

where  $C_2(A)$  is the coefficient of the second-degree Casimir operator of the group in the adjoint representation and defined by  $C_2(A)\delta_{ab} = \text{tr}[\tau_a\tau_b]$  (for details see [O’R86]). Although the beta function is in general scheme-dependent,  $\beta_0$  and  $\beta_1$  are scheme-independent. For further details on the various renormalization schemes, as well as the issue of scheme dependence of the renormalization group equations and the beta function, see e.g. [Mut98, Pok87].

With the help of definition (1.66) the desired connection between  $a$  and  $g$  can now be established: as the renormalized coupling  $g_R$  is held fixed,

$$0 = a \frac{d}{da} g_R = a \frac{\partial g_R}{\partial g} \frac{dg}{da} + a \frac{\partial g_R}{\partial a} \quad (1.71)$$

$$\implies \tilde{\beta}(g_R) \stackrel{a \rightarrow 0}{=} -a \frac{dg}{da}, \quad (1.72)$$

where an implicit dependence of  $\tilde{\beta}$  on  $\mu_r$  is assumed, and in the last step it has been used that in the presence of an ultraviolet cut-off

$$g_R(g, \mu_r, a) = g + A(\mu_r, a)g^3, \quad (1.73)$$

where  $A(\mu_r, a)$  stems from one-loop perturbation theory and all higher terms have been dropped (see e.g. [Pok87, IZ80]). But there is still the renormalized coupling  $g_R$  to be eliminated from the above relation, because we need an equation relating bare quantities. We observe, however, that

$$\tilde{\beta}(g) = \tilde{\beta}(g_R) + (g - g_R) \frac{d\tilde{\beta}}{dg_R} + \dots \quad (1.74)$$

$$= \tilde{\beta}(g_R) + \mathcal{O}(g^5), \quad (1.75)$$

in view of equations (1.73) and (1.67). Therefore, the first two coefficients of the “bare” and the “renormalized” beta functions coincide, and we may safely consider the two functions as equal, as long as the renormalized coupling  $g_R$  is small — otherwise, the perturbative expansion would be invalid, anyway. Eventually we get:

$$\tilde{\beta}(g) \stackrel{a \rightarrow 0}{=} -a \frac{dg}{da}. \quad (1.76)$$

This means that the perturbatively calculated beta function delivers the approximate physical extension of the lattice spacing  $a$  in the neighbourhood of  $a = 0$ , where the relation becomes exact. This can be seen from another point of view, too: eventually we are interested in the continuum limit of the theory. Thus, we have to look for a set of parameters (which, in this case, is  $\beta \sim \frac{1}{g^2}$ ) where the correlation length  $\xi \sim \frac{1}{a}$  of physical quantities becomes infinite, i.e. we are looking for *critical points* in the parameter space. Critical points are points that reflect a *second-order phase transition* of the lattice, when regarded as a

statistical system. They are also *fixed points* of the renormalization group, and distinguish themselves by zeroes in the corresponding beta functions:

$$g_c \text{ critical} \implies \beta(g)|_{g=g_c} = 0,$$

which is compatible with equation (1.76). Put differently, the continuum limit *is* the second-order phase transition, which is what has to be looked for. Further details concerning critical phenomena in statistical systems can be found in [Ami84, BDFN92, ID89].

Equation (1.76) can be solved for  $a(\beta)$ , with the perturbative expansion (1.67) of  $\tilde{\beta}(g)$  being inserted. To first order the result is ( $\beta = \frac{2N}{g^2}$ ):

$$a(\beta) = a' \exp\left(-\frac{\beta - \beta'}{4N\beta_0}\right), \quad (1.77)$$

the value of the integration constant  $a'$  being dependent on the renormalization scheme, and  $\beta'$  is such that  $a(\beta') = a'$ . As mentioned above, a preferable quantity to fix the scale in lattice gauge theories is the string tension  $\kappa$ . On dimensional grounds,  $\kappa = \frac{1}{a'^2}$ ,  $a(\beta_\kappa) = 1/\sqrt{\kappa}$ , so:<sup>18</sup>

$$a^2(\beta) = \frac{1}{\kappa} \exp\left(-\frac{\beta - \beta_\kappa}{2N\beta_0}\right). \quad (1.78)$$

The second-order result is

$$a^2(\beta) = \frac{1}{\kappa} \left(\frac{\beta_\kappa\beta_0 + 2N\beta_1}{\beta\beta_0 + 2N\beta_1}\right)^{-\frac{\beta_1}{\beta_0^2}} \exp\left(-\frac{\beta - \beta_\kappa}{2N\beta_0}\right). \quad (1.79)$$

Now that the scale  $a$  is fixed by means of the renormalization scheme above, expectation values of observables  $\langle O \rangle$  which are calculated on the lattice can be assigned physical values by simply comparing the bare value

$$\langle O \rangle(a(\beta), \beta) \quad (1.80)$$

with the bare value of the quantity used for renormalization, in our case the string tension

$$\kappa_{\text{phys}} = \lim_{a \rightarrow 0} \langle \kappa \rangle(a(\beta), \beta). \quad (1.81)$$

In other words, equation (1.81) is solved for  $a$ , which in turn is inserted in equation (1.80).

The following discussion is a central issue in this work, as it shows the way to distinguish possible lattice artifacts from real estimators, which do have a continuum limit.

---

<sup>18</sup>Note that, in principle,  $\kappa$  only has to be proportional to  $\frac{1}{a'^2}$ , but any proportionality constant can be absorbed in a redefinition of  $\beta'$ .

The differential relation (1.76) between the beta function of the theory and the physical scale  $a$  is, as has been shown, the more valid, the smaller  $a$  is, i.e. in the neighbourhood of a fixed point of the renormalization group. In this work, we are interested in  $SU(N)$  Yang–Mills theory, with the beta function given by (1.67). Together with (1.73) and the fact that fixed points correspond to zeroes of the beta function, it is at once clear that in order to reach the continuum limit, we have to study the behaviour of the observable under consideration in the limit  $\beta \rightarrow \infty$ , as one trivial fixed point, the *Gaussian fixed point*, is the point  $g_R = g = 0$ .<sup>19</sup> If the estimator  $\langle O \rangle$  which is calculated on the lattice corresponds to a *physical* observable, it must tend to a constant value  $O_{\text{phys}}$  in the limit  $\beta \rightarrow \infty$ . On the other side, if it does not, it most probably is a *lattice artifact*, a quantity which is measurable when defined on the lattice, but does not possess any well-defined continuum counterpart, and thus is bare of any physical meaning. This realization is of vital importance when it comes to the discussion of the physicality of centre vortices, or the objects caricatured by them, respectively, in the next chapter.

### 1.3 Definitions and Conventions

In this work  $SU(2)$  Yang–Mills theory on the lattice is studied. Although the central statements and experiences are expected to hold for  $SU(N)$  theory in general, we will, for the sake of simplicity, confine ourselves to the case of two colour degrees of freedom.

The first two coefficients of the beta function are:

$$\beta_0 = \frac{11}{24\pi^2} \quad (1.82)$$

$$\beta_1 = \frac{17}{96\pi^4}. \quad (1.83)$$

The one-loop, and two-loop solutions, respectively, for  $a(\beta)$  then are:

$$a^2(\beta) = \frac{1}{\kappa} \exp\left(-\frac{6\pi^2}{11}(\beta - 2)\right) \quad (\text{one-loop}) \quad (1.84)$$

$$a^2(\beta) = \frac{1}{\kappa} \left(\frac{11 + 34\pi^2}{\frac{11}{2}\beta + 34\pi^2}\right)^{-\frac{102}{121}} \exp\left(-\frac{6\pi^2\beta}{11}\right) \quad (\text{two-loop}). \quad (1.85)$$

The string tension  $\kappa$  is arbitrarily taken to be  $\kappa = (440 \text{ MeV})^2$ , which is approximately the value acquainted by the study of the Regge trajectories as explained in the previous section. The actual value is not of any great importance, as  $SU(2)$  theory is a model theory, anyway, and any observables calculated with

---

<sup>19</sup>Other fixed points may well exist, but are as yet not known.

that value taken as a reference value for renormalization can easily be rescaled if the value of  $\kappa$  changes.

In addition, we make use of the relation

$$c\hbar = 3.1615 \cdot 10^{-26} \text{ Jm} \quad (1.86)$$

$$= 197.327 \text{ fm MeV}. \quad (1.87)$$

In *natural units*, where  $c = \hbar = 1$ , we get the relation:

$$197.327 \text{ fm MeV} = 1. \quad (1.88)$$

If the lattice spacing  $a$  is given a definite value by means of renormalization as explained in the previous section, the temperature scale is also defined on an asymmetric lattice by virtue of relation (1.88).



## Chapter 2

# Centre Dominance and Vortex Condensation

*Various model theories, which stress the role of the variables belonging to the centre of unitary gauge group, are briefly reviewed. There, spin models like the Ising model as well as gauge models like the Wegner model, exhibit a certain similarity in the behaviour. In especial, in the four-dimensional Wegner model, vortices occur as collective degrees of freedom due to the presence of a non-trivial centre of the gauge group. In Yang–Mills theory, a projection method is presented which extracts in a certain way the vortex content of a gauge configuration. These thin vortices exhibit perturbative scaling behaviour signalling an underlying structure of the full, unprojected theory, containing thick vortices of physical meaning. A toy model shows that for the generic behaviour of unprojected Yang–Mills theory to be reproduced, some kind of interaction between these thin vortices must be considered.*

After the preliminaries of the first chapter, which were meant to set the stage for what is to follow, we shall now embark on the main point of this chapter and the central issue of this thesis, the possible mechanisms of the confinement of quarks. Although it is as central as quark confinement is, the subject of gluon confinement is deferred from this work, as the confinement criteria used are not applicable to this case.

Thus, whereas in the previous chapter, various technicalities and employments to extract physical information have been presented, dynamical as well as topological properties of the Yang–Mills ground state are in the foreground of this chapter.

As has already been mentioned on a previous occasion, the issue of quark confinement will be dealt with without any dynamical quarks at all in this work. This means that we assume that at the heart of a yet unknown confinement mechanism, purely gluonic properties dominate, which needs a justification.

Indeed, as is known from a perturbative treatment, and has been indicated in the previous chapter, a calculation of the one-loop beta function  $\beta(g)$  of QCD reveals that the fermionic contribution leads to a tendency away from the typical non-abelian behaviour of  $\beta(g)$ , and with enough quark flavours at hand, no asymptotic freedom would be got.

When the lattice-regularized Yang–Mills theory was invented in the 70s, various numerical as well as analytical efforts were made to trace the cause of the non-existence of coloured asymptotic states. The former have already been presented, and in this section some of the necessarily scarce analytical results shall be summarized, but not for the sake of historical interest. Several vital notions and expressions will find their introduction in a review-like embedding, but will become rediscovered as well as reexamined within the framework of centre-projected Yang–Mills theory in section 2.3. But first, some important group-theoretical aspects of gauge theory are explained, especially the issues of faithfulness of representations, the homomorphism theorem of group theory, and some topological aspects of Lie groups.

## 2.1 Gauge Groups and Their Topology

Gauge theories by definition have as a central constructive element a local continuous symmetry. The symmetry group is a *Lie group*, i.e. a group which has at the same time all the properties of a differentiable manifold. For the most known theories the associated gauge group is a unitary group like  $U(1)$  or  $SU(N)$ .

A *representation*  $R$  is a map from the gauge group  $G$  to the set of linear operators acting on a vector space  $V$ :

$$R : G \rightarrow GL(V) \tag{2.1}$$

$$g \mapsto R(g) \tag{2.2}$$

The dimension of the vector space  $V$  is called the *dimension*  $d_R$  of the representation. If the representation is a bijective map, it is called a *faithful* representation. If the vector space  $V$  is the tangent space to  $G$  at the identity element  $\mathbb{1}$ , the *Lie algebra*, the representation is called the *adjoint* representation  $R_A$ :

$$R_A : G \rightarrow GL(\mathfrak{g}) \tag{2.3}$$

$$g \mapsto R_A(g). \tag{2.4}$$

The *fundamental* representation is the lowest-dimensional faithful representation. It therefore is an group isomorphism, and the fundamental representation shares all group-theoretical and topological properties of the group itself. In a certain sense it actually *defines* the group.

The vector spaces acted on by the gauge group are constituted by the fields the Lagrange density  $\mathcal{L}$  defining the theory under consideration is constructed with.

Whereas *matter fields* are transformed by the fundamental representation, the gauge fields are transformed by the adjoint representation. Let us now state a very important theorem of group theory, the *homomorphism theorem* (see e.g. [Gil74, O'R86]): let  $\phi$  be a homomorphism, i.e. a surjective map, from a group  $G$  to a group  $G'$ , and  $\ker \phi$  its kernel, i.e.  $\text{Im } \ker \phi = \{\mathbb{1}\}$ . Then  $G/\ker \phi$  is isomorphic to  $G'$ :

$$G/\ker \phi \simeq G'. \quad (2.5)$$

As seen from  $G'$ ,  $G$  is called a *covering group* of  $G'$ , and  $G'$  is a subgroup of  $G$ . For example, take  $G = SU(2)$  and  $G' = SO(3)$ . In quantum mechanics courses, it is learnt that there is a two-to-one mapping from  $SU(2)$  to  $SO(3)$ . The kernel of this mapping consists of two elements:  $\{\mathbb{1}, -\mathbb{1}\}$ . Now identify each element of  $SU(2)$  with the one which one gets by multiplying it with  $-\mathbb{1}$ , and one gets a coset  $SU(2)/\mathbb{Z}_2$  which is isomorphic to  $SO(3)$ . If, as in this example, the covering group is simply connected, it can be shown to be unique, and it is called the *universal covering group* of  $G'$ . Every group possesses a universal covering group [Gil74].

It is also important to note that  $\ker \phi$  is not only a subset of  $G$ , but a subgroup of  $G$ , moreover an *invariant subgroup*. For there also exists a theorem which states that with  $H$  being a subgroup of  $G$ , the coset  $G/H$ , too, is a subgroup of  $G$  if and only if  $H$  is an invariant subgroup of  $G$ . Thus we get a decomposition of  $G$  as follows:

$$G = H \wedge G/H, \quad (2.6)$$

where the product  $\wedge$  denotes the *semi-direct product* of the two groups.<sup>1</sup> Seen from the topological point of view, the reason why it is the semidirect product and not the direct product  $\times$  is because this decomposition is valid only locally but not globally (see the discussion of fibre bundles in chapter 1).

In the case of the unitary groups, the situation is as follows: all non-abelian special unitary groups  $SU(N)$  are simply connected and constitute their own universal covering group, whereas in the case of the abelian group  $U(1)$ , the universal covering group is isomorphic to  $\mathbb{R}$ .

An important application of the homomorphism theorem is its application to the adjoint representation  $R_A(SU(N))$  of the unitary groups. It has the following properties:

$$R_A(SU(N)) \simeq PSU(N) = SU(N)/\mathbb{Z}_N \quad (2.7)$$

$$\pi_1(SU(N)) \simeq 0 \iff \pi_1(SU(N)/\mathbb{Z}_N) \simeq \mathbb{Z}_N, \quad (2.8)$$

where  $PSU(N)$  is called a *projective unitary group*,  $\pi_1$  denotes the first homotopy group or *fundamental group* of the group manifold,  $\mathbb{Z}_N$  is the cyclic group of the

---

<sup>1</sup>Remember: a well-known example for a semi-direct product group is the *Poincaré group*  $ISO(3, 1)$  which has as subgroups the *Lorentz group*  $SO(3, 1)$  and the *translation group*  $T_4$ , but which is not the direct product group.

order  $N$ , and  $0$  stands for the trivial group. Starting from the fundamental representation, the adjoint representation can explicitly be determined:

$$G \rightarrow R_A(G) \quad (2.9)$$

$$U \mapsto R_{ij}(U) = 2\text{Tr}(U\tau_i U^\dagger \tau_j), \quad (2.10)$$

$\tau_i$  being the generators of the group in the fundamental representation.

This all means that the adjoint representation does not distinguish between group elements that differ by an element of the *centre*  $\mathcal{Z}(G)$  of the group, which consists of all elements of  $G$  that commute with all other elements of  $G$ . For the unitary groups,  $\mathcal{Z}(SU(N)) \simeq \mathbb{Z}_N$ , so this is the cause for the popular saying that “gluons are blind to the centre of the gauge group”. On a compact manifold, these circumstances have important implications on the topology of gauge fields, as will be further depicted in the next chapter.

## 2.2 Confinement by Vortex Condensation in $\mathbb{Z}_N$ models

In the beginning of the 1970s, lattice regularization was realized as an invaluable tool for the investigation of the non-perturbative properties of quantum field theories. Pure gauge theories, especially, and their phase structure, became the centre of interest of numerous analytical, as well as numerical considerations, as by the time quantum chromodynamics as a non-abelian gauge theory has crystallized out into a serious explanation model for the strong interaction.

On a discrete space-time lattice the notion of continuity is lost. Remarkably, this gives us more freedom in formulating a gauge theory. But although a gauge model with a discrete gauge group does not have a classical continuum limit, this does not necessarily carry over to the quantum theory. If the system exhibits a second-order phase transition at an appropriate zero of its beta function, one should be able to define a continuum quantum field theory (see the exposition in 1.2.4).

Thus, at first, discrete gauge groups were considered, due to the simplicity of their treatment, and as a testing ground for new techniques. The cyclic groups  $\mathbb{Z}_N$ , which are discrete subgroups of the continuous unitary groups  $U(N)$ , played a very important role and still do. As will be recognized later, the centre of a gauge group seems to be of vital importance for the question of confinement of static quarks, and the centre of a special unitary group  $SU(N)$  happens to be just the cyclic group  $\mathbb{Z}_N$ :  $\mathcal{Z}(SU(N)) = \mathbb{Z}_N$ , consisting of the elements

$$\mathbb{Z}_N = \{e^{2\pi ik/N} | k = 0 \dots N - 1\}, \quad (2.11)$$

(cf. the previous section).

At a very early point of time it was realized that there exist certain astounding similarities between a  $\mathbb{Z}_N$  spin model (*Heisenberg model*) in  $d$  dimensions and a  $\mathbb{Z}_N$  gauge model (*Wegner model*) in  $2d$  dimensions [Weg71]. For instance, the  $d$ -dimensional  $\mathbb{Z}_2$  model (*Ising model*) is known to have a non-trivial phase structure. There exists a critical temperature  $T_c$  below which a phase transition towards spontaneous magnetization occurs. The magnetization thus serves as a local order parameter. For the sake of lucidity, we confine ourselves on a short exposition of the  $d = 2$  case. On a larger scale regions with different magnetization are found, the *Weiss domains*. The boundaries between different regions (*Peierls contours*), which are closed lines, effectively play the role of degrees of freedom of the statistical system under consideration, and due to the symmetries of the system, they are the *only* (collective) excitations. The four-dimensional  $\mathbb{Z}_2$  gauge model also offers the possibility to define vortex-like structures which turn out to be the only possible excitations respecting the symmetries. In three dimensions monopoles instead of vortices appear. Unlike a  $\mathbb{Z}_N$  spin model, however, a gauge theory does not admit a local order parameter due to the Elitzur theorem. Thus, to distinguish different phases, a non-local order parameter like the Wilson loop expectation value  $W(R, T)$  is needed to be pulled up.

For the sake of comparison, let us first recall some properties of the two-dimensional Ising model (for a more detailed review, see e.g. [Gro88]). The basic variables, denoted by  $\sigma(x) \in \{\pm 1\}$  are attached to the lattice sites, or *vertices*. A link variable  $u(x, y)$  is defined by the product of two adjacent vertex variables  $\sigma(x), \sigma(y)$ :

$$u(x, y) = \sigma(x)\sigma(y). \quad (2.12)$$

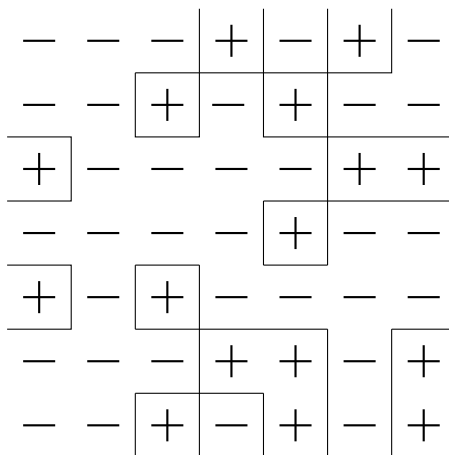


**Figure 6:** The two-dimensional Ising model. The Peierls contours separate regions with spin up from regions with spin down.

As depicted in figure 6, the set of link variables  $\{u_{-}|u_{-} = -1\}$  with negative value form closed paths on the dual lattice. These closed paths are the *Peierls contours*, which separate regions with spin up from regions with spin down. They are the

*only* excitations in the Ising model, because a configuration  $\{\sigma\}$  is determined by its Peierls contours up to a global spin rotation  $\sigma \mapsto -\sigma$ . In other words, the  $d = 2$  Ising model is in fact a “contour theory”.

The two-point correlation function  $\langle \sigma(x)\sigma(y) \rangle$  is determined by the probability distribution of Peierls contours that wind either around  $x$  or around  $y$ . If  $p_n$  is the probability that there are  $n$  such contours, then

$$\langle \sigma(x)\sigma(y) \rangle = \sum_n (-1)^n p_n. \quad (2.13)$$

A detailed analytical study [Rue99] yields that the absence of spontaneous magnetization and the exponential fall-off of the correlation function obtain in the high temperature phase where there is a condensation of the domain walls, so that long Peierls contours are abundant.<sup>2</sup> Conversely, at low temperatures, long Peierls contours are very rare, since the creation of such a contour costs energy  $E$  proportional to its length, and the entropy  $S$ , which is also proportional to the length, cannot make up for this since its contribution to the chemical potential  $\mu = E - TS$  of a contour is suppressed by a factor  $T \sim \beta^{-1}$ . In other words, short contours winding around  $x$  do not have any information about the other point  $y$  in  $\langle \sigma(x)\sigma(y) \rangle$ . They can therefore not produce a fall-off as  $y \rightarrow \infty$ .

The situation in the  $\mathbb{Z}_2$  Wegner model in  $d = 3, 4$  dimensions is quite analogous [Weg71]. As we are dealing with a gauge theory, the basic variables are now link variables  $U_\mu(x) \in \{\pm 1\}$ . For an action, the Wilson action is chosen.<sup>3</sup> The usual definition of a plaquette variable  $P_{\mu\nu}$  (see chapter 1) is a product of numbers, i.e.  $P_{\mu\nu} \in \{\pm 1\}$ , too. As a consequence of the Bianchi identity (see equation (1.35)), one has for every cube  $C$ :

$$\prod_{P_{\mu\nu} \in C} P_{\mu\nu}(x) = 1, \quad (2.14)$$

which means that the set of plaquettes  $\{P_- | P_- = -1\}$  with negative value form closed paths ( $d = 3$ ) or closed surfaces ( $d = 4$ ), respectively, on the dual lattice. In four dimensions these surfaces constitute the vortex world-sheets, and these are again the *only* (collective) excitations of the model, because a configuration  $\{U_\mu\}$  is determined by its vortices up to a gauge transformation.

---

<sup>2</sup>This explanation is also known as the *Peierls argument*.

<sup>3</sup>This shows that the Wilson action had already been in use before its employment for Yang-Mills theory.

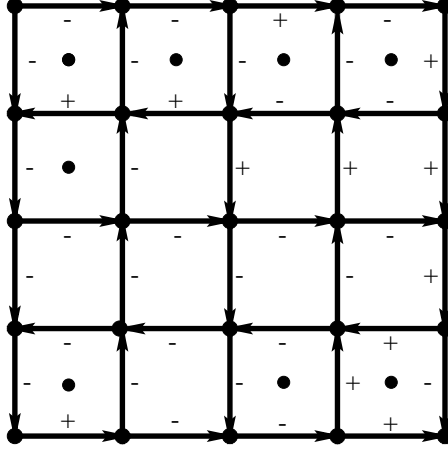


**Figure 7:** Plaquettes  $P_{\mu\nu}$  with value  $-1$  in the  $\mathbb{Z}_2$  model, labelled with a dot. They form closed paths on the dual lattice (not shown in the figure).

The analogue of the two-point correlation function in the  $d = 2$  Ising model here is the Wilson loop expectation value  $\langle \text{tr } W(\mathcal{C}) \rangle$ . It is determined by the probability distribution of vortices that wind around the path  $\mathcal{C}$ . If  $p_n$  is the probability that there are  $n$  of them,

$$\langle \text{tr } W(\mathcal{C}) \rangle = \sum_n (-1)^n p_n. \quad (2.15)$$

Again, a thorough analytical calculation [Rue99] yields that at strong bare coupling ( $\beta \rightarrow 0$ ), vortices condense so that long ones abound, which leads to an area law for  $\langle \text{tr } W(\mathcal{C}) \rangle$ . At weak bare coupling ( $\beta \rightarrow \infty$ ), however, long vortices are very rare, for the same reason as discussed for Peierls contours in the Ising model. Therefore, the only vortices that contribute to the Wilson loop expectation value (2.15) are those which wind tightly around  $\mathcal{C}$ . But these are only able to produce a perimeter law:

$$\langle \text{tr } W(\mathcal{C}) \rangle \xrightarrow{P \rightarrow \infty} e^{-\mu P}, \quad (2.16)$$

where  $P$  is the perimeter of the Wilson loop. In other words, they do not have any information about the size of the area enclosed by  $\mathcal{C}$ .

Consider now the intersection of a vortex world-sheet  $\Sigma_{\text{vortex}}$  with a timelike hyperplane  $K$  in four dimensions. By definition, it consists of spacelike plaquettes with  $P_{ij}(x) = -1$ . Therefore, if we take into account that

$$a^2 g F_{ij}(x) = 1 - P_{ij}(x), \quad (2.17)$$

where the connection between the plaquette variable and the field strength established in chapter 1 has been used, we see that there is thus a quantum of magnetic flux passing through each of these plaquettes. If, without any loss of generality e.g.  $i, j = 2, 3$ , we have  $B_1 = -\frac{2}{a^2 g}$ . If  $P_{23}$  had been  $+1$ ,  $B_1$  would

be zero. The intersection of a vortex world sheet with a timelike hyperplane is therefore identified as a magnetic flux loop.

It is useful to internalize the four-dimensional  $\mathbb{Z}_2$  Wegner model, which is of special interest to us: we have an area law for the Wilson loop expectation value  $\langle \text{tr} W(\mathcal{C}) \rangle$  in the strong (bare) coupling regime ( $\beta \rightarrow 0$ ), because of the condensation of long vortices, which in a three-dimensional time slice are magnetic flux loops. At weak (bare) coupling ( $\beta \rightarrow \infty$ ), a condensate of small vortices leads to a perimeter law for  $\langle \text{tr} W(\mathcal{C}) \rangle$ , as those are the only one contributing to  $\langle \text{tr} W(\mathcal{C}) \rangle$ , winding tightly around  $\mathcal{C}$ . We will encounter this situation again in the centre-projected Yang–Mills theory at finite temperatures in chapter 3.

In the *Mack–Petkova model* [MP79, MP80, MP82a],  $SU(2)$  Yang–Mills theory on the lattice is investigated from a general point of view, but with a slightly modified Wilson action, which amounts to restricting the admissible configurations  $\{U_\mu(x)\}$ . Based on the ideas originating in [tH78, tH79] on the connection between vortex condensation and singular gauge transformations changing the topology of the configuration — which will further be exposed in chapter 3 — a sufficient condition for an area law behaviour of the Wilson loop expectation value  $W(R, T)$  is deduced via a re-interpretation of the  $SU(2)$  theory as a  $\mathbb{Z}_2$  theory in the presence of “thick” vortices, which are  $SU(2)/\mathbb{Z}_2$  degrees of freedom. Analytical [M81] as well as lattice Monte Carlo calculations [MP82b] have been performed in order to substantiate the hypothesis of quark confinement due to the condensation of vortices. The difficulty, however, turned out to be taking the results obtained for the strong coupling limit ( $\beta \rightarrow 0$ ) over to the continuum limit  $\beta \rightarrow \infty$ , so that the question still had not been settled. In the next section, we will encounter a prescription to extract the vortex content of a given Yang–Mills configuration which exhibits the desired scaling behaviour.

It is useful to note at this point that the notion of a “thick vortex” in contrast to a “thin vortex”, which has been considered so far and which by definition has a thickness of one lattice spacing only, is necessary if a vortex-like structure shall be carried over to the continuum theory. Indeed, as early as in [Yaf80] the necessity of the “spreading” of the magnetic flux is stressed as a key feature for confinement due to an area law behaviour for the Wilson loop expectation value.

## 2.3 The Emergence of Vortices in Yang–Mills Theory

It shall now be embarked upon the issue of how the considerations made above on  $\mathbb{Z}_N$  degrees of freedom and vortices turn into something of vital importance for lattice  $SU(N)$  gauge theory with standard Wilson action, and how vortex configurations enter into the non-abelian  $SU(N)$  gauge field. A particular assignment of vortices to a given Yang–Mills lattice configuration is presented, the



*centre projection*, originating from an idea by [DFGO97], and further developed in [DFG<sup>+</sup>98, FGOa, FGO99, BFGO]. Whereas in the mean-time, first calculations are being done for an  $SU(3)$  gauge group [FGOb], we shall concentrate further on the  $SU(2)$  case. First, because it is simpler from the calculational point of view, and no principal differences are expected for the more realistic case of  $SU(3)$ , as the mechanism presented is independent of the rank of the group. Second, because in this work, great importance is attached to the issue of finite-temperature field theory and the question of the realization of a possible deconfinement phase transition within the framework of a model  $SU(2)$  theory. This will be the subject of the third chapter.

A lattice configuration  $\{U_\mu(x)\}$  is characterized by the link variables  $U_\mu(x)$ , which take values in the gauge group, in our case  $SU(2)$ . Gauge transformations  $\Omega(x)$  act on the link variables as follows:

$$U_\mu(x) \mapsto \Omega(x + \mu)U_\mu(x)\Omega^\dagger(x). \quad (2.18)$$

We are now interested in a very special gauge transformation, namely that which maximizes the central components of  $\{U_\mu(x)\}$ , or more precisely:

$$U_\mu(x) \mapsto U^\Omega = \Omega(x + \mu)U_\mu(x)\Omega^\dagger(x) \quad (2.19)$$

such that

$$\sum_{x,\mu} \text{tr} [U_\mu^\Omega(x)]^2 \stackrel{!}{=} \max., \quad (2.20)$$

which is a functional condition on  $\Omega(x)$ . Another, equivalent condition is to find a gauge transformation  $\Omega(x)$  that maximizes the following functional:

$$U_\mu(x) \mapsto U^\Omega = \Omega(x + \mu)U_\mu(x)\Omega^\dagger(x) \quad (2.21)$$

such that

$$\sum_{x,\mu,i} \text{tr} [U_\mu^\Omega(x)\sigma_i U_\mu^{\Omega^\dagger}(x)\sigma_i] \stackrel{!}{=} \max., \quad (2.22)$$

as this functional differs from the previous one only by an unimportant constant.  $\sigma_i$  are just the Pauli matrices, which are the  $SU(2)$  generators in the fundamental representation. The gauge thus defined is called the *maximal centre gauge* **MCG**.

If the desired transformation  $\Omega_c$  is found, the transformed configuration  $\{U_\mu^c(x)\}$  has the identical physical content as the untransformed one. Therefore, no approximation or simplification has been achieved so far. The far-reaching intervention now enters the game with the total neglect of the non-central components of the link variables  $U_\mu^c(x)$ , or, in other words, the link variables  $U_\mu^c(x)$  are projected onto the central component  $\mathcal{Z}(U_\mu^c(x))$ :

$$U_\mu^c(x) \mapsto \mathcal{Z}(U_\mu^c(x)) = z_\mu(x) \quad (2.23)$$

$$\text{with } z_\mu(x) \in \mathbb{Z}_2. \quad (2.24)$$

As a result of this procedure of gauging and projecting, a given  $SU(2)$  lattice gauge configuration has been mapped onto a  $\mathbb{Z}_2$  lattice gauge configuration, and this mapping is called the *centre projection*  $\mathcal{P}$ :

$$\{U_\mu(x)\} \xrightarrow{\mathcal{P}} \{z_\mu(x)\}, \quad (2.25)$$

The resulting  $\mathbb{Z}_2$  gauge theory is expected to be totally different, however, from the  $\mathbb{Z}_2$  Wegner model described in section 2.2. Whereas in the Wegner model, the Wilson action defined in terms of  $\mathbb{Z}_2$  variables has been used, what has been done here is starting from a full Yang–Mills configuration and singling out degrees of freedom that deem important to us, by numerical construction. After that, we deliberately neglect the other degrees when calculating observables.

Now having a  $\mathbb{Z}_2$  configuration at hand, we know already that the only collective degrees of freedom are *thin vortices*, which by definition have the thickness of one lattice spacing. Reflecting the fact that these vortex degrees of freedom arise from the centre projection  $\mathcal{P}$  of a given Yang–Mills configuration, the vortices are also called  $\mathcal{P}$ -vortices. In the next section, some properties of the  $\mathcal{P}$ -vortices will be illuminated, the most important one being the scaling behaviour of the planar vortex density.

Some words are in order here to mention some methodological details. Firstly, we comment upon the gauge-fixing algorithm used. We have introduced the maximal centre gauge as condition (2.20) or (2.22) for the Yang–Mills configuration. In numerical lattice calculations of the Monte Carlo type, these functional conditions, which apply to the gauge configuration as a whole, are impossible to meet exactly. Therefore, as a numerical approximation, iterative algorithms are used to fulfil conditions (2.20) or (2.22) in localized regions on the lattice by turns, one at a time. In this work, the gauge fixing condition is solved exactly for the links adjacent to a single lattice point. Subsequently, every lattice point is swept over and iteratively, the whole lattice configuration is converging towards the global solution.

The second point concerns the difference between the *direct centre gauge* and the *indirect centre gauge* [DFG<sup>+</sup>98]. In this work, what is meant by maximal centre gauge is always *direct centre gauge*, so we need not explain it. By performing the *indirect centre gauge*, one first fixes another gauge in an intermediate step, namely the *maximally abelian gauge* **MAG**, defined by the functional condition on the link variables

$$\sum_{x,\mu} \text{tr} \left[ U_\mu^\Omega(x) \sigma_3 U_\mu^{\Omega^\dagger}(x) \sigma_3 \right] \stackrel{!}{=} \max. \quad (2.26)$$

In a subsequent step, the gauge configuration is replaced by the so-called *abelian projected* configuration  $\{U_\mu^A(x)\}$  by replacing each link variable  $U_\mu(x)$  with an abelian link variable  $U_\mu^A(x)$  defined by setting all off-diagonal elements to zero. Afterwards, this abelian theory undergoes the same gauge-fixing and projection

procedure towards the centre-projected theory as before. In other words, in order to obtain a  $\mathbb{Z}_2$  configuration, a two-fold projection is applied:

$$\{U_\mu(x)\} \xrightarrow{\mathcal{P}_A} \{U_\mu^A(x)\} \xrightarrow{\mathcal{P}} \{z_\mu(x)\}, \quad (2.27)$$

where  $\mathcal{P}_A$  denotes the abelian projection. The importance of the abelian projection has its origin in the hypothesis of the *dual Meissner effect*, an idea proposed first in the mid-1970s and at the beginning of the 1980s in [Man76, tH81, tH82]. The idea thereby roughly is that confinement is due to the condensation of Dirac magnetic monopoles which emerge as gauge artifacts in various kinds of abelian gauges, thus inducing the confinement of colour-electric charges, similar to the behaviour of a superconductor of the second kind in the so-called *Shubnikov phase*, where the magnetic flux of an external magnetic field is either repelled from the superconducting medium, or, two hypothetical magnetic monopoles are confined to each other and bound by a linear potential. We will briefly comment on magnetic monopoles within the vortex picture in chapter 4.

## 2.4 Perturbative Scaling and the Continuum Limit

In the last section we have arrived at a mapping which relates a given Yang–Mills configuration  $\{U_\mu(x)\}$  to a  $\mathbb{Z}_2$ -vortex configuration  $\{z_\mu(x)\}$ , the centre projection  $\mathcal{P}$ . One may well wonder whether this very truncated configuration encloses the same physical information (which, as one assumes rightly in advance, it does not) or whether at least this reduction of degrees of freedom is not so dramatic in effect as one might estimate from the typical values of the link variables before and after the projection  $\mathcal{P}$  (see below).

In order to get a feeling for in how far the resulting  $\mathbb{Z}_2$ -vortex configuration is useful for calculating physical quantities, the centre-projected string tension  $\kappa_c$  is addressed, which is calculated by means of the Creutz ratios introduced in the last chapter. To be specific, the following procedure is executed: a set of equilibrated Yang–Mills lattice configurations  $\{U_\mu(x)\}$  is centre-projected. The centre-projected configurations  $\{z_\mu(x)\}$  are then taken for the usual algorithms for measuring the Creutz ratios and the string tension. This inspection has first been done by [DFGO97] and their results shall just be reproduced at this point.

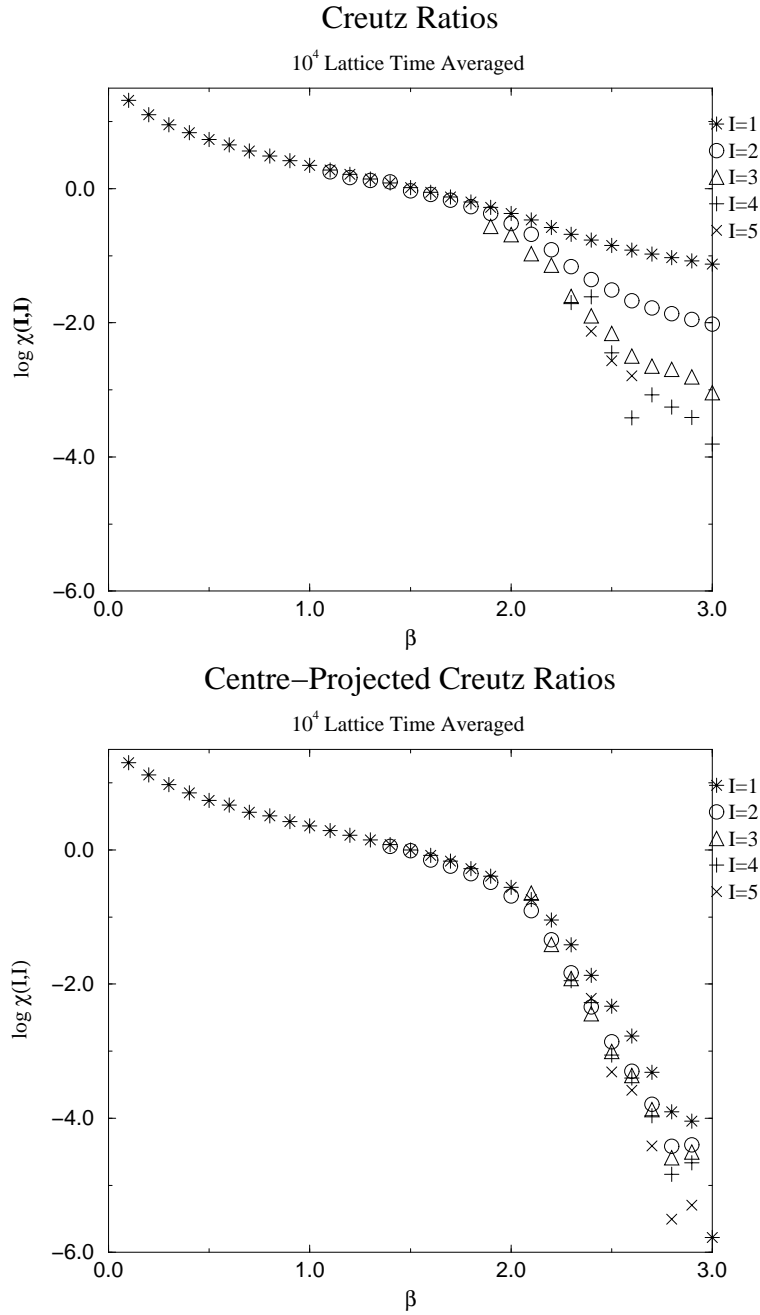


**Figure 8a/b:** Creutz ratios  $\chi(R, R)$  calculated from the full Yang–Mills configuration vs. centre-projected Creutz ratios. The elimination of the contributions of the perturbative gluon exchange can explicitly be seen.

Figures 8a and 8b are a plot of Creutz ratios  $\chi$  vs. bare inverse coupling  $\beta$ , extracted from Wilson loops formed by the full Yang–Mills configuration and the centre-projected  $\mathbb{Z}_2$  configuration, respectively. The lattice size was chosen to be  $10^4$ . In a Creutz ratio plot of a Yang–Mills lattice measurement like figure 8a

the deviation of the curves from the scaling line is due to the perturbative gluon exchange in the weak coupling regime  $\beta \rightarrow \infty$  (see e.g. [Cre83]). What is rather striking is that  $\chi(R, R)$  for  $R > 2$  in figure 8b practically lie on top of each other, and, moreover, on the same scaling line that usually is just the envelope of the Creutz ratios as in figure 8a! The centre projection seems to virtually “sweep away” the short-distance Coulomb potential, and the remaining linear potential is revealed in the short-distance region  $\beta \rightarrow \infty$ .

In [DFGO97] another interesting observation was made: let the Creutz ratios  $\chi(R, R)$  be calculated in the usual way using the full, unprojected  $SU(2)$  gauge configuration  $\{U_\mu(x)\}$ . But for the calculation of  $\chi(R, R)$ , drop all those Wilson loops, which are *not pierced by a  $\mathbb{Z}_2$ -vortex in the corresponding centre-projected configuration*  $\{z_\mu(x)\}$ . This selection process turns out to be so dramatic, that the string tension  $\kappa$  extracted from the Creutz ratios drops to zero! The hypothesis is that the Yang–Mills configuration therefore seems to contain vortex-like structures already in the full, unprojected theory. By the centre-projection  $\mathcal{P}$  these *thick vortices* are squeezed into the thin  $\mathcal{P}$ -vortices of the resulting  $\mathbb{Z}_2$ -configuration. Of vital importance here is the scaling behaviour of the planar vortex density shown below, as this is a necessary condition to rule out the possibility that these thin vortices are nothing else than lattice artifacts, bare of any physical relevance. One has to bear in mind, however, that thin vortices alone do not survive the continuum limit, themselves being objects of infinitesimal thickness. The situation reminds somewhat of the notions depicted already in [MP79] and [Yaf80], where the necessity of the “spreading” of magnetic flux is regarded in order to be able to take the theory over to the continuum limit  $\beta \rightarrow \infty$ . We will come back to that point below. The relevance of the  $\mathbb{Z}_2$  degrees of freedom in  $SU(2)$  lattice Yang–Mills theory, together with their properties as objects of physical relevance discussed below, is called *centre dominance* or *vortex dominance*, as vortices are the only degrees of freedom in a  $\mathbb{Z}_2$  theory.

Now if it is the hypothetical thick vortices that ought to constitute the underlying physical quantity to the  $\mathcal{P}$ -vortices, which only arise when the centre projection makes the thick vortices shrivel up to infinitesimally thin chords, there might remain some physicalness in the vortex configuration throughout the whole process of centre projection. To this point, the *planar vortex density*, defined as the number of  $\mathcal{P}$ -vortices piercing a unit area within some two-dimensional hyperplane has been investigated [LRT98, LTER99]. To be specific, we have considered the planar vortex density at different values of the bare inverse coupling constant  $\beta$ .

In order to get a more explicit picture of the vortex structure of the centre-projected theory, we again visualize the vortex distribution in a three-dimensional timeslice, comparing two different “resolutions” of the lattice due to a different choice of  $\beta$ , which leads to a different physical size of the lattice constant  $a$  (see chapter 1).

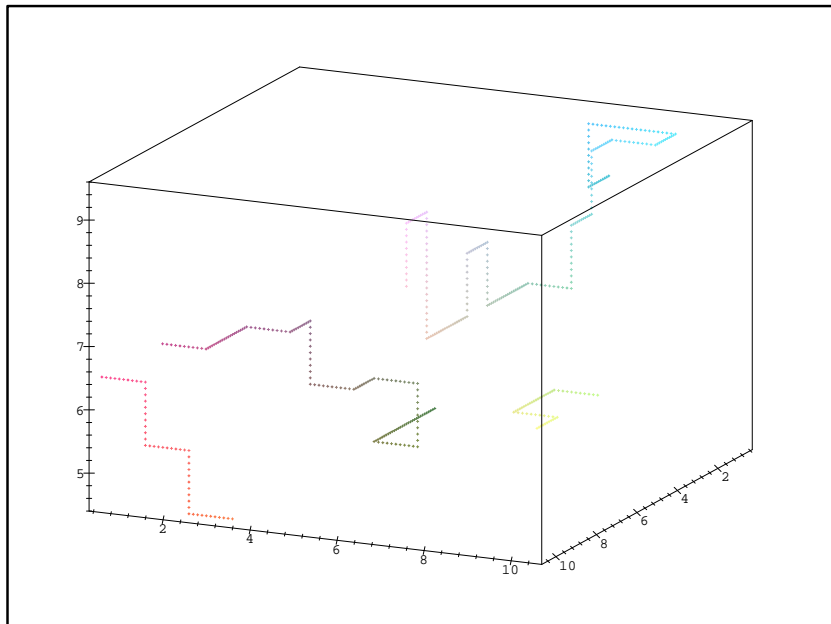
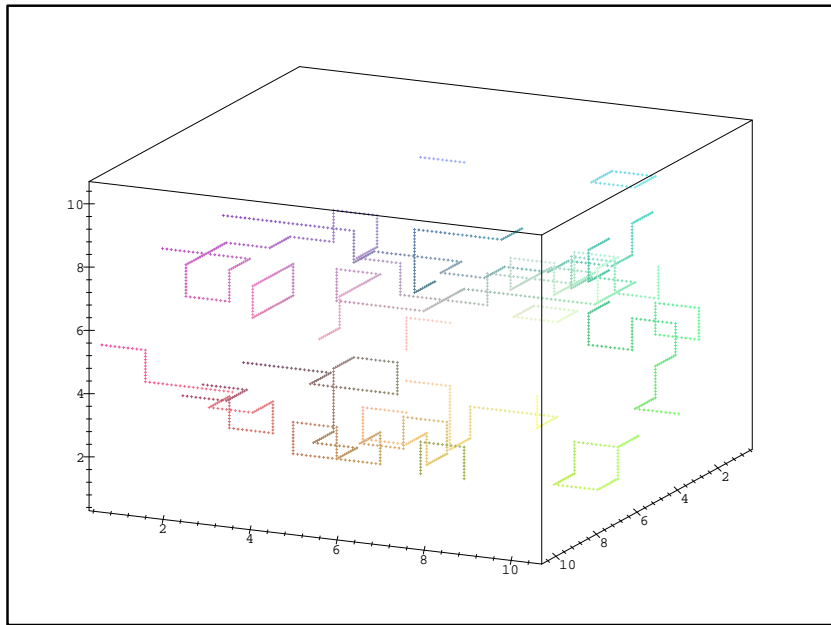


**Figure 9a/b:** Visualization of the vortex structure of a centre-projected Yang–Mills configuration  $\{z_\mu(x)\}$  at two different values of the bare inverse coupling  $\beta$ . *Upper:*  $\beta = 2.5$ . *Lower:*  $\beta = 3.0$ .

In figures 9a and 9b two generic  $\mathbb{Z}_2$  configurations for  $\beta = 2.5$  and  $\beta = 3.0$  are shown for a  $10^3$  cube of a  $10^4$  lattice. The initial observation is that the vortex

conglomeration is more dilute in the case of  $\beta = 3.0$  than in the case of  $\beta = 2.5$ . This behaviour is anticipated if it is assumed that an underlying structure of thick vortices as physical objects in the full, unprojected theory exists. This, however, is just a subjective estimate, and does not yet exclude the possibility that the vortex structure emerging after centre projection is just a lattice artifact. Therefore we have measured the *planar vortex density*  $\rho$ , defined as

$$\rho a^2 = \frac{\bar{N}}{L^2}, \quad (2.28)$$

where  $\bar{N}$  is the mean number of vortices piercing a two-dimensional ( $L \times L$ )-hyperplane.

The following data have been obtained by using lattices of size  $12^4$  and  $16^4$  [LTER99]. For these lattice sizes, the finite-size dependence of dimensionless quantities is negligible compared with the statistical errors. However, as is well-known, considerable finite-size effects persist in the extraction of the mass scale, as. e.g. encoded in the lattice spacing  $a$  as a function of  $\beta$  [FHK93]. Taking as a renormalization scale the string tension  $\kappa_c = (440 \text{ MeV})^2$  extracted from the Creutz ratios of the centre-projected configuration, we extract  $\kappa_c a^2(\beta = 2.3) = 0.12(3)$ . In a large-scale analysis [FHK93] an interpolation of the numerical data with the help of one-loop scaling to the renormalization point  $\beta = 2.3$  reveals  $\kappa_c a^2 = 0.136$  for a  $10^4$  lattice,  $\kappa_c a^2 = 0.121$  for a  $16^4$  lattice, and  $\kappa_c a^2 = 0.107$  for a  $32^4$  lattice. Compatible with this, we use  $\kappa_c a^2(\beta = 2.3) = 0.12$  as a reference scale for assigning physical units to measured quantities. When finite-size effects are mentioned below, this always refers to the aforementioned difficulty in defining the mass scale at a given  $\beta$ .

In order to extract vortex properties, we fix the  $SU(2)$  configurations to the maximal centre gauge **MCG** as described in the previous section. To eliminate the influence of Gribov copies as explained below, random gauge transformations after the gauge-fixing procedure are performed, this procedure being repeated several times. It turns out that three of these runs are sufficient at zero temperature. In the next chapter we will see that close to the deconfinement phase transition, an increasing influence of the Gribov copies makes up to six iterations necessary.

The scale dependence of the vortex density is shown in figure 10. We find a perfect scaling behaviour of the planar vortex density  $\rho$  in the range  $\beta \in [2.25, 2.55]$  for lattice sizes  $12^4, 16^4$ . We finally extract  $\rho = 3.6 \pm 0.2 \text{ fm}^{-2}$ . The relatively large error in  $\rho$  stems from the inherent uncertainty in the determination of the scale due to the aforementioned finite-size effects.

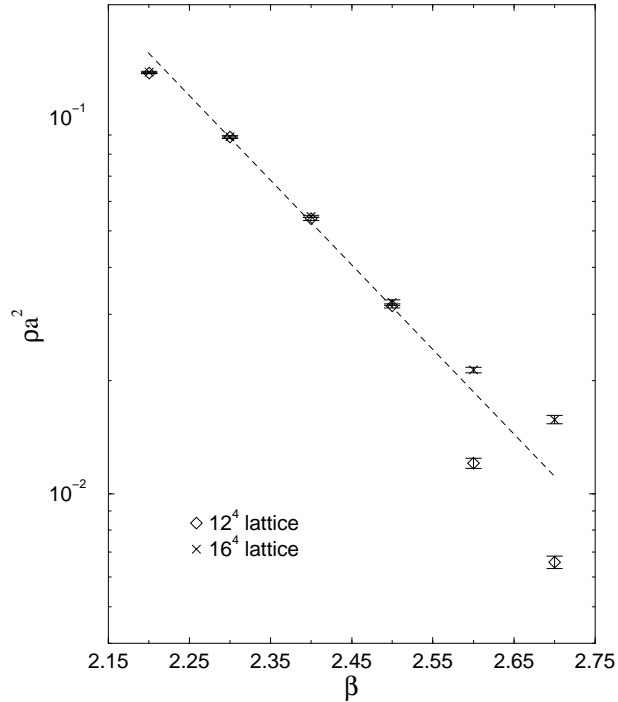


**Figure 10:** Scaling of the planar density  $\rho$  of vortex intersection points with a given space-time plane.

**Note in corrigendum:** The value above, which is larger than the one quoted in [LRT98], is in agreement with the one in [DFG<sup>+</sup>98] within the error bars. The faulty estimate, at first given for  $\rho$  given in [LRT98], was due to the fact that the Coulomb part of the full zero temperature static quark potential had been underestimated, which subsequently led to an overestimate of the reference scale. As a consequence, mass scales given in [LRT98], and also in [ELRT98], should be rescaled upwards by a factor of 1.35. Note also that the corrected value of  $\kappa_c/\rho = 1.4 \pm 0.1$  — as opposed to the old value of  $\kappa_c/\rho = 2.5$  — implies that a model of randomly distributed intersection points of vortices with a two-dimensional hyperplane (*random vortex model*, see next section) overestimates, rather than underestimates, the string tension as a function of the planar vortex density  $\rho$ , as such a model leads to a value of  $\kappa_c/\rho = 2$  as explained in the next section. However, this does not affect the motivation for the lattice measurements in [ELRT98] nor their validity, up to the aforementioned necessary rescaling of the mass scale. There, correlations of an attractive type were observed between vortex intersection points as presented in the next section, and it seems plausible that such correlations curtail the randomness of the distribution of these points, thus reducing the string tension  $\kappa_c$ . Indeed, in section 3.4, it will become clear that it is a pairing of the vortex intersection points which ultimately leads to deconfinement.

**Note on the effect of Gribov copies on the scaling behaviour:** As has been explained in 1.2.1, a gauge-fixing functional  $F[A_\mu]$  — under certain



boundary conditions — never has a unique solution, but admits an infinite set of solutions called Gribov copies. For lattice gauge theory, where the basic variables are the link variables  $U_\mu(x)$ , which in a way are the integrated quantities to the gauge field  $A_\mu$ , this means that a gauge-fixing functional condition like (2.20) or (2.22) need not be valid globally in function space, but can admit local solutions for the gauge configuration  $\{U_\mu^\Omega(x)\}$ . As shown in [KT99], if the maximal centre gauge is fixed after a previous gauge-fixing to Landau gauge, centre dominance is lost. The explanation for this apparent inconsistency is that the previous fixing to Landau gauge drives the gauge configuration too far away from the configuration corresponding to the *absolute maximum* of the gauge-fixing functional in (2.20) or (2.22). A subsequent gauge-fixing by means of some kind of local gauge-fixing algorithm like the one used in this work then inevitably leads to a gauge configuration constituting in general only a *local maximum* of the gauge-fixing functional in (2.20) or (2.22). To eliminate the effect of Gribov copies as much as possible, we perform a certain number of random gauge transformation after each process of fixing the maximal centre gauge, and then fix the gauge again. This procedure is repeated several times, and eventually, out of the set of configurations all constituting a local maximum to (2.20) or (2.22), the one with the largest value for the functional is chosen as the “valid” configuration, whereby the effect of Gribov copies is minimized. It must be stressed, however, that the existence of Gribov copies does not change anything about the validity of the whole concept of centre projection, as strictly the functional conditions (2.20,2.22) are naturally solved by the absolute maximum alone.

The issue of Gribov copies in lattice gauge theories has first been investigated in [Sha84] and their influence on lattice Monte Carlo measurements has first been investigated for  $SU(3)$  Yang–Mills theory in Landau gauge in [MPR91].

## 2.5 Random Vortex Model and Correlations

The results found so far indicate that much of the physical information of a lattice Yang–Mills configuration is encoded in a vortex-like structure which emerges when the configuration is submitted to the centre projection. The resulting vortex theory is not (yet) exactly known in the sense that the functional form of an effective action has been found. Neither is known whether these thick vortices, should they really exist, are the only structures in the Yang–Mills ground state, although they might dominate. But the effects of such an effective action can be measured by considering correlations in the positions of vortices, which eventually yield information about the interaction of the vortices. This, in turn, has a vital impact on the confining properties of the vortex vacuum, in view of equation (2.15). For this reason the two-point correlation function  $c(r)$  has been measured which will be defined in the following.

Before that, a very simple toy model shall be considered which will be found to

already contain very important properties of the centre vortex theory as measured on the lattice by means of Monte Carlo calculations. As expressed by (2.15), the Wilson loop expectation value is determined by  $p_n$ , the probability that the area  $A$  enclosed by the Wilson loop  $W(\mathcal{C} = \partial A)$  is pierced by vortices  $n$  times, which we call the *intersection probability*. For the *random vortex model* it shall be assumed that the vortices do not interact. Let us consider a four-dimensional  $L^4$ -lattice. The probability  $p$  that a vortex piercing through a two-dimensional  $(L \times L)$ -hyperplane also pierces  $A$  is assumed to be  $p = A/L^2$ . If  $N$  vortices pierce through  $L^2$ , then the probability  $p_n$  that precisely  $n \leq N$  vortices pierce  $A$  is

$$p_n = \binom{N}{n} p^n (1-p)^{N-n}. \quad (2.29)$$

Hence, the Wilson loop expectation value can explicitly be calculated to be

$$\begin{aligned} \langle \text{tr } W(\mathcal{C}) \rangle_{\text{rand}} &= \sum_{n=0}^{\infty} (-1)^n p_n \\ &= (1-2p)^N. \end{aligned} \quad (2.30)$$

But, as presented in the previous section, our lattice calculations revealed that the planar vortex density  $\rho a^2 = \bar{N}/L^2$  is a physical quantity. We therefore obtain in the continuum limit

$$\begin{aligned} \langle \text{tr } W(\mathcal{C}) \rangle_{\text{rand}} &= \lim_{N \rightarrow \infty} \left( 1 - \frac{2\rho A}{N} \right)^N \\ &= \exp(-2\rho A). \end{aligned} \quad (2.31)$$

Equation (2.31) yields an area law, from which the string tension

$$\kappa_{\text{rand}} = 2\rho \approx (535 \text{ MeV})^2, \quad (2.32)$$

based on a value for the planar vortex density  $\rho$  of  $3.6/\text{fm}^2$  (see the previous section). The value turns out to be about 48% too high, an indication that the vortices must not be considered as free, but correlations between them are obviously significant.

Consider a two-dimensional  $(L \times L)$ -hyperplane, which is pierced by vortices at the *intersection points*, which are, due to their definition, neither part of the lattice, nor part of the dual lattice. Rather, it is the plaquette pierced by the vortex which is distinguished. Nevertheless, the meaning of the intersection points is clear.

We introduce a quantity  $s_j$ , with  $j$  labelling all the different plaquettes in the lattice:  $s_j$  is 1, if plaquette  $j$  is pierced by the vortex, and 0 otherwise. The lattice average  $\langle s \rangle$  is independent of  $j$  due to homogeneity and isotropy, at least in the continuum limit. It is nothing else but the dimensionless part of the planar vortex density:

$$\langle s \rangle = \rho a^2. \quad (2.33)$$

Consider now the correlation function<sup>4</sup>

$$c_{ij} = \frac{\langle s_i s_j \rangle}{\langle s \rangle^2}, \quad (2.34)$$

where in the following, the plaquettes  $i$  and  $j$  lie in the same hyperplane with one of the two hyperplane coordinates equal [ELRT98]. Neglecting the obliquely situated pairs of intersection points does not mean a breach of isotropy, only a loss of statistical data. Let the two points lie  $l$  lattice spacings apart, so that their distance is  $r = la$ .  $\langle c_{ij} \rangle$  will only depend on  $r$  and henceforth be denoted as  $c(r)$ . It is the probability that two intersection points are found to be separated by the distance  $r$ , which is why  $c(r)$  is also called the *radial distribution function*. From another point of view, it can be interpreted as the conditional probability that an intersection point is found at a distance  $r$ , provided that at  $r = 0$  there already exists one such point. A value of  $c(r) \equiv 1$  would imply zero correlation, which is the case for the random vortex model. Any value different from that implies the higher correlations, the higher the deviation from 1 is. The distance scales over which the deviations persist give a rough estimate of the range of the vortex interaction.

Since we assume the planar vortex density to be a physical quantity, the radial distribution function  $c(r)$  might also behave like one. Therefore, in order to verify the scaling behaviour of  $c(r)$ , it is necessary to examine the correlation function at different bare couplings  $\beta$ , where it is crucial to take into account the running of the lattice spacing  $a(\beta)$  entering the physical distance  $r = la$ .

In order to estimate the statistical errors as well as the influence of systematic errors, three methods have been used to extract  $a(\beta)$  in physical units:

- Firstly, we have measured the dimensionless string tension estimator  $\kappa_c a^2(\beta)$  for values of  $\beta$  within the scaling window  $2 < \beta < 2.8$ . Using  $\kappa_c = (440 \text{ MeV})^2$ , this procedure directly yields  $a(\beta)$  in physical units.
- Secondly, we have assumed the validity of the perturbative scaling law, equation (1.84) from the last chapter, i.e. we have assumed “ideal scaling” and have extracted  $a(\beta)$  from that.
- Thirdly, we have extracted  $a(\beta)$  from measuring the dimensionless planar vortex density estimator  $\rho a^2(\beta)$  within the scaling window, and using  $\rho = 3.6/\text{fm}^2$  as physical reference scale.

Within the statistical error bars, all three methods of extrapolating to the continuum limit should yield the same results. The figures 11a and 11b show our numerical results for the radial distribution function  $c(r)$ .

---

<sup>4</sup> $c_{ij}$  is related to the *correlation coefficient*  $r$  in statistics by  $c_{ij} = r + 1$ .

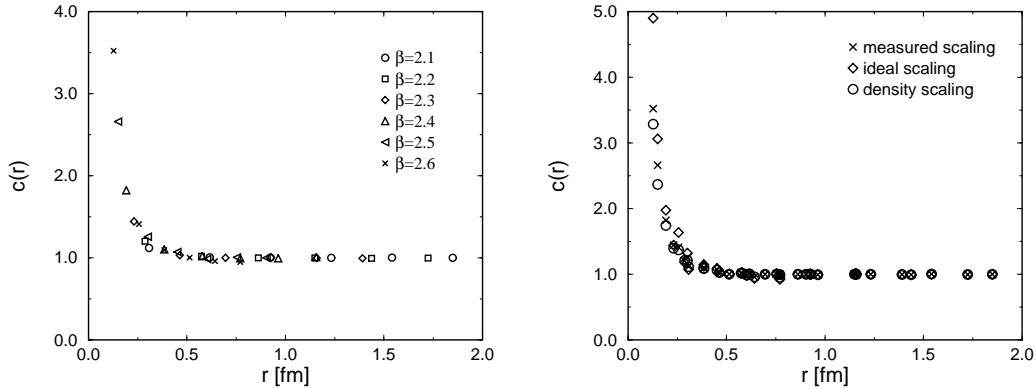


**Figure 11a/b:** The renormalized radial distribution function  $c(r)$  *Left:* Renormalization by “ideal scaling”. *Right:* All three methods of renormalization contrasted with each other.

We have used  $10^4$  and  $12^4$  lattices in order to estimate the finite size effects. Calculations with both lattice sizes yield the same results within the statistical error bars. In figure 11a, the renormalization has been done assuming “ideal scaling”. The crucial observation is that the result indeed indicates that the radial distribution function  $c(r)$ , just like the planar vortex density  $\rho$ , exhibits the right scaling behaviour and hence behaves like a physical quantity.

In figure 11b, all three methods of renormalization are contrasted with each other for a  $10^4$  lattice.

The shape of the radial distribution function  $c(r)$  plotted in figures 11a,b reveals that an attractive interaction operates between the vortices. Note that the range of this interaction constitutes a rather vaguely defined notion. One way of defining it is to look for the first cross-over of the radial distribution function below unity.<sup>5</sup> For the present data, the cross-over is at  $r_{\text{cr}} \approx 0.6$  fm, where it must be noted that in this region the statistical errors are already of the same magnitude as the deviation from unity. The value  $r_{\text{cr}} \approx 0.6$  fm must be regarded as an upper limit on the interaction range. Another possible definition would arise from the fit of an exponential decay law to the data, whence one could extract a typical screening length. In this case this would lead to a lower limit to the interaction range of about  $r_{\text{cr}} \approx 0.2$  fm.

It must be borne in mind that the planar correlations measured here still represent a rather unspecific yardstick for the structure of the vortex vacuum. They subsume a variety of more detailed effects; not only are they sensitive to the actual interaction between neighbouring vortices, but also e.g. to the shape distributions of the individual vortices in the directions orthogonal to the plane

<sup>5</sup>Note that such a cross-over has to exist, since an appropriate integral over  $c(r)$  must reproduce the total number of intersection points.

under consideration. Further investigations of the effects due to curvature terms are shortly commented upon in the chapter 4.



## Chapter 3

# Centre Dominance at Finite Temperature

*Field theory at finite temperatures is reviewed. The topological consequences of the formulation of a gauge theory in a finite volume is explained. The invariance of the gauge field under gauge transformations taking their value in the centre of the gauge group leads to the possibility of twisted boundary conditions on the gauge fields. The most general regular gauge transformation compliant with these boundary conditions can be translated to a composition of a normal gauge transformation and a centre-valued flip of some set of link variables in lattice gauge theory. The respective invariance properties of a certain non-local operator, the Polyakov loop operator, allow to define an order parameter for a symmetric state and a state with spontaneously broken centre symmetry, denoting the confinement phase and the deconfinement phase, respectively. It is shown that the vortex dominance continues to hold also above the deconfinement phase transition, which is induced by the transition between a percolating and a non-percolating phase of the vortex line clusters.*

In chapter 2 convincing results were presented which substantiate the picture of a Yang–Mills vacuum containing vortex-like structures, which by centre projection — effectively a reduction of degrees of freedom — come to light.

Much evidence has been gathered that, at least with respect to the confinement properties of the Yang–Mills ground state, the centre degrees of freedom are of vital importance<sup>1</sup>, as the full string tension is produced with the  $\mathbb{Z}_2$  variables alone.

An interesting question now is, and will be the second main point in this work, in how far the existence of a deconfinement phase above a critical temperature  $T_c$  can be explained within the framework of the centre vortex picture.

---

<sup>1</sup>One may indeed punningly speak of *central* importance in a literal sense!

Therefore, after giving a brief survey on the formalism of finite-temperature field theory and its realization in lattice gauge theory, something is said about the very likely existence of a deconfinement phase in QCD and a quark–gluon plasma, before in section 3.4 the Monte Carlo results of our lattice measurements will be presented.

### 3.1 Finite Temperature in Field Theory

Let us recall field theory from the point of view of statistical physics. The following presentation is essentially in the line of [BL93], but can be taken from any standard text book on quantum field theory at finite temperature. There the fundamental quantity is the partition function

$$Z = \text{Tr} e^{-\beta \hat{H}}, \quad (3.1)$$

where  $\hat{H}$  is the Hamilton operator of the system, and  $\beta = \frac{1}{kT}$  is essentially the inverse of the temperature  $T$ , apart from the unimportant Boltzmann constant  $k$ , which is set to 1 in most cases.

In Hamiltonian field theory, the basic quantity is the field operator  $\hat{\phi}_H(\vec{x}, t)$  in the Heisenberg picture. Its eigenstates are defined by

$$\hat{\phi}_H(\vec{x}, t)|\phi(\vec{x}, t)\rangle = \phi(\vec{x})|\phi(\vec{x}, t)\rangle. \quad (3.2)$$

The relation to the Schrödinger picture field operators  $\hat{\phi}_S(\vec{x}) := \hat{\phi}_H(\vec{x}, t = 0)$  is given by

$$\hat{\phi}_S(\vec{x})|\phi(\vec{x}, t = 0)\rangle := \phi(\vec{x})|\phi(\vec{x})\rangle, \quad (3.3)$$

so at  $t = 0$  the eigenvector systems of  $\hat{\phi}_S$  and  $\hat{\phi}_H$  coincide. It is the eigenstates of the Schrödinger picture field operator which have to be taken for evaluating the trace, as these constitute a complete orthonormal frame for the Hilbert space of the system at any time:

$$Z = \int_{\phi(\vec{x})} \langle \phi(\vec{x}), t = 0 | e^{-\beta \hat{H}_S} | \phi(\vec{x}), t = 0 \rangle, \quad (3.4)$$

where the integral symbolizes the fact that the the eigenvalues of the field operators form a continuum, not a discrete set. Let us now remember that the *propagator*, i.e. the matrix element of the time evolution operator  $U(t', t'') = \mathcal{T} e^{-i\hat{H}_S(t' - t'')}$  in position space ( $\mathcal{T}$  being the time-ordering operator), is just

$$\langle \phi''(\vec{x}), t'' | \phi'(\vec{x}), t' \rangle = \langle \phi''(\vec{x}), t = 0 | e^{-i\hat{H}(t'' - t')} | \phi'(\vec{x}), t = 0 \rangle \quad (3.5)$$

$$\sim \int \mathcal{D}\phi \int \mathcal{D}\pi \exp \left( i \int_{t'}^{t''} dt \int d^3x \left( \pi \frac{\partial \phi}{\partial t} - \mathcal{H}(\pi, \phi) \right) \right), \quad (3.6)$$



where  $\pi(\vec{x}, t)$  is the canonically conjugate field function of  $\phi(\vec{x}, t)$ , and the path integral is taken over all functions  $\pi$  and over functions  $\phi$  which satisfy the boundary conditions

$$\phi(\vec{x}, t = t'') = \phi''(\vec{x}) \quad (3.7)$$

$$\phi(\vec{x}, t = t') = \phi'(\vec{x}). \quad (3.8)$$

If the two expressions (3.4) and (3.6) are compared with each other, the functional integral expression for the partition function  $Z$  can easily be established:

$$Z \sim \int_{\phi(\vec{x})} \int \mathcal{D}\phi \int \mathcal{D}\pi \exp \left( \int_0^\beta d\tau \int d^3x \left( i\pi \frac{\partial\phi}{\partial t} - \mathcal{H}(\pi, \phi) \right) \right), \quad (3.9)$$

where  $\phi$  and  $\pi$  are now functions of  $\vec{x}$  and  $\tau = it$ , and  $\phi$  satisfies the boundary conditions

$$\phi(\vec{x}, \tau = \beta) = \phi(\vec{x}, \tau = 0) \quad (3.10)$$

$$= \phi(\vec{x}), \quad (3.11)$$

i.e. any eigenfunction of  $\hat{\phi}(\vec{x})$ .

Therefore, we can rewrite (3.9) as

$$Z \sim \int \mathcal{D}\phi \int \mathcal{D}\pi \exp \left( \int_0^\beta d\tau \int d^3x \left( i\pi \frac{\partial\phi}{\partial t} - \mathcal{H}(\pi, \phi) \right) \right), \quad (3.12)$$

where the integration is done over all periodic functions with  $\phi(\vec{x}, \tau = \beta) = \phi(\vec{x}, \tau = 0)$ .

The transition from the Hamiltonian formulation to the Lagrangian formulation can now be carried out in the case that  $\mathcal{H}(\pi, \phi)$  admits a separation of the variables  $\pi$  and  $\phi$ . More precisely, if  $\mathcal{H}(\pi, \phi)$  is of the form

$$\mathcal{H}(\pi, \phi) = \frac{\pi^2}{2} + V(\phi), \quad (3.13)$$

the  $\pi$  integral is Gaussian and therefore trivial.<sup>2</sup> Then

$$Z = \tilde{N}(\beta) \int \mathcal{D}\phi \int \exp \left( - \int_0^\beta d\tau \int d^3x (\mathcal{L}(\phi, \bar{\partial}_\mu \phi)) \right), \quad (3.14)$$

$$\text{with } \bar{\partial}_\mu = \left( i \frac{\partial}{\partial \tau}, \vec{\nabla} \right). \quad (3.15)$$

$\tilde{N}(\beta)$  contains both the constant stemming from the Gaussian  $\pi$ -integral, and the normalization factor, which up to equation (3.12) had been dropped.

---

<sup>2</sup>In the case that  $\mathcal{H}(\pi, \phi)$  is separable, but not of the specific type (3.13), the  $\pi$  integration can also be separated away and, at least in principle, been done, but one does not end up with the Lagrangian formalism.

To sum up, what has been learnt is that the partition function of a quantum field theory at a finite temperature  $T \sim \frac{1}{\beta}$  is expressed by a functional integral over functions in a four-dimensional Euclidean space, with one dimension being of finite extent ( $\beta$ ) and compact, due to the periodic boundary conditions (3.10). Space-time is therefore topologically equivalent to  $\mathbb{R}^3 \times S^1$ .

This situation is translated to gauge theory, which we now want to study at finite temperature. For the sake of generality, and because of the practical realization in actual lattices taken for Monte Carlo calculations, we consider the case with all four dimensions compactified, i.e. space-time is homeomorphic to a four-torus  $T^4$ . Apart from finite-size effects in the scaling behaviour of physical quantities which we will not be interested in at the moment, the compactification of the base manifold, if we stick to the geometrical language, has important consequences for the gauge freedom of the Yang–Mills system. In the following, some short consideration about the topology of gauge fields on the torus ought to be in order.

## 3.2 The Topology of Gauge Fields on the Torus

Periodicity of space-time does not necessarily imply periodicity of the fields defined on it if the fields are not any measurable quantities. This is well-known for the case of a fermion field, where anti-periodic boundary conditions are indeed necessary to be compatible, eventually, with the spin-statistics theorem. In the case of a gauge theory, there is even an entire set of boundary conditions available, all compliant to the physical requirement that measurable quantities should be periodic in space-time. This was in thoroughness investigated by [tH78, tH79], and a short summary of his results shall be given. For a more comprehensive account of the situation of gauge fields defined on compact manifolds, especially tori, see [GA].

Let us consider a four-dimensional torus  $T^4$ , a two-dimensional hyperplane of which is sketched in figure 12. Firstly, we are considering continuum gauge theory, so our basic field variables are the local gauge fields  $\mathbf{A}(x) = A^a(x)\tau^a$ , which in the language of geometry, define a section in an associated vector bundle over  $T^4$ , the vector space being the Lie algebra of the gauge group, and the structure group  $SU(N)$  acting on the  $\mathbf{A}(x)$  from the left, but in the affine-adjoint representation, which is isomorphic to the adjoint representation. The index  $\mu$  is dropped as the space-time vector properties of  $\mathbf{A}(x)$  are irrelevant to this discussion:

$$\mathbf{A}(x) \mapsto [\widetilde{\Omega}(x)]\mathbf{A}(x) \quad (3.16)$$

$$:= \Omega(x)\mathbf{A}(x)\Omega^\dagger(x) + i\Omega(x)\partial\Omega^\dagger(x) \quad (3.17)$$

$$A^a(x) \mapsto [\Omega(x)]^{ab}A^b(x) - [\Omega(x)]^{ab}\theta^b(x) \quad (3.18)$$

$$\text{with } [\Omega(x)]^{ab} = \text{tr}(\Omega^\dagger(x)\tau^a\Omega(x)\tau^b) \quad (3.19)$$

$$= \exp(i\theta^c(x)f^{abc}), \quad (3.20)$$

where  $\Omega(x)$  denotes the gauge transformation as  $SU(N)$  element in the fundamental representation, and  $[\Omega(x)]$  in the adjoint representation, while  $[\widetilde{\Omega}(x)]$  symbolizes the affine-adjoint transformation operator.

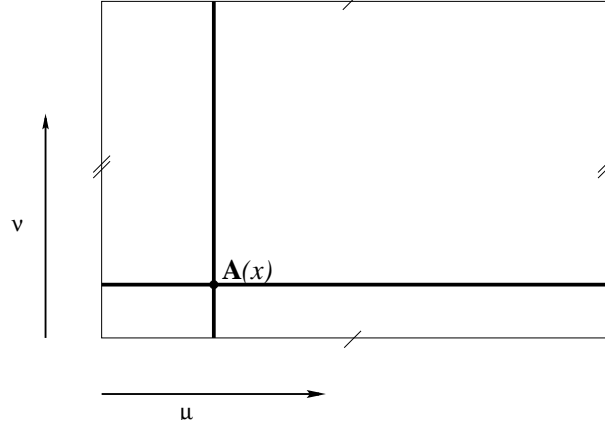


**Figure 12:** A two-dimensional slice of the four-dimensional torus. The ticks symbolize the identification of the respective opposite sides, resulting in the toroidal topology  $T^2$  of the slice.

$\mathbf{A}(x)$  is a differentiable vector field in every open subset  $\mathcal{U}$  or *patch* of  $T^4$ , but in general not on the entire manifold. In overlapping regions (cf. chapter 1)  $\mathcal{U}_1 \cap \mathcal{U}_2$ ,  $\mathbf{A}_1$  and  $\mathbf{A}_2$  must be related by an element of the structure group  $SU(N)$  which can always be reduced to  $PSU(N) = SU(N)/\mathbb{Z}_N$ , because  $\mathbf{A}$  transforms according to the adjoint representation. Let us regard the two-dimensional hyperplane of figure 12 and let  $N_{(\mu)}$  ( $N_{(\nu)}$ ) be the extent in the  $\mu$  ( $\nu$ ) direction. Then, in particular,

$$\mathbf{A}(x + N_{(\mu)}) =: \mathbf{A}(x + \mu) = [\widetilde{\Omega}_{(\mu)}] \mathbf{A}(x). \quad (3.21)$$

The cocycle condition of chapter 1, equation (1.3), now implies that, in particular,

$$\begin{aligned} \mathbf{A}(x + \mu + \nu) &= [\widetilde{\Omega}_{(\nu)}(x + \mu)][\widetilde{\Omega}_{(\mu)}(x)] \mathbf{A}(x) \\ &= [\widetilde{\Omega}_{(\mu)}(x + \nu)][\widetilde{\Omega}_{(\nu)}(x)] \mathbf{A}(x), \end{aligned} \quad (3.22)$$

$$\implies [\widetilde{\Omega}_{(\nu)}][\widetilde{\Omega}_{(\mu)}] = [\widetilde{\Omega}_{(\mu)}][\widetilde{\Omega}_{(\nu)}], \quad (3.23)$$

as the first equality holds for every connection  $\mathbf{A}$ . But  $[\widetilde{\Omega}_{(\mu)}], [\widetilde{\Omega}_{(\nu)}]$  are elements of the affine-adjoint representation, which is isomorphic to  $SU(N)/\mathbb{Z}_N$ , so that for the elements of the gauge group  $SU(N)$  the following, more general, relation holds:

$$\Omega_{(\nu)}\Omega_{(\mu)} = \Omega_{(\mu)}\Omega_{(\nu)}z_{\mu\nu}, \quad (3.24)$$

$z_{\mu\nu}$  belonging to the centre of the gauge group:  $z_{\mu\nu} \in \mathcal{Z}(SU(N)) = \mathbb{Z}_N$ , and if  $z_{\mu\nu} \neq \mathbb{1}$  the gauge configuration is said to have *twisted boundary conditions*.

Note an important difference to the situation sketched in chapter 1, where it was explained that in a principal fibre bundle, the connection one-form is always differentiable in the entire bundle, whereas here there are overlap regions  $U_1, U_2$ , where the gauge fields  $\mathbf{A}_1, \mathbf{A}_2$  need only be connected by a gauge transformation. Here the gauge fields play the role of a vector field, transforming according to the adjoint representation of the gauge group. It is an associated bundle to the *adjoint bundle*, the principal bundle with a structure group  $SU(N)/\mathbb{Z}_N$ . If  $z_{\mu\nu}$  is not zero, there is an *obstruction* to lift an  $SU(N)/\mathbb{Z}_N$  bundle to an  $SU(N)$  bundle over  $T^4$ .<sup>3</sup> This obstruction is related to the second homology group of the torus with coefficients in  $\mathcal{Z}(SU(N)) = \mathbb{Z}_N$ , which is not trivial. In the  $SU(2)$  case we have the *second Čech cohomology group*  $H^2(T^4; \mathbb{Z}_2)$  and its special elements, the *second Stiefel–Whitney classes*, which are both non-trivial with twisted boundary conditions. In other words, the existence of a more general set of boundary conditions is due to the invariance of the gauge fields to the group centre  $\mathbb{Z}_N$ . This leads to a generalized set of regular gauge transformations, as we will see below. A general introduction to obstruction theory and the problem of lifting of maps can be found in [Spa66]. For a deeper treatise of the special problem of gauge theories on compact manifolds see e.g. [Sed82].

In the fundamental representation,  $z_{\mu\nu}$  is of the form

$$z_{\mu\nu} = e^{\frac{2\pi i}{N} n_{\mu\nu}}, \quad (3.25)$$

$n_{\mu\nu}$  being called the *twist tensor*. It is antisymmetric and thus has six integer entries which are defined modulo  $N$ . They are usually denoted by

$$m_i = \frac{1}{2} \varepsilon_{ijk} n_{jk} \quad (3.26)$$

$$k_i = n_{0i}, \quad (3.27)$$

and have a certain similarity to the electric and the magnetic field embedded inside the field strength tensor, and are not without reason called the *total electric* and *total magnetic flux vectors* in  $T^4$ , respectively. The reason will become clear below. It is clear that  $n_{\mu\nu}$  defines  $N^{\frac{D(D-1)}{2}} = N^6$  (for  $D = 4$  dimensions) topological classes of gauge configurations. Note that these classes disappear if a field in the fundamental representation of  $SU(N)$  is added to the system, as these fields would make unacceptable jumps at the boundary.

Now let  $\Omega(x)$  be a gauge transformation acting on the system,  $\Omega(x) \in \{T^4 \rightarrow SU(N)\}$ . The most general gauge transformation in compliance with the invariance of physical states, i.e. one which leaves the twist tensor invariant, is a

---

<sup>3</sup>Remember: given a map  $f : X_1 \rightarrow Y$  and a map  $g : X_2 \rightarrow Y$ , does there exist a map  $h : X_2 \rightarrow X_1$ , such that  $f \equiv gh$ ? The map  $h$  is then called a *lift* of  $f$ .

$\mathbb{Z}_N$ -periodic transformation for which the following relation must hold:

$$\mathbf{A}(x) \rightarrow [\widetilde{\Omega(x)}]\mathbf{A}(x) \quad (3.28)$$

$$\text{with } [\widetilde{\Omega(x+\mu)}] = [\widetilde{\Omega(x)}] \quad (3.29)$$

$$\text{but } \Omega(x+\mu) = \Omega(x)z_\mu, \quad (3.30)$$

with  $z_\mu := e^{2\pi i k_\mu/N} \in \mathbb{Z}_N$ . In this case,  $\Omega(x)$  is called a *regular gauge transformation*.

One may also define a particular kind of *singular gauge transformations* [tH78, tH79], which are well-defined everywhere except on a  $(D-2)$ -dimensional closed submanifold  $\Sigma$ . In the  $D=4$  case, they produce an integer unit of magnetic or electric flux, dependent on the type of three-dimensional slice one considers. We denote a gauge transformation singular along a closed hypersurface  $\Sigma$  by  $\Omega^\Sigma(x)$ . In a three-dimensional slice  $K$ , this hypersurface defines a curve  $\mathcal{C}'$  (see figure 13). The restriction of  $\Omega^\Sigma(x)$  on  $K$  is called the *disorder operator* or *'t Hooft loop* and denoted by  $\Omega(\mathcal{C}')$ .

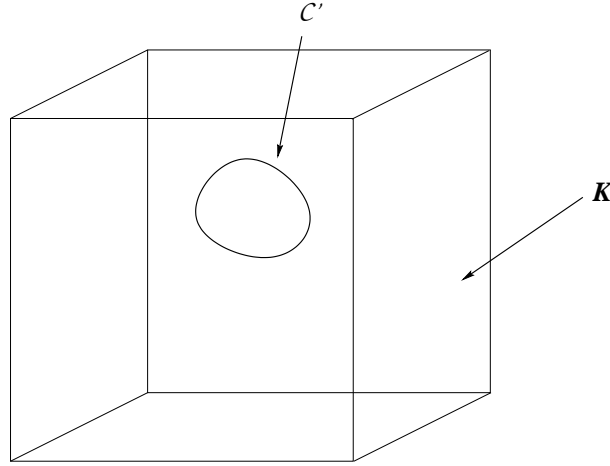


**Figure 13:**  $\mathcal{C}'$  is the intersection of the singularity hypersurface  $\Sigma$  with the three-dimensional slice  $K$ . The restriction of the singular gauge transformation  $\Omega^\Sigma(x)$  on  $K$  is the 't Hooft disorder operator  $\Omega(\mathcal{C}')$  and can be understood as the creation operator of a magnetic flux loop if  $K$  is spatial.

One may verify that for consistency of the theory, the following commutation relations between the Wilson loop operator  $W$  and the 't Hooft loop operator  $\Omega$  must hold [tH78]:

$$[W(\mathcal{C}), W(\mathcal{C}')] = 0 \quad (3.31)$$

$$[\Omega(\mathcal{C}), \Omega(\mathcal{C}')] = 0 \quad (3.32)$$

$$W(\mathcal{C})\Omega(\mathcal{C}') = \Omega(\mathcal{C}')W(\mathcal{C})z, \quad (3.33)$$

where  $z$  is an element of the centre  $\mathcal{Z}(SU(N)) = \mathbb{Z}_N$  of the gauge group  $SU(N)$ , and either  $\mathcal{C}$  or  $\mathcal{C}'$  is null-homotopic. The Wilson loop and the 't Hooft loop are dual to each other. In a three-dimensional time slice,  $W(\mathcal{C})$  creates an integer unit of electric flux<sup>4</sup> along  $\mathcal{C}$ , and  $\Omega(\mathcal{C}')$  creates an integer unit of magnetic flux along  $\mathcal{C}'$ , the integer value itself being dependent on  $z$ . If the 't Hooft loop is null-homotopic, the twisted boundary conditions are not changed. But if the 't Hooft loop belongs to a non-trivial homotopy class,  $n_{\mu\nu}$  is changed by integer units in some entry. Thus, a singular gauge transformation may change the twisted boundary conditions of the configuration. It should be clear by now why the integer-valued quantities  $m_i, k_i$  have been called total magnetic and electric flux, respectively.

Now, we will turn again to an  $SU(N)$  gauge theory defined on a lattice. Here, the basic variables — the link variables  $U_\mu(x)$  — are bilocal operators and elements of the gauge group itself. Elements of the centre  $\mathcal{Z}(SU(N))$  of the gauge group  $SU(N)$  act non-trivially on them. In the following we will now concentrate on the effect of a  $\mathbb{Z}_N$ -periodic gauge transformation on the lattice. The effect of a  $\mathbb{Z}_N$ -periodic gauge transformation is very simple to visualize. For simplicity, consider a two-dimensional hyperplane homeomorphic to  $T^2$  sliced out of  $T^4$ . Looking at figure 14 it is easy to realize that a gauge transformation with  $\Omega(x_1, x_2 = a_2) = z\Omega(x_1, x_2 = 0)$  has the same effect as a periodic gauge transformation  $\Omega_0(x)$  plus a flip of all link variables  $U_2(x_1, x_2 = a_2 - 1)$  by the same centre element  $z$ :

$$U_2(x_1, x_2 = a_2 - 1) \mapsto zU_2(x_1, x_2 = a_2 - 1). \tag{3.34}$$

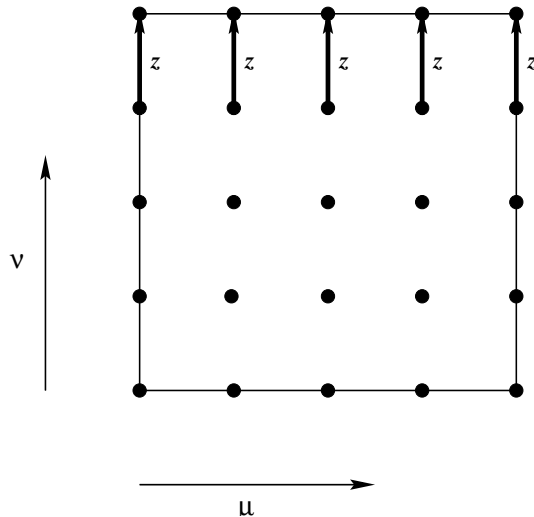


**Figure 14:** A gauge transformation which is  $\mathbb{Z}_N$ -periodic in the  $\nu$ -direction can be decomposed as an periodic gauge transformation, accompanied by a  $z_\nu$ -flip of every link variables at a fixed  $x_\nu$ .

<sup>4</sup>cf. the interpretation of the Wilson loop as a quark-antiquark world-line in chapter 1

But this flip leaves the plaquette variables  $P_{\mu\nu}(x)$  invariant, so this transformation is a *symmetry transformation*, as the action (1.28) is unchanged.<sup>5</sup> Therefore, also in lattice gauge theory, *centre symmetry* is a symmetry of the action.

However, as is well-known, a symmetry of the action need not be a symmetry of the ground state. The case of a ferromagnetic system below the *Curie temperature* is a well-known example. Out of an ensemble of possible states all related to each other by a symmetry transformation, only one is chosen to be realized by nature. In our case the symmetry at hand is not even a continuous one, let alone a local one, but a global discrete symmetry, which can be spontaneously broken. In order to determine whether the symmetric or the spontaneously broken phase is realized, an order parameter is needed. This order parameter must be a non-local one, due to the same reasons given in the first chapter for the choice of the Wilson loop expectation value  $\langle \text{tr } W(\mathcal{C}) \rangle$ , but that alone is not enough. Every plaquette and therefore every Wilson loop  $W(\mathcal{C})$  that is *null-homotopic* is invariant under centre transformations and therefore not a means for distinguishing the two possible phases. The expectation value  $\langle \text{tr } L \rangle$  of the *Polyakov loop*  $L(\vec{x})$ , however, which is defined by

$$L(\vec{x}) = \mathcal{P} \prod_{x_4=0}^{N_4-1} U_4(\vec{x}, x_4), \quad (3.35)$$

is suited. The Polyakov loop defines a path  $\mathcal{C}$  winding once around the torus in the time direction, and under a  $\mathbb{Z}_N$ -periodic gauge transformation it transforms as

$$L(\vec{x}) \mapsto z_4 L(\vec{x}), \quad (3.36)$$

$z_4$  being defined as in (3.30), where the 4-direction is chosen to be the time direction.

From now on, we will take the time direction to be compactified to  $S^1$ , the three space directions being regarded as infinite. The reason is that using lattice calculations, one tries to find out how the properties of the physical system change if the temperature is driven up, but still in the infinite (three-)volume limit. Thus, everything that has been stated so far about  $\mathbb{Z}_N$ -periodic gauge transformations and centre symmetry only applies to the time direction. For argumentational purpose, our space-time is then  $\mathbb{R}^3 \times S^1$ , even though in real numerical lattice Monte Carlo calculations only finite lattices can be realized. Thus, in a strict sense, numerical lattice calculations never are at infinite volume, or at zero temperature. The point, however, is whether the extent  $N_i (i = 1, 2, 3)$  in the three space directions is large enough if the correlation length  $\zeta$  is taken as a scale. If  $N_i \gg \zeta$ , even a finite lattice can be taken to be a realization of a zero-temperature, or infinite-volume, lattice. To realize a lattice at a finite temperature  $T$ , an asymmetric lattice with  $N_4 < N_i (i = 1, 2, 3)$  is used. But for the

---

<sup>5</sup>Necessarily, only if the extent in each of the directions is greater than one lattice unit!

finite temperature to take effect,  $N_4$  has to be comparable to the correlation length  $\zeta$ . If this is the case, then the temperature can be calculated with the use of the renormalization procedure presented in chapter 1.

To understand the appropriateness of  $\langle \text{tr } L \rangle$  as an order parameter for distinguishing a centre-symmetrical phase from a non-symmetrical one, one must merely remember that centre symmetry is a symmetry of the action, i.e. in expectation values of the form

$$\langle \text{tr } L \rangle = \int \mathcal{D}U \text{tr } L(U) e^{-S[U]} \quad (3.37)$$

a certain value of  $L(U)$  contributes as much as a centre-transformed one  $zL(U)$ . Therefore, because of  $\sum_k z_k = 0$ , in a symmetric phase the expectation value must be zero, whereas in a spontaneously broken phase, it may well acquire a non-zero value:

$$\langle \text{tr } L \rangle = 0 \quad (\text{symmetric phase}) \quad (3.38)$$

$$\langle \text{tr } L \rangle \neq 0 \quad (\text{spontaneously broken phase}). \quad (3.39)$$

Whether or not, and if, by which choice of parameters, the one or the other phase is realized, now is a question addressed to numerical lattice calculations, as an analytical treatment is momentarily outside the scope of the possible. In the next section the role of  $\langle \text{tr } L \rangle$  within the context of quark liberation is illuminated, with the phase transition hinted at in the last few paragraphs being identified with the *deconfinement phase transition* within the context of pure Yang–Mills theory.

In [tH78] instead of choosing the expectation value of the Polyakov loop operator, that of the above-defined disorder operator  $\Omega(\mathcal{C})$  was proposed as an additional order parameter for determining the phase being realized by the system, arguing on general grounds. The existence of at least three possible phases was conjectured, and consequent analytical calculations [Tom81] supported the picture.

Let us just summarize at last that by studying the behaviour of the Polyakov loop expectation value, one may verify whether at a definite point in parameter space, i.e. at the phase transition point, the original  $SU(N)$  symmetry is broken spontaneously down to a mere  $SU(N)/\mathbb{Z}_N$  symmetry. This spontaneous symmetry breaking does not contradict Elitzur's theorem, however, as the broken symmetry group acts globally on the fields.

### 3.3 The Deconfinement Phase Transition

It is generally believed that from a certain critical temperature  $T_c$  upwards the notion of hadrons as effective degrees of freedom under the influence of the strong interaction breaks down. Furthermore, the belief is that at the same critical



temperature *chiral symmetry* is restored. This means that in the *deconfinement phase*, i.e. above the critical temperature, the QCD degrees of freedom and the physical degrees of freedom are supposed to be identical. The hadronic matter is expected to undergo a phase transition into a *quark-gluon plasma*, where the characteristic low-energy features like confinement and spontaneous chiral symmetry breaking are lost, and the behaviour of matter is dominated by the asymptotic freedom of QCD.

This phase transition is expected to occur at some temperature  $T_c \approx m_\pi$ ,  $m_\pi$  being the pion mass, where copious thermal production of pions sets in. Although neither any rigorous theoretical argument nor reliable experimental data exist to substantiate this hypothesis, some indications exist by which one is led to this supposition. For a review of this topic see e.g. [Shu88].

The problem to solve therefore is: does QCD predict a deconfinement phase transition, and if so, what is the nature of it? Lacking any analytical method to tackle the problem, one has to resort to lattice Monte Carlo calculations, which allow, at least in principle, to obtain an answer to the question.

At zero temperature, the potential of a static quark-antiquark pair at a distance  $R$  can be determined by studying the Wilson loop expectation value  $W(R, T)$  in the limit of large Euclidean times  $T \rightarrow \infty$  as has been explained in 1.2.3, with the lattice extent in the time direction being infinite. At finite temperatures the lattice has a finite extent in the time direction, and this limit cannot be taken any more. Thus, the Wilson loop no longer plays the role of an order parameter.

Fortunately, we have already come across a substitute for it, the Polyakov loop  $L(\vec{x})$ . It has already been shown in the previous section that it has the properties of an order parameter distinguishing a centre-symmetric phase from a spontaneously broken one. Now, it shall be shown that these two phases also have dramatically different physical properties. The centre-symmetric phase being a *confinement phase* for static external quarks, and the spontaneously broken phase being a *deconfinement phase*. So, at this stage, it will be deduced that centre symmetry indeed plays a crucial role in the confinement mechanism.

The argument given in the following is rather qualitative and similar in nature to the one in 1.2.3. For a more detailed discussion, the reader shall be referred to [Pol78, Sus79]. We consider continuum theory at finite temperature, i.e. space-time is isomorphic to  $\mathbb{R}^3 \times S^1$ . We get for the partition function of a system with

one static external quark at  $\vec{x}$ , which is represented by a state  $|\Psi(\vec{x})\rangle \in \mathcal{H}_x$ :

$$Z \sim \text{Tr} e^{-\beta \hat{H}} \quad (3.40)$$

$$= \sum_n \langle \Psi_{\text{vac}} | \Psi_{(n)}(\vec{x}, 0) \text{tr} e^{-\beta \hat{H}} \Psi_{(n)}^\dagger(\vec{x}, 0) | \Psi_{\text{vac}} \rangle \quad (3.41)$$

$$= \sum_n \langle \Psi_{\text{vac}} | \text{tr} e^{-\beta \hat{H}} \Psi_{(n)}(\vec{x}, \beta) \Psi_{(n)}^\dagger(\vec{x}, 0) | \Psi_{\text{vac}} \rangle \quad (3.42)$$

$$\sim \langle \Psi_{\text{vac}} | \text{tr} e^{-\beta \hat{H}} \Psi_{(0)}(\vec{x}, \beta) \Psi_{(0)}^\dagger(\vec{x}, 0) | \Psi_{\text{vac}} \rangle \quad (3.43)$$

$$= \langle \Psi_{\text{vac}} | \text{tr} e^{-\beta \hat{H}} L(\vec{x}) | \Psi_{\text{vac}} \rangle \quad (3.44)$$

$$= \langle \text{tr} L(\vec{x}) \rangle, \quad (3.45)$$

where  $|\Psi_{\text{vac}}\rangle$  is the vacuum state,  $\Psi_{(n)}^\dagger(\vec{x}, 0)$  is the creation operator of a static external quark with  $n$  labelling the eigenstates of  $\hat{H}$ , and  $\beta \sim \frac{1}{T}$ . In the last line the periodic boundary conditions have been used, the line before is due to renormalization effects (see [Pol78, Sus79]). Note that the expectation value is calculated for the canonical ensemble.

Eventually, we see that the expectation value of the Polyakov loop,  $\langle \text{tr} L \rangle$ , is proportional to the *free energy*  $F$  of the system containing a single static external quark:

$$\langle \text{tr} L \rangle \sim \text{Tr} \left( e^{-\beta \hat{H}} \mathcal{P} e^{-\int_0^\beta d\tau \hat{A}_4(\vec{x}, t)} \right) \quad (3.46)$$

$$= e^{-\beta F}. \quad (3.47)$$

It is now clear how a vanishing or a non-vanishing Polyakov loop expectation value has to be interpreted physically: for  $\langle \text{tr} L \rangle$  to be zero, an infinite free energy is needed, which means that such a state is impossible. To be more precise: it is not so much that the required free energy is infinity – this would be a phenomenon well-known in quantum physics and could be overcome by just redefining the zero level of the energy, just like the renormalization of the zero point energy of the harmonic oscillator by subtracting the infinite part. It is the fact that the free energy of the system without a single quark is zero already without additional renormalization, which means that there is an infinite *mass gap* between the two states, and *this* makes the one-static-quark state impossible!

Consider now the correlation function

$$\Gamma(R) = \langle \text{tr} L(\vec{x}) L^\dagger(\vec{0}) \rangle \quad (3.48)$$

$$\text{with } R = |\vec{x} - \vec{0}|. \quad (3.49)$$

If the correlations at large values of  $R$  tend to zero, i.e. if  $\Gamma$  obeys the *cluster decomposition principle*:

$$\langle \text{tr} L(\vec{x}) L^\dagger(\vec{0}) \rangle \xrightarrow{|\vec{x} - \vec{0}| \rightarrow \infty} |\langle \text{tr} L \rangle|^2, \quad (3.50)$$

then

$$\langle \text{tr } L \rangle = 0 \quad (3.51)$$

$$\implies \Gamma(R) = e^{-\beta V(R)} = 0 \quad (\text{confinement}) \quad (3.52)$$

and

$$\langle \text{tr } L \rangle \neq 0 \quad (3.53)$$

$$\implies \frac{\Gamma(R)}{|\langle \text{tr } L \rangle|^2} = e^{-\beta V(R)} \xrightarrow{R \rightarrow \infty} \text{const.} \quad (\text{deconfinement}), \quad (3.54)$$

where  $V(R)$  is the static quark potential introduced in chapter 1. The last equation is due to the Wilson loop formula (1.56), and, in a strict sense, only valid in the limit  $T \rightarrow \infty$ , which can never be reached at a finite temperature.

Altogether we have established the desired connection between the spontaneous breaking of centre symmetry and the deconfinement phase transition.

Now that the importance of the Polyakov loop expectation value as an order parameter for confinement has been clarified, it remains to investigate lattice Yang–Mills theory from this angle. This has first been done by [MS81a, MS81b, KPS81] for  $SU(2)$  gauge theory. The results have been reproduced by our own measurements and are included in figure 15 in the next section.

## 3.4 Centre Dominance at Finite Temperature

### 3.4.1 Centre Projection and the Deconfinement Phase Transition

The interesting question now is: is the deconfinement phase transition also reproduced in centre-projected lattice Yang–Mills theory? We therefore have measured  $\langle \text{tr } L \rangle$  with centre-projected configurations  $\{z_\mu(x)\}$  and contrasted the result with the one obtained in full, unprojected Yang–Mills theory in figure 15.

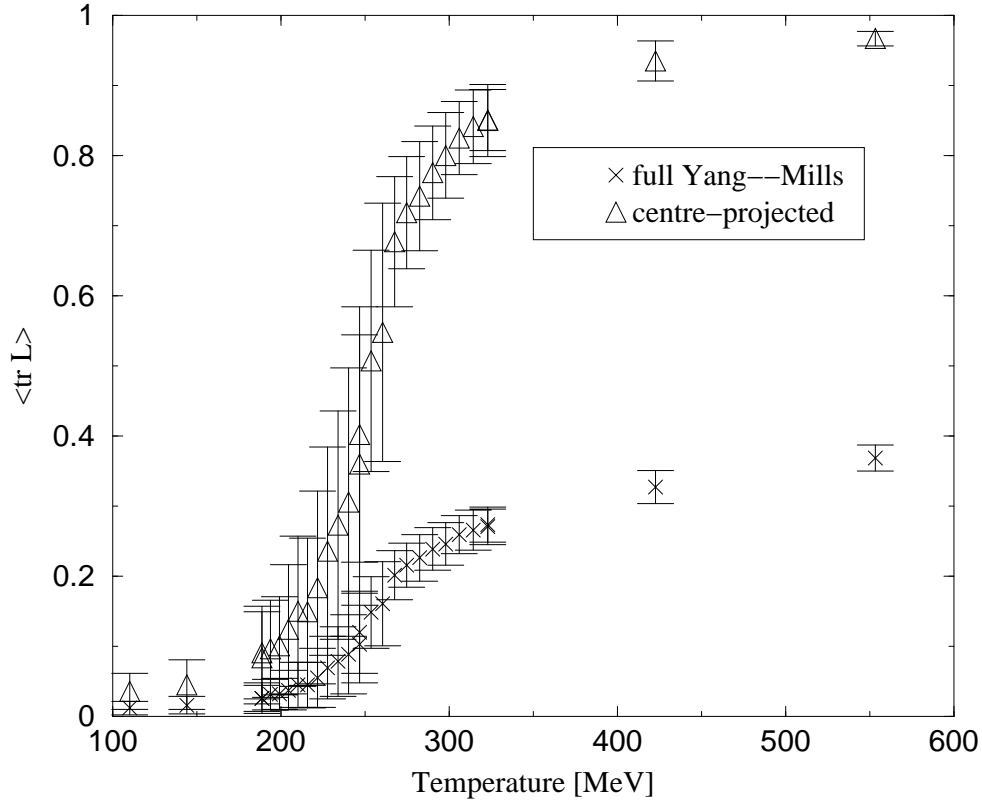


**Figure 15:** The expectation value  $\langle \text{tr } L \rangle$  of the Polyakov loop operator. The triangles show the results for the centre-projected configurations, the crosses for full, unprojected Yang–Mills theory.

The measurements have been performed on a  $(12^3 \times 3)$ -lattice with the bare inverse coupling  $\beta$  varying between  $[2.0, 2.6]$ . By varying  $\beta$  instead of  $N_t$  we have a finer means of tuning the inverse temperature  $1/T = N_t a(\beta)$ .

The renormalization of this measurement has been done by assigning a physical value for the lattice spacing  $a$  through the scale defined by the centre-projected string tension  $\kappa_c = (440 \text{ MeV})^2$ . As can be deduced from figure 15, at a physical temperature  $T_c \approx 260 \text{ MeV}$ ,  $\langle \text{tr } L \rangle$  acquires a non-zero value in an abrupt way. It is, however, not possible to tell from this picture that there exists a phase transition, be it a continuous or a discontinuous one. In order to find an answer to this question, very large lattices have to be taken in order to reduce the finite-size effects, bearing in mind that in a strict sense, there cannot be a phase transition in a finite system.

The actual value of  $\langle \text{tr } L \rangle$  is of course different for the unprojected and the centre-projected case, respectively. However, this is of no importance, as long as it is not zero, and in any formula  $\langle \text{tr } L \rangle$  enters only together with a proportionality constant.

In order to nail down the transition point more precisely, we define it to be the point at which the mean variation  $\Delta \langle \text{tr } L \rangle$  has its maximum.

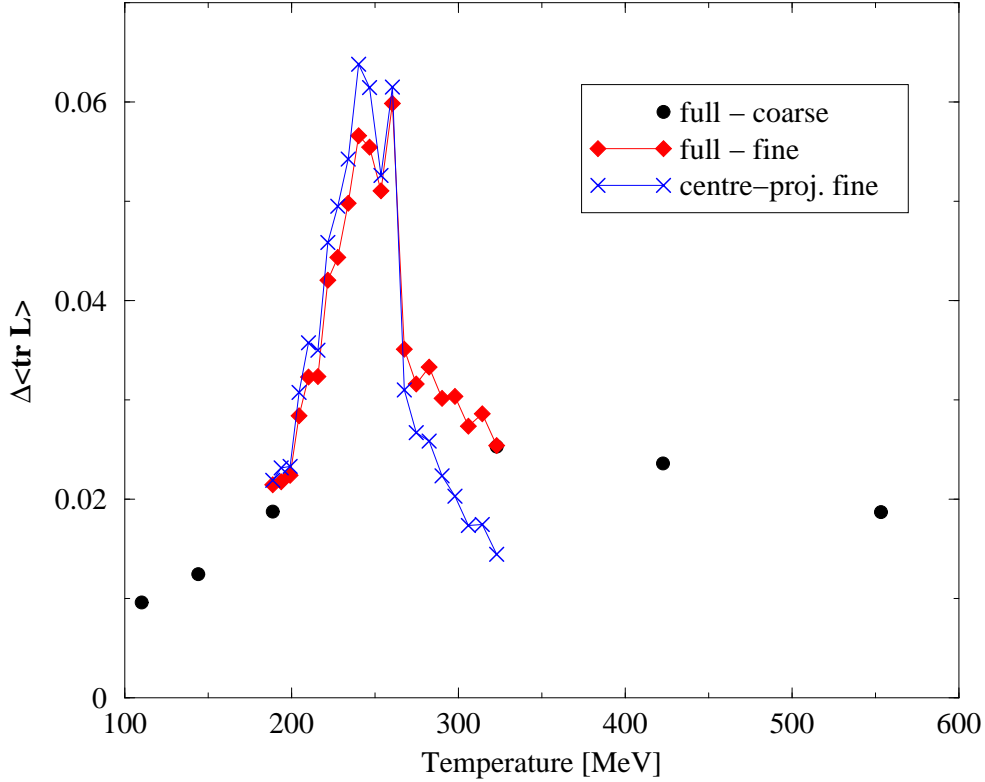


**Figure 16:** The deconfinement phase transition signalled by the mean deviation  $\Delta\langle\text{tr } L\rangle$  of the Polyakov loop.

Figure 16 shows the result for the same measurement as in figure 15. The big filled dots constitute measurement points taken with a coarse increase of  $\beta$  between 2.0 and 2.6, whereas the filled diamonds are taken with a finer stepping of 0.01 between  $\beta = 2.20$  and  $\beta = 2.40$ . The crosses, finally, constitute the measurement points taken on a centre-projected lattice of the same size. The figure clearly shows the transition point to occur at exactly the same temperature for both the centre-projected and the full, unprojected theory, i.e. at about 260 – 270 MeV taking the string tension to be  $\kappa = (440 \text{ MeV})^2$  as a renormalization scale. As the absolute values of the mean deviations  $\Delta\langle\text{tr } L\rangle$  for the centre-projected configuration has been different, the respective graph has been scaled down in  $y$ -direction by a factor of three, which, however, has no interpretative consequences, but only enhances the visual perception. Also, note again that the tick values given for the temperature scale do not have any importance, as an initially arbitrary value for a hypothetical  $SU(2)$  string tension was chosen, the  $\beta$ -dependence of the lattice spacing  $a$  and thus of the temperature  $T$  being extracted from zero temperature string tension measurements.

### 3.4.2 The String Tension at Finite Temperature

Since centre elements of the gauge group commute with each other, the Polyakov loop correlator evaluated with centre-projected configurations is equal to the Wilson loop of identical spatial width and extending along the entire time direction. Therefore, at finite temperature, centre vortices contribute to the static quark potential in the same way as they do at zero temperature. The question to be answered is whether, at finite temperature, vortices still provide the entire long-range static quark potential, i.e. if centre dominance prevails above  $T_c$ , or if other effects become important. This would mean that centre vortices lose their role as relevant infrared collective degrees of freedom.

We have tested this empirically [LTER99]. On the one hand, we have evaluated Polyakov loop correlation function  $\Gamma_c(R) = \langle \text{tr} L(\vec{x}) L^\dagger(\vec{0}) \rangle$  defined in the previous section, using centre-projected links on a  $12^3 \times N_t$  lattice with  $N_t = 5, 6, 7$  for different  $\beta \in [2.26, 2.4]$ , i.e. different inverse temperatures  $1/T = N_t a(\beta)$  were achieved by varying  $\beta$ . The  $\beta$ -dependence of the lattice spacing  $a$  and thus of the temperature  $T$  has been extracted from zero temperature string tension measurements. While these measurements are thus fraught with sizeable uncertainties due to finite-size effects in  $a(\beta)$ , the statistical fluctuations still turn out to be the dominant source of error.

The centre-projected temporal string tension<sup>6</sup>  $\kappa_c(T)$  as a function of the temperature  $T$  was extracted from the above-defined correlation function  $\Gamma_c(R)$  by fitting a linear law to the potential  $V(R)$  of relation (3.54). A Coulomb term is not necessary, since, as will be illustrated by an example below, centre projection removes the perturbative Coulomb part from  $V(R)$  just as at  $T = 0$  [DFGO97, LTER99]. In addition, however, it should be kept in mind that the static quark potential at finite temperature in general also contains a logarithmic dependence on  $R$  [BFH<sup>+</sup>93]. Thus, fitting a purely linear law to  $V(R)$  does not yield the coefficient of the linear term, which, by definition constitutes the string tension  $\kappa_c$ ; instead, one obtains an “effective” string tension, which provides a good parametrization of the long-range static quark potential in the limited range of separations accessible to lattice experiments. Since the accuracy of our measurements is limited, we cannot separate the linear and logarithmic parts of the potential, and we thus quote instead the effective string tension in the sense explained above. In full Yang–Mills theory this quantity is known to behave as follows: it retains its zero-temperature value to within approximately 10 % up to the temperature  $0.8T_c$ , where  $T_c$  is the deconfinement phase transition temperature, and then quickly drops to zero. For the  $SU(2)$  theory, we have only been able to find some rather sparse older data to substantiate this [KL84]. On the other hand, for full  $SU(3)$  QCD including dynamical fermions, new high-precision measurements exist [DKKL99], which corroborate the aforementioned behaviour of the effective string tension.

---

<sup>6</sup>This is the physical string tension.

Our results for the centre-projected theory are displayed in the plot of figure 17a. We find that within the error bars, the centre-projected string tension  $\kappa_c(T)$  reproduces the behaviour of the full string tension  $\kappa(T)$  quoted above. Thus, we observe centre dominance in the long-range part of the static quark potential at finite temperatures  $T < T_c$ , all within the framework of our accuracy and the limited range of separations available.

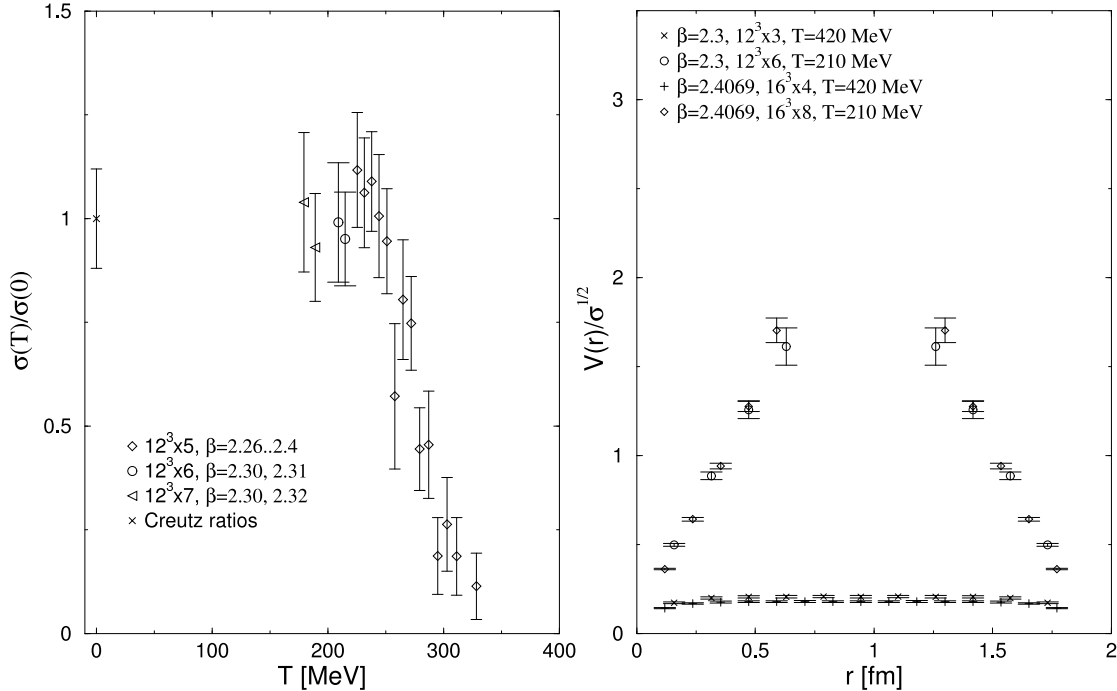


**Figure 17a/b:** *Left:* The centre-projected string tension  $\kappa_c(T)$ ; the four lowest-temperature points on the  $12^3 \times 5$  lattice are measured at  $\beta < 2.3$ , and thus may already be subject to systematic scaling violations. *Right:* The static quark potential at two sample temperatures, as extracted from Polyakov loop correlators in a centre-projected configuration, in units of the zero-temperature string tension. Note that the string tension is denoted by  $\sigma$  in this picture.

Moreover, the centre-projected string tension  $\kappa_c$  signals the deconfinement phase transition to occur at  $T_c = 260 \pm 10$  MeV, where the input scale was the zero temperature centre-projected string tension of  $\kappa_c(0) = (440 \text{ MeV})^2$ . This value is in complete accordance to the results obtained for the transition point by a measurement of the Polyakov loop expectation value  $\langle \text{tr } L \rangle$  in the centre-projected theory in the previous subsection, and in good agreement with the high-precision measurements of [BFH<sup>+</sup>93]. Again it can be seen that the transition to the deconfined phase with a vanishing string tension  $\kappa_c = 0$  is accurately reproduced by the centre-projected theory.

As a further illustration, we also calculated the Polyakov loop correlation function  $\Gamma_c(R)$  defined in the previous section, using in particular  $\beta = 2.3$  for a  $12^3 \times N_t$  lattice, and  $\beta = 2.4069$  for a  $16^3 \times N_t$  lattice, while varying the number of lattice points  $N_t$  in time direction, in order to obtain different inverse temperatures  $1/T = N_t a(\beta)$ . The  $\beta$  values and lattice sizes in both cases correspond to a physical size of the spatial cube of  $L_s = N_s a(\beta) \approx 1.9$  fm, while the lattice spacing changes by a factor  $a(\beta = 2.3)/a(\beta = 2.4069) = \frac{4}{3}$ . This particular choice of parameters allows to test the scaling behaviour of the lattice observables with vastly diminished fluctuations due to finite size effects. Of course, the overall uncertainty in the mass scale remains (cf. the discussion above). In the case of  $\Gamma_c(R)$  this does not turn out to be crucial; the statistical fluctuations are the main source of error. However, when measuring vortex densities (see next subsection), this method substantially improves the observed scaling properties, since the statistical errors are not so dominant.

Using the Monte Carlo results for  $\Gamma_c(R)$  in the centre-projected theory, the static quark potential  $V(R)$  at diverse temperatures both below and above the deconfinement phase transition was extracted (cf. equation (3.54)). Two examples, corresponding to  $N_t = 3.6$  for  $\beta = 2.3$  and  $N_t = 4.8$  for  $\beta = 2.4069$ , are given in figure 17b. For  $T < T_c$ , the potential rises linearly even at small distances. As observed previously for the case of zero temperature (see chapter 2), the centre projection removes the short-range Coulomb interaction.

## 3.5 Vortex Polarisation and Percolation

### 3.5.1 Anisotropy of Vortices

Given this success of the vortex picture, the question of the nature of the deconfinement phase transition in this picture poses itself. One of the simplest hypotheses would appear to be the following: while the centre vortices, by construction, are one lattice spacing thick (*thin vortices*), they represent smooth configurations in the original gauge fields before the centre projection is applied, with a physical thickness in the continuum limit (see chapter 2). Possibly vortices running perpendicularly to the time direction are simply too thick to fit into the space-time manifold of time extent  $1/T$  for  $T > T_c$ . This would mean that the *temporal planar vortex density*  $\rho_t$  vanishes. Vanishing density of such points precludes fluctuations in the number of such points, making an area law decay of  $\Gamma_c(R)$  impossible. In order to test this scenario, we have measured  $\rho_t$  at different temperatures  $T$ . We have taken the same parameter set for  $\beta$  and  $N_t$  as in section 3.4, i.e.  $\beta = 2.3$  for a  $12^3 \times N_t$  lattice and  $\beta = 2.4069$  for a  $16^3 \times N_t$  lattice while varying the extent in time direction  $N_t$  in order to obtain different inverse temperatures  $1/T = N_t a(\beta)$ . The result for the vortex density is shown in figure 18a.



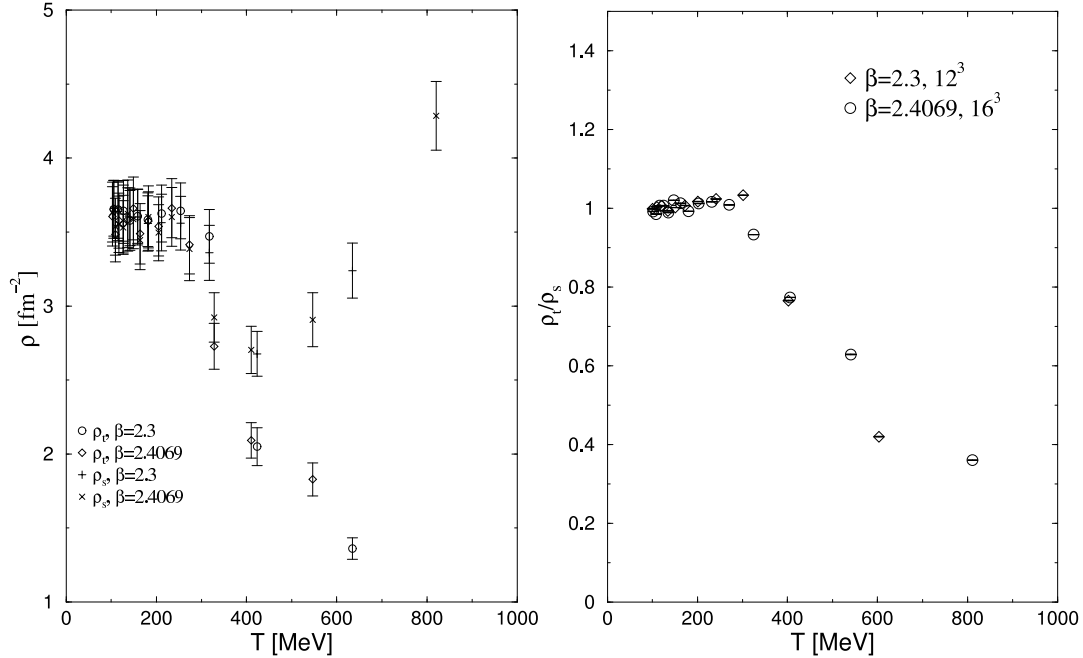


**Figure 18a/b:** *Left:* The spacelike and timelike planar vortex densities  $\rho_s$  and  $\rho_t$ . *Right:* The ratio  $\rho_t/\rho_s$ .

Evidently, while  $\rho_t$  experiences a drop as the temperature increases past  $T_c$ , its behaviour is smooth, and at  $T \approx 2T_c$ , it still retains roughly a third of its zero temperature value. Thus, the hypothesis advanced above of deconfinement being due to a vanishing of  $\rho_t$  was too simplistic. There still exists a non-vanishing temporal planar vortex density above  $T_c$ , but the random character of the distribution of these vortices must disappear for deconfinement to be realized. We will come back to this presently.

Before doing so, note that for comparison, we have also measured the spatial planar vortex density  $\rho_s$ . The ratio  $\rho_t/\rho_s$  is shown in figure 18b. For low temperatures,  $\rho_s$  and  $\rho_t$  coincide, as they must, due to Euclidean  $O(4)$  invariance. At temperatures slightly above  $T_c$ ,  $\rho_s$  decreases along with  $\rho_t$ . At higher temperatures, however,  $\rho_s$  begins to increase. This seems consistent with a simple picture of the spatial intersection points still being distributed randomly, which leads to a linear relation between the spatial planar density  $\rho_s$  and the corresponding spatial string tension  $\kappa_s$  extracted from spacelike Wilson loops (cf. the discussion on the random vortex model in chapter 2, in especial equation (2.32)). This spatial string tension in turn is known to behave like  $\sqrt{\kappa_s} \sim g^2(T)T$  for  $T \geq 2T_c$ , according to arguments based on the method of *dimensional reduction* [AP81], and their verification in lattice experiments [BFH<sup>+</sup>93]. As mentioned above, in the case of the temporal planar vortex density  $\rho_t$ , this simple random picture must by contrast become invalid above  $T_c$ .

We have learned now that it is necessary to inspect more closely the properties of vortices piercing the area spanned by the two Polyakov loops entering the

correlation function  $\Gamma_c(R)$ . A necessary condition for an area law suppression of the loop correlator expectation value is an ever better mutual cancellation, as the area spanned by the Polyakov loops is increased, between configurations where the area is pierced an even or an odd number of times by vortices, respectively. We have therefore measured the probabilities of these two cases as a function of the temperature for an area of spatial width 0.9 fm. For  $\beta = 2.3$ , this corresponds to 6 lattice spacings in a  $12^3 \times N_t$  lattice, whereas for  $\beta = 2.4069$ , it corresponds to 8 lattice spacings in a  $16^3 \times N_t$ , i.e. in both cases the distance between the Polyakov loops is half the linear extent of the lattice universe. The result of these Monte Carlo experiments is shown in figure 19, which displays the fraction  $p(T)$  of cases where an area specified as above is pierced an even number of times by vortices. This quantity exhibits a sharp transition at the deconfinement temperature  $T_c \equiv 280$  MeV. If  $p \not\rightarrow \frac{1}{2}$  for large areas, there cannot be an area law decay of the Polyakov loop correlation function  $\Gamma_c(R)$  and therefore deconfinement occurs.

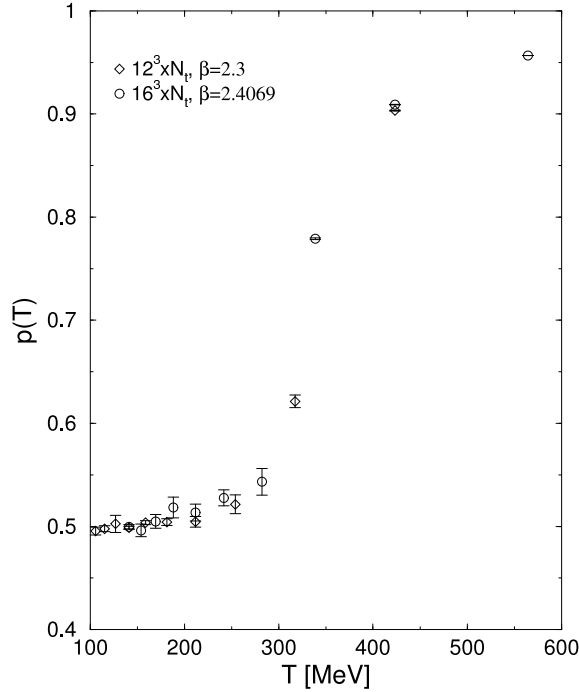


**Figure 19:** Fraction  $p$  of cases in which an area spanned by two Polyakov loops is pierced by vortices an even number of times, as a function of the temperature  $T$ .

The clear signal of the deconfinement transition exhibited by the ratio  $p$  above is not surprising, since it constitutes nothing but a slightly more physical variant of the usual order parameter given by the Polyakov loop expectation value  $\langle \text{tr } L \rangle$ . The centre-projected Polyakov loop correlation function  $\Gamma_c(R)$  is given in terms of  $p$  as follows:

$$\langle \text{tr } L(\vec{x}) L^\dagger(\vec{y}) \rangle = p \cdot 1 + (1 - p) \cdot (-1) = 2p - 1. \quad (3.55)$$

Thus,  $p$  corresponds, up to a rescaling and a shift, to the correlation function  $\Gamma_c(R)$  itself.

Therefore, in defining the probability  $p$ , we have not really introduced a new, distinct, order parameter for the deconfinement phase transition. Rather, the vortex picture simply provides an alternative language for describing  $\Gamma_c(R)$  by characterizing the manner in which vortex intersection points occur in the area spanned by the two Polyakov loops. The deconfinement transition occurs when the intersection points begin to show up predominantly in pairs of finite separation above  $T_c$ , whereas they are distributed randomly below  $T_c$ .

### 3.5.2 Vortex Clustering and Percolation

As we have just seen, there exists a substantially non-zero temporal density of vortex intersection points. Therefore, deconfinement must be due more specifically to a correlation between these intersection points, such that the distribution of these points ceases to be sufficiently random to generate an area law. It shall now shortly be motivated that a correlation conducive to confinement occurs if vortices only tend to form clusters smaller than some maximal size, i.e. if they do not tend to *percolate*.

Consider a lattice universe of some finite extent, and let us assume that the vortex intersection points come in pairs at most a distance  $d$  apart. Then the only pairs that can contribute a factor of  $(-1)$  to a planar Wilson loop are those whose midpoints lie in a strip of width  $d$  centred on the trajectory of the loop.

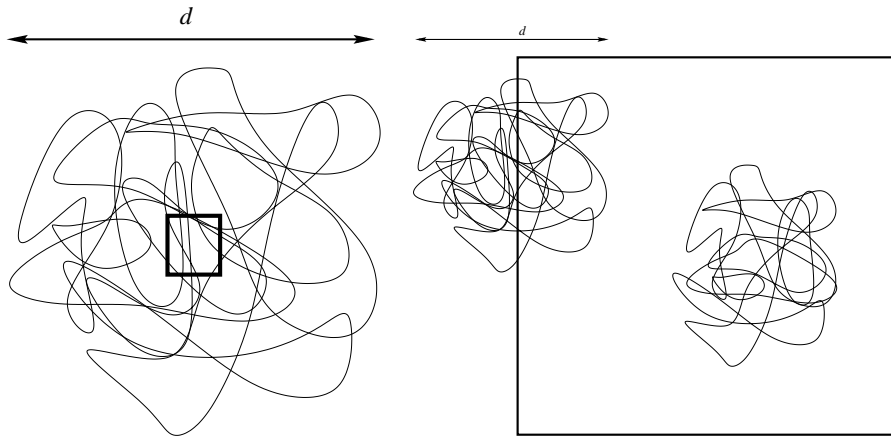


**Figure 20:** A vortex cluster of extension  $d$  defines the maximum distance of a pair of intersection points. The thick-edged square is a Wilson loop. *Left:* In a vortex percolation phase, the whole Wilson loop is pierced more or less with equal probability. *Right:* In a non-percolating phase, only the vortex clusters distributed near the perimeter of the Wilson loop contribute a factor of  $(-1)$  with a probability  $p$ .

Let  $p$  be the probability that a pair which satisfies this condition actually does contribute  $(-1)$ . This probability is an appropriate average over the distances of the midpoints of the pairs from the Wilson loop, their angular orientations, the distribution of separations between the points making up the pairs, and the local geometry of the Wilson loop up to the scale  $d$ . The probability  $p$  does, however, not depend on the macroscopic extent of the Wilson loop. A pair which is placed at random on a slice of the universe of area  $L^2$  contributes a factor of  $(-1)$  to the Wilson loop with the probability  $pA/L^2$ , where  $A$  is the area of the above-defined strip. To leading order,  $A = Pd$ , with  $P$  being the perimeter of the Wilson loop.<sup>7</sup> Now, placing  $N$  pairs on a slice of the universe of area  $L^2$  at random, the probability that  $n$  of them contribute a factor of  $(-1)$  to the Wilson loop is

$$P_N(n) = \binom{N}{n} \left( \frac{pPd}{L^2} \right)^n \left( 1 - \frac{pPd}{L^2} \right)^{N-n}, \quad (3.56)$$

and, consequently, the expectation value  $\langle \text{tr } W \rangle$  of the Wilson loop in the limit of large lattice sizes is

$$\langle \text{tr } W \rangle = \sum_{n=0}^N (-1)^n P_N(n) \xrightarrow{N \rightarrow \infty} \exp(-\rho p P d), \quad (3.57)$$

where  $\rho a^2 = 2N/L^2$  is the planar vortex density. One thus observes a perimeter law if the space-time extent of vortices or vortex networks is bounded. For confinement in order to be realized, the vortex clusters must extend over the entire space-time manifold, in other words, *percolation* must take place. Conversely, therefore, in the deconfinement phase, vortices must cease to be of arbitrary length, in a sense to be made more precise below, within this hypothetical picture. The main result of the following exposition is that this seems indeed to be the case, implying that the deconfinement phase transition can be characterized as a *vortex percolation transition*. In order to test whether this type of mechanism is at work, we investigated the extent of the vortex clusters [ELRT].

Vortices constitute closed two-dimensional surfaces in four space-time dimensions. Taking a fixed time slice or space slice, they are one-dimensional loops. In the following, specifically the size of vortex loop clusters in either time or space slices will be investigated. In this way, the relevant information is exhibited more clearly than by considering the full two-dimensional surfaces in four-dimensional space-time.

Given a centre-projected lattice configuration  $\{z_\mu(x)\}$  in a three-dimensional slice, the corresponding vortices can be constructed on the dual lattice as follows: as a definite example, consider a fixed time slice. Then the vortices are represented by lines made up of links on the dual lattice.<sup>8</sup> Particularly, consider

<sup>7</sup>Subleading corrections are induced by the local loop geometry.

<sup>8</sup>The definition of the objects dual to one another is of course dependent on the dimension

a plaquette on the original lattice, lying e.g. in the  $z = z_0$ -plane, and extending from  $x_0$  to  $x_0 + a$  and from  $y_0$  to  $y_0 + a$ . By definition, if the links making up this plaquette multiply to  $-1$ , then a thin vortex pierces that plaquette. This means that a certain link on the dual lattice is part of a vortex, namely the one connecting the dual lattice points  $(x_0 + \frac{a}{2}, y_0 + \frac{a}{2}, z_0 - \frac{a}{2})$  and  $(x_0 + \frac{a}{2}, y_0 + \frac{a}{2}, z_0 + \frac{a}{2})$ .

Having constructed the vortex configuration on the dual lattice, one can proceed to define the vortex clusters. Starting from that link, one tests which adjacent links, i.e. links which share a dual lattice site with the first link, are also part of the vortex. This is repeated with all new members of the cluster until all links making up the cluster have been found. This way, it is possible to separate the different vortex clusters.

Given the vortex clusters, their extension can be measured. Consider all pairs of links in a cluster and evaluate the distance in between each of the pairs. The maximal such distance defines the extension of that cluster. In figures 21–24, histograms are displayed, in which, for every cluster, the frequency distribution of the total number of constituent links is shown. The histograms are normalized such that the integral over the distribution function gives unity.

Constructed this way, the histograms give a very transparent characterization of typical vortex configurations. The content of each bin represents the percentage of the total vortex length in the configurations, i.e. the vortex material available, which is organized into clusters of the corresponding extension. Accordingly, these distributions will be referred to as *vortex material distributions* in the following. In a percolating phase, the vortex material is peaked at the largest extension possible in a lattice universe under consideration.<sup>9</sup> In a non-percolating phase, the vortex material distribution is peaked at a finite extension independent of the size of the lattice universe. Figures 21–23 pertain to space slices, whereas figure 24 further below summarizes analogous results for time slices. The extension, given on the horizontal axis, is measured in units of the maximal extension possible, namely  $\sqrt{2 \cdot (12/2)^2 + (N_t/2)^2}$  lattice spacings on a space slice of the given lattice.

---

$D$  of the embedding manifold. In our case,  $D = 3$  as we consider a three-dimensional time slice as our surrounding space.

<sup>9</sup>Note that, due to periodic boundary conditions, this maximal extension in a  $N_s \times N_s \times N_t$  space slice of the four-dimensional space-time lattice, for example, is  $\sqrt{(N_s/2)^2 + (N_s/2)^2 + (N_t/2)^2}$  lattice spacings.

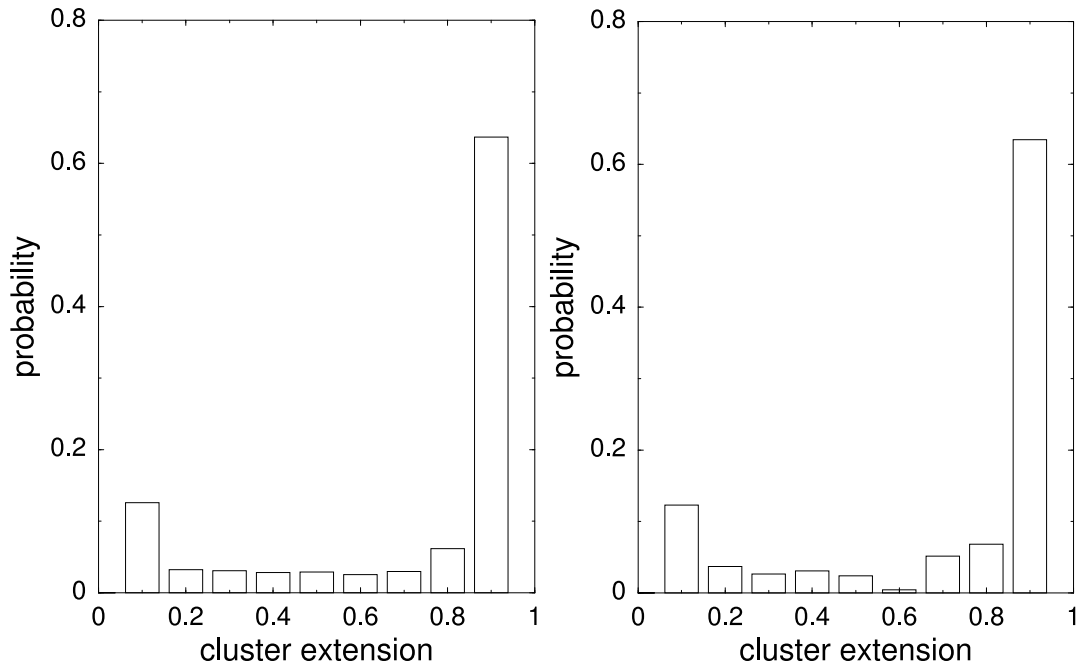


**Figure 21a/b:** *Left:*  $12^3 \times 8$  lattice at  $\beta = 2.4$ , equivalent to a temperature of  $T = 0.7T_c$ . *Right:*  $12^3 \times 7$  lattice at  $\beta = 2.4$ , equivalent to  $T = 0.8T_c$ .

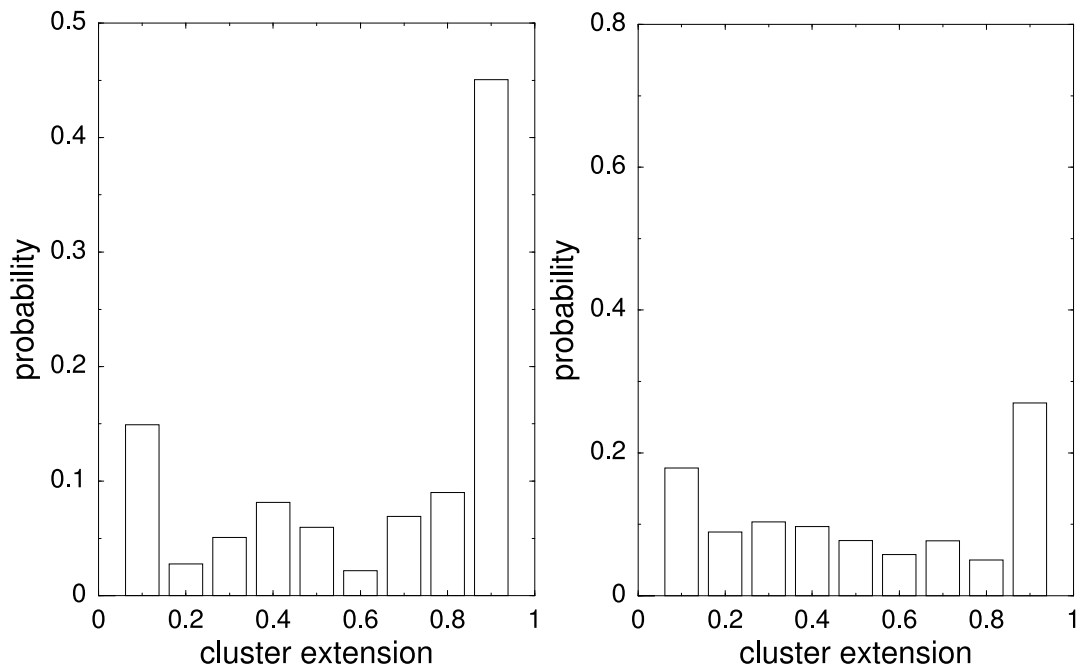


**Figure 22a/b:** *Left:*  $12^3 \times 6$  lattice at  $\beta = 2.4$ , equivalent to  $T = 0.9T_c$ . *Right:*  $12^3 \times 5$  lattice at  $\beta = 2.4$ , equivalent to  $T = 1.1T_c$ .

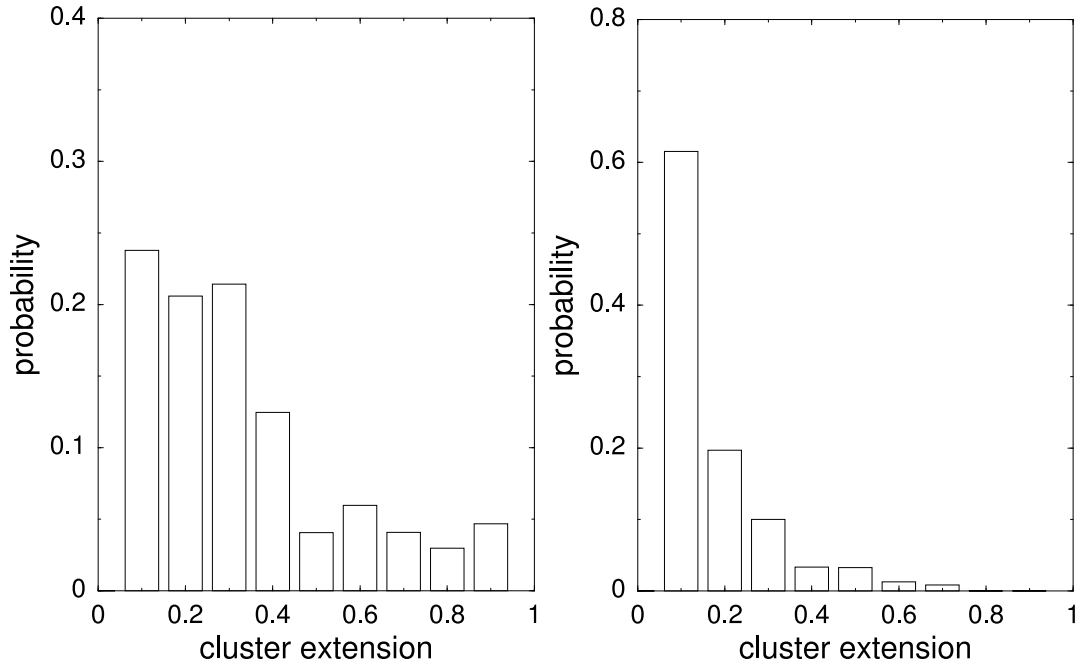


**Figure 23a/b:** *Left:*  $12^3 \times 4$  lattice at  $\beta = 2.4$ , equivalent to  $T = 1.4T_c$ .  
*Right:*  $12^3 \times 3$  lattice at  $\beta = 2.4$ , equivalent to  $T = 1.8T_c$ .

In space slices of the lattice universe, one observes a transition from a percolating to a non-percolating phase at the Yang–Mills deconfinement phase transition. Below  $T_c$ , the vortex material distribution is strongly peaked at the maximal extension possible; when the temperature rises above  $T_c$ , however, the distribution becomes concentrated at short lengths. The behaviour in the vicinity of the deconfinement temperature  $T_c$  deserves a more detailed discussion. While the contents of the bin of maximal extension fall sharply between  $T = 0.8T_c$  and  $T = 1.1T_c$ , a residual one quarter of vortex material remains concentrated in loops of maximal extension at the temperature identified as  $T = 1.1T_c$ . This is too large a proportion to let pass by without further consideration. In [ELRT], we have repeated the measurement at  $T = 1.1T_c$  on a  $16^3 \times 3$  lattice, and again did not find a depletion of the bin of maximal extension. On the other hand, one should be aware that there is a considerable uncertainty — of the order of 10 % — in the overall physical scale in these lattice experiments, affecting in particular the identification of the deconfinement temperature  $T_c$  itself, as has already been discussed in detail earlier in this chapter. At the present level of accuracy,  $T = 1.1T_c$  cannot be considered significantly separated from  $T_c$ ; one cannot state with confidence that the measurement formally identified with a temperature  $T = 1.1T_c$  must unambiguously be associated with the deconfinement phase. Note that also in standard string tension measurements via the Polaykov loop correlation function  $\Gamma(R)$ , one does not attain a sharper signal of the deconfinement phase transition if one uses comparable lattice sizes and statistics. Indeed, earlier in

the last section, we still extracted a string tension of about 10 % of the zero-temperature value at the temperature formally identified as  $T = 1.1T_c$ .<sup>10</sup>

In balance, it is argued that a percolation transition in space slices occurs together with the deconfinement phase transition, both in view of the strong heuristic arguments connecting the two phenomena in the centre vortex picture, and in view of the drastic change in the vortex material distribution between  $T = 0.8T_c$  and  $T = 1.1T_c$ . The latter suggests that the vortex material distribution can in practice be used as an alternative order parameter for the deconfinement phase transition. When the vortices rearrange at the transition temperature to form a non-percolating phase, the vortex intersection points defined above occur in pairs less than a maximal distance  $d$  apart. This leads to a perimeter law for the Polyakov loop correlation function, and therefore to deconfinement.

Consider now by contrast the vortex material distribution obtained in time slices.

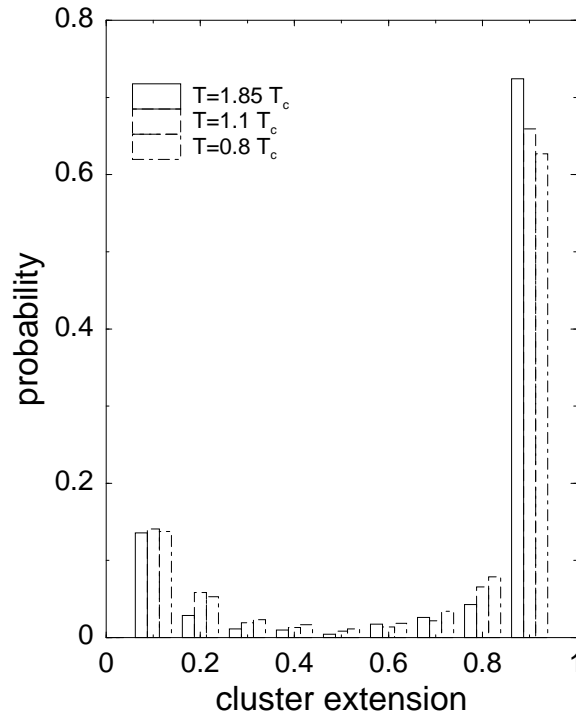


**Figure 24:** Vortex material distribution measured in time slices of  $12^3 \times N_t$  lattices at  $\beta = 2.4$ . Bins corresponding to three different temperatures are shown simultaneously:  $N_t = 3$ , equivalent to  $T = 1.85T_c$ ,  $N_t = 5$ , equivalent to  $T = 1.1T_c$ , and  $N_t = 7$ , equivalent to  $T = 0.8T_c$ .

<sup>10</sup>Clearly, in all measurements at finite temperature performed on a finite-sized lattice, discretization effects do not permit a phase transition to be realized in a strict sense. A theoretical discontinuity in a plot of the Polyakov loop expectation value  $\langle \text{tr } L \rangle$ , for instance, will always be smeared to a continuous graph.



According to figure 24, this distribution is strongly peaked at the maximal possible extension at all temperatures, even above  $T_c$ . Thus, vortex line clusters in time slices always percolate; there is not any marked change in their properties as the temperature rises above  $T_c$ . Note that this does not entail any consequences for the behaviour of the Polyakov loop correlation function  $\Gamma_c(R)$ , since Polyakov loops do not lie within time slices. However, the persistence of vortex percolation into the deconfined phase when time slices are considered represents one way of understanding the persistence of the spatial string tension  $\kappa_s$  above  $T_c$ . Given percolation, it seems plausible that intersection points of vortices with spatial Wilson loops continue to occur sufficiently randomly to generate an area law.

There is another, complementary way of understanding the spatial string tension  $\kappa_s$ , which will be discussed in detail in the next subsection.

Moreover, note that figures 21–24 together imply that the vortices, regarded as two-dimensional surfaces in four-dimensional space-time, percolate both in the confinement and in the deconfinement phase, albeit in an anisotropic way. Only by considering a three-dimensional slice does one filter out the percolation transition in the topology of vortex configurations. It should be emphasized that the percolation of the two-dimensional vortex surfaces in four-dimensional space-time in the deconfinement phase does not negate the heuristic picture of deconfinement put forward above. Given that vortex line clusters in space slices cease to percolate in the deconfined phase, intersection points of vortices with timelike planes necessarily come in pairs less than a maximal distance  $d$  apart, regardless of whether the different vortex line clusters do ultimately connect if one follows their world sheets into the additional spatial dimension. It is the pair correlation of the intersection points which induces the deconfinement phase transition.

### 3.5.3 Winding Vortices in the Deconfinement Phase

In order to gain a more detailed picture of the deconfinement phase, it is useful to carry out the following analysis. Consider again the space slice of the lattice universe, in which vortex clusters have a short extension above  $T_c$ . In particular, consider lattices of time extent  $N_t \cdot a$  with odd  $N_t$ ,  $a$  being the lattice spacing; in the following numerical experiment  $N_t = 3$ . On such a lattice, the vortex material distribution is measured analogously to the the measurements above, but with one slight modification: the bins of the histograms are not defined by the cluster extension, but simply by the number of dual lattice links contained in the clusters.

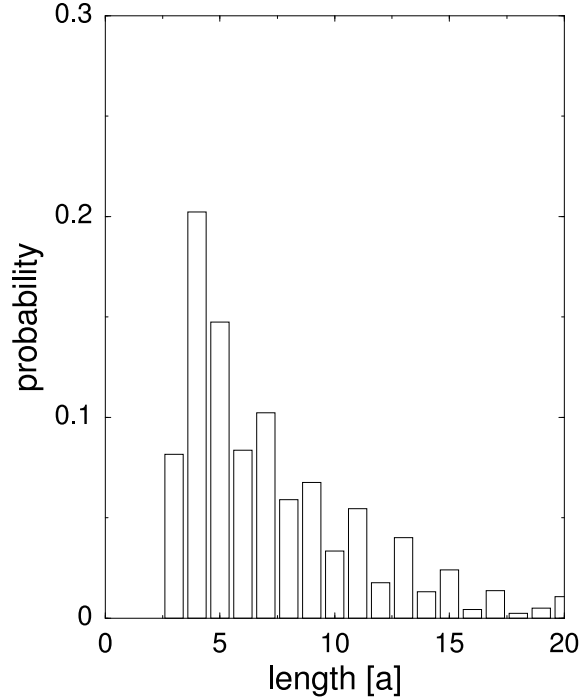


**Figure 25:** Vortex material distribution in space slices as a function of the total vortex line length contained in the clusters.  $\beta = 2.4$  which is equivalent to a temperature  $T = 1.85T_c$ . There is a residual but insignificant proportion of vortex clusters containing more than 20 dual lattice links not displayed in the plot.

It turns out that, in the deconfinement phase, specifically at  $T = 1.85T_c$ , roughly 55 % of the vortex material is concentrated in clusters made up of an odd number of links, cf. figure 25. On a lattice with  $N_t = 3$ , these are necessarily vortex loops which wind around the lattice in time direction by virtue of the periodic boundary conditions, where the loops containing an odd number of links larger than 3 exhibit residual transverse fluctuations in the spatial directions, as also visualized in figure 26 below.

One thus obtains a quite specific characterization of the short vortices appearing in the deconfinement regime. This phase can evidently be visualized largely in terms of short winding vortex loops with residual transverse fluctuations if one considers a space slice of the lattice universe. Note that this picture also explains the partial vortex polarization observed in density measurements, shown in 3.5.1.

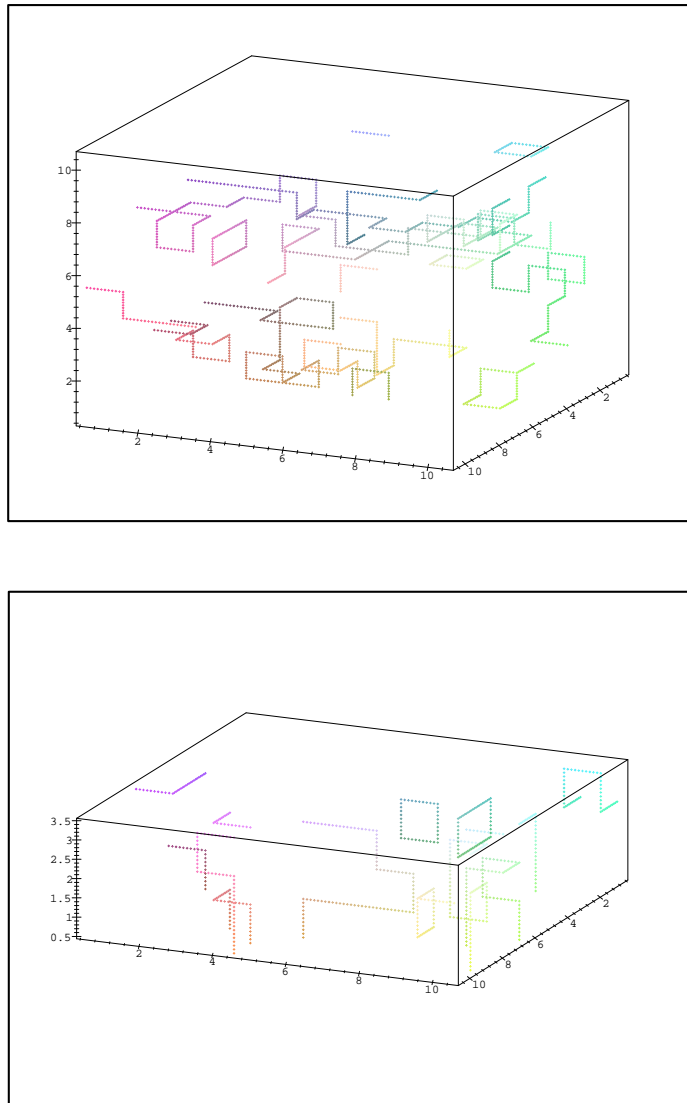


**Figure 26:** Visualization of typical vortex configurations. *Upper:* On a symmetric lattice, which corresponds to zero temperature. *Lower:* On an asymmetric lattice, which corresponds to a finite temperature.



# Chapter 4

## Conclusions and Outlook

On the basis of the measurements presented in this work, a detailed description of the confinement and deconfinement phases of Yang–Mills theory within the framework of centre vortices emerges.

In the confinement phase, vortex line clusters in space slices of the lattice universe percolate. This allows intersection points of vortices with planes bounded by two Polyakov loops to occur sufficiently randomly to generate an area law. By contrast, in the deconfinement phase, typical vortex configurations in space slices of the lattice universe are characterized by short vortex loops, which are winding to a large part in the Euclidean time direction. This causes intersection points of vortices with planes containing Polyakov loop correlators to occur in pairs less than a maximal distance  $d$  apart, which leads to a perimeter law. Simple analytical model arguments clarifying the emergence of this qualitative difference have been presented. In summary, the deconfinement phase transition in the vortex picture can thus be understood as a transition from a percolating to a non-percolating phase.

It should be emphasized that the percolation properties of vortices focussed on in 3.5.2 are more stringently related to confinement than the polarization properties. There is not any a priori logical connection between the observed partial vortex polarization by itself and deconfinement. On the one hand, even in presence of a significant polarization, confinement would persist as long as the vortex loops retain an arbitrarily large length, namely by winding sufficiently often around the Euclidean time direction. On the other hand, even in an ensemble without any polarization, deconfinement will occur if the vortices are organized into many small isolated clusters. Therefore, vortex polarization should be viewed more as an accompanying effect than the direct cause of deconfinement. Of course, a correlation between the absence of percolation in space slices of the lattice universe and vortex polarization is not surprising. If the fluctuations of the vortex loops in spatial directions are curtailed, e.g. due to a phase containing many short vortices winding in the time direction becoming favoured, then clearly the connectivity of vortex clusters in the spatial directions is reduced, and

they may cease to percolate. In this sense, polarization indirectly can facilitate deconfinement. However, the percolation concept is related much more directly, and with much less ambiguity, to the question of confinement. Since the Wilson loop expectation value should be independent of the choice of area which one may regard it to span, it is conceptually sounder not to consider densities occurring in such areas, but global properties of the vortices such as their linking number with the Wilson loop. The probability of the occurrence of a particular linking number is strongly influenced by the connectivity of the vortex networks. Correspondingly, there is a clear signal of the phase transition in the vortex material distributions displayed in 3.5.2; these quantities can be used as alternative order parameters for the phase transition. By contrast, the vortex densities seem to behave smoothly across the deconfinement phase transition as shown in 3.5.1.

Turning to the spatial string tension, there are two complementary ways to qualitatively account for its persistence in the deconfinement phase of Yang–Mills theory. If one considers a time slice of the lattice universe, the associated vortex line configurations do not display any marked change of their clustering properties across the deconfinement transition. Even in the deconfinement phase, vortex loops in time slices percolate. In view of this, it seems plausible that intersection points of vortices with spatial Wilson loops continue to occur sufficiently randomly to generate an area law. It should be noted, however, that this percolation is qualitatively different from the one observed in the confinement phase in that it only occurs in the three space dimensions, whereas the configurations are relatively weakly varying in the Euclidean time direction. In other words, in the deconfinement phase, one finds a dimensionally reduced percolation phenomenon only visible either in the whole four-dimensional space-time manifold, or in three-dimensional time slices thereof.

On the other hand, if one considers space slices of the lattice universe, the deconfinement phase is characterized largely by short vortex loops winding around in time direction. However, these short vortices can pierce the area spanned by a large spatial Wilson loop an odd number of times, even far from its perimeter. This should be contrasted with the picture one obtains for the Polyakov loop correlation function  $\Gamma_c(R)$ . There, shortness of vortices implies that their intersection points with the plane containing the Polyakov loop correlator occur in pairs less than a maximal distance  $d$  apart, leading to a perimeter law behaviour of  $\Gamma_c(R)$ , and therefore to deconfinement. For spatial Wilson loops, this mechanism is inoperative due to the existence of the winding vortices. On the contrary, if one assumes the locations of the various winding vortices to be uncorrelated, one obtains precisely the heuristic model of 2.5, in which vortex intersection points are distributed randomly in the plane containing the Wilson loop, leading to an area law. Therefore, finite length vortex loops do not contradict the existence of a spatial string tension.

Of course, there is not any reason to expect the locations of the winding vortices to be completely uncorrelated in the high-temperature Yang–Mills ensemble.

In fact, comparing the values for the spatial string tension  $\kappa_s$  from [BFH<sup>+</sup>93] and the relevant density  $\rho_s$  of vortex intersection points in planes extending in two spatial directions as in 3.5.1, the ratio  $\kappa_s/\rho_s$  acquires a value of about  $\kappa_s/\rho_s \approx 3$  at  $T \approx 2T_c$ . This should be contrasted with the value  $\kappa = 2\rho$  obtained in the random vortex model discussed in 2.5. If one further takes into account that a sizeable part of  $\rho_s$  is still furnished by non-winding vortex loops, then one should actually use the density  $\rho'_s < \rho_s$  corresponding to winding vortices only in the above consideration. This yields an even larger ratio  $\kappa_s/\rho'_s$ . Therefore, the winding vortices in the deconfinement phase seem to be subject to sizeable correlations.

While the relevant characteristics of the vortex configurations in the different regimes have been described in detail in this work, the present understanding of the underlying dynamics in the vortex picture is still tenuous. There are, however, some indications that the deconfining percolation transition can be understood in terms of simple entropy considerations. Increasing the temperature implies shortening the Euclidean time direction of the lattice universe. This means that the number of possible percolating vortex configurations decreases simply due to the reduction of space-time volume. At the same time as the number of possible percolating vortex clusters is reduced, the number of available short vortex configurations is enhanced by the emergence of a new class of short vortices at finite temperatures, namely the vortices winding in time direction. In view of this, it seems plausible that a transition to a non-percolating phase is facilitated as the temperature is raised. This picture ought to be compared with the analytical calculations performed for the  $\mathbb{Z}_2$  Wegner model [Weg71], or for the Mack–Petkova model [MP79, MP80, MP82a] in the strong coupling limit, as indicated in 2.2, which led to similar results.

There are two pieces of evidence supporting this explanation, one of which has already been given above. Namely, the deconfinement phase indeed contains a large proportion of short winding vortices. More than half of the vortex material is transferred to the newly available class of short winding vortices in the deconfinement phase. The second piece of evidence is related to the behaviour of stiff random surfaces in four space-time dimensions [Eng]. This model assumes that the vortices are random surfaces associated with a certain action cost per unit area and a penalty for curvature of the vortex surface. By construction, evaluating the partition function of this model simply corresponds to counting the available vortex configurations under certain constraints imposed by the action. The cost per surface area effectively imposes a certain mean density of vortices, while the curvature penalty imposes an ultraviolet cut-off on the fluctuations of the vortex surfaces. Beyond this, no further dynamical information enters. It turns out that already this simple model generates a percolation phase transition analogous to the one observed here for the  $\mathcal{P}$ -vortices of centre-projected Yang–Mills theory. This suggests that the deconfining percolation transition of centre-projected Yang–Mills theory can be understood in similarly simple terms,

without any need for detailed assumptions about the form of the full centre vortex effective action.

To sum up, centre projection has provided a means for reducing the degrees of freedom of  $SU(N)$  Yang–Mills theory in a way that the infrared behaviour of the full, unprojected Yang–Mills theory is reproduced to a high degree. In this work, Monte Carlo measurements have been presented for the  $SU(2)$  case, but first calculations have already been performed for the  $SU(3)$  gauge group in [FGOb]. The resulting  $\mathbb{Z}_N$  theories bear many analogues to various  $\mathbb{Z}_N$  models which admit analytical calculations. The centre vortex theory, however, has the unique property to exhibit perturbative scaling behaviour. This is a necessary condition for the theory to possess a continuum limit. But it must be borne in mind that the additional condition of the spreading of the magnetic flux, which has been realized very early already, is crucial for the formulation of a continuum theory. To date, however, the continuum structure of these “thick vortices” is not known. Indications exist that already at the level of the maximally abelian gauge on the lattice, a rudimentary vortex structure may exist [Ten]. Also, there is a high degree of correlation between the localizations of magnetic monopoles in the maximally abelian gauge and centre vortices in the maximal centre gauge, a fact which has already been mentioned in [DFG<sup>+</sup>98], and realized to hold even above the deconfinement phase transition [Ten].

Very recently, an investigation into the topology of the two-dimensional vortex surfaces in four-dimensional space-time has been reported in [BFGO], including the case of finite temperatures. The investigation focusses on properties such as orientability and genus of the vortex surfaces, and changes in these characteristics as one passes the phase transition. At the moment, developments are being undertaken to construct a continuum vortex theory merging some of the aspects considered on centre-projected lattice Yang–Mills theory [ERb, ERa]. As a part of these considerations, the construction of a non-vanishing topological charge by means of vortices and magnetic monopoles alone is performed. A fractional topological charge is induced by the intersection of vortex sheets and magnetic monopole world-lines. The existence of fractional topological charge in configurations that are singular nature in two-dimensional hypersurfaces has already been shown in [FHP81, FHP82], but the connection between these two approaches is as yet totally unclear.



# Appendix A

## Useful Formulae for $SU(N)$ Gauge Groups

In the following,  $\tau_i$  are the generators of the  $SU(N)$  gauge group.

$$[\tau_a, \tau_b] = if_{abc}\tau_c \quad (\text{A.1})$$

$$\{\tau_a, \tau_b\} = \frac{1}{N}\delta_{ab}\mathbb{1} + d_{abc}\tau_c \quad (\text{fund. repr.}) \quad (\text{A.2})$$

$$\frac{1}{2}if_{abc} = \text{tr}([\tau_a, \tau_b]\tau_c) \quad (\text{A.3})$$

$$\frac{1}{2}d_{abc} = \text{tr}(\{\tau_a, \tau_b\}\tau_c) \quad (\text{fund. repr.}) \quad (\text{A.4})$$

Trace rules for fundamental representation:

$$\text{tr}[\tau_a] = 0 \quad (\text{A.5})$$

$$\text{tr}[\tau_a\tau_b] = \frac{1}{2}\delta_{ab} \quad (\text{A.6})$$

$$\text{tr}[\tau_a\tau_b\tau_c] = \frac{1}{4}(d_{abc} + if_{abc}) \quad (\text{A.7})$$

$$\text{tr}[\tau_a\tau_b\tau_c\tau_d] = \frac{1}{4N}\delta_{ab}\delta_{cd} + \frac{1}{8}(d_{abe} + if_{abe})(d_{cde} + if_{cde}) \quad (\text{A.8})$$

Trace rules for adjoint representation ( $(\tau_a)_{bc} = -if_{abc}$ ):

$$\text{tr}[\tau_a] = 0 \quad (\text{A.9})$$

$$\text{tr}[\tau_a\tau_b] = N\delta_{ab} \quad (\text{A.10})$$

$$\text{tr}[\tau_a\tau_b\tau_c] = \frac{N}{2}if_{abc} \quad (\text{A.11})$$

$$\text{tr}[\tau_a\tau_b\tau_c\tau_d] = \delta_{ab}\delta_{cd} + \delta_{ad}\delta_{bc} + \frac{N}{4}(d_{abe}d_{cde} - d_{ace}d_{bde} + d_{ade}d_{bce}) \quad (\text{A.12})$$

Sum rules:

$$d_{abc}d_{abc} = \left(N - \frac{4}{N}\right)(N^2 - 1) \quad (\text{A.13})$$

$$f_{abc}f_{abc} = N(N^2 - 1) \quad (\text{A.14})$$

$$d_{abb} = 0 \quad (\text{A.15})$$

$$d_{abc}d_{dbc} = \left(N - \frac{4}{N}\right)\delta_{ad} \quad (\text{A.16})$$

$$f_{abc}f_{dbc} = N\delta_{ad} \quad (\text{A.17})$$

$$f_{abr}f_{cdr} = \frac{2}{N}(\delta_{ac}\delta_{bd} - \delta_{ad}\delta_{bc}) \\ + d_{acr}d_{dbr} - d_{adr}d_{bcr} \quad (\text{A.18})$$

$$f_{ade}f_{bef}f_{cfd} = \frac{N}{2}f_{abc} \quad (\text{A.19})$$

$$f_{abr}f_{cdr} + f_{acr}f_{dbr} + f_{adr}f_{bcr} = 0 \quad (\text{A.20})$$

$$f_{abr}d_{cdr} + f_{acr}d_{dbr} + f_{adr}d_{bcr} = 0 \quad (\text{A.21})$$

Explicit values for structure constants of the  $\mathfrak{su}(3)$  algebra:

$a$	$b$	$c$	$2f_{abc}$	$a$	$b$	$c$	$2d_{abc}$	$a$	$b$	$c$	$2d_{abc}$
1	2	3	2	1	1	8	$2/\sqrt{3}$	3	6	6	-1
1	4	7	1	1	4	6	1	3	7	7	-1
1	5	6	-1	1	5	7	1	4	4	8	$-1/\sqrt{3}$
2	4	6	1	2	2	8	$2/\sqrt{3}$	5	5	8	$-1/\sqrt{3}$
2	5	7	1	2	4	7	-1	6	6	8	$-1/\sqrt{3}$
3	4	5	1	2	5	6	1	7	7	8	$-1/\sqrt{3}$
3	6	7	-1	3	3	8	$2/\sqrt{3}$	8	8	8	$-2/\sqrt{3}$
4	5	8	$\sqrt{3}$	3	4	4	1				
6	7	8	$\sqrt{3}$	3	5	5	1				

# Bibliography

- [Ami84] D. J. Amit. *Field Theory, the Renormalization Group, and Critical Phenomena*. World Scientific, Singapore, 2nd edition, 1984.
- [AP81] T. Appelquist and R. D. Pisarski. High-temperature Yang–Mills theories and three-dimensional quantum chromodynamics. *Phys. Rev.* D23:2305–2317, 1981.
- [BDFN92] J. J. Binney, N. J. Dowrick, A. J. Fisher, and M. E. J. Newman. *The Theory of Critical Phenomena — An Introduction to the Renormalization Group*. Clarendon Press, Oxford, 1992.
- [BFGO] R. Bertle, M. Faber, J. Greensite, and S. Olejník. The structure of projected center vortices in lattice gauge theory. hep-lat/9903023.
- [BFH<sup>+</sup>93] G. S. Bali, J. Fingberg, U. M. Heller, F. Karsch, and K. Schilling. The spatial string tension in the deconfined phase of the (3 + 1)-dimensional  $SU(2)$  gauge theory. *Phys. Rev. Lett.* 71:3059–3062, 1993.
- [BL93] D. Bailin and A. Love. *Introduction to Gauge Field Theory*. IOP, Bristol, 2nd edition, 1993.
- [BV79] O. Babelon and C.-M. Viallet. The geometrical interpretation of the Faddeev–Popov determinant. *Phys. Lett.* 85B:246–248, 1979.
- [Cas74] W. E. Caswell. Asymptotic behavior of non-abelian gauge theories to two-loop order. *Phys. Rev. Lett.* 33:244–245, 1974.
- [CL84] T.-P. Cheng and L.-F. Li. *Gauge Theory of Elementary Particle Physics*. Oxford University Press, Oxford, 1984.
- [Cre83] M. Creutz. *Quarks, Gluons and Lattices*. Cambridge University Press, Cambridge, 1983.
- [DFG<sup>+</sup>98] L. Del Debbio, M. Faber, J. Giedt, J. Greensite, and S. Olejník. Detection of center vortices in the lattice Yang–Mills vacuum. *Phys. Rev.* D58:094501, 1998.

- [DFGO97] L. Del Debbio, M. Faber, J. Greensite, and S. Olejník. Center dominance and  $Z_2$  vortices in  $SU(2)$  lattice gauge theory. *Phys. Rev. D* 55:2298–2306, 1997.
- [DKKL99] C. DeTar, O. Kaczmarek, F. Karsch, and E. Laermann. String breaking in lattice quantum chromodynamics. *Phys. Rev. D* 59:031501, 1999.
- [Eli75] S. Elitzur. Impossibility of spontaneously breaking local symmetries. *Phys. Rev. D* 12:3978–3982, 1975.
- [ELRT] M. Engelhardt, K. Langfeld, H. Reinhardt, and O. Tennert. Deconfinement in  $SU(2)$  Yang–Mills theory as a center vortex percolation transition. *Phys. Rev. D* 61:054504, 2000.
- [ELRT98] M. Engelhardt, K. Langfeld, H. Reinhardt, and O. Tennert. Interaction of confining vortices in  $SU(2)$  lattice gauge theory. *Phys. Lett. B* 431:141–146, 1998.
- [Eng] M. Engelhardt. by private communication.
- [ERa] M. Engelhardt and H. Reinhardt. Center projection vortices in continuum Yang–Mills theory. hep-lat/9907139.
- [ERb] M. Engelhardt and H. Reinhardt. Center vortex model for the infrared sector of Yang–Mills theory —confinement and deconfinement. hep-lat/9912003.
- [FGOa] M. Faber, J. Greensite, and S. Olejník. Center projection with and without gauge fixing. hep-lat/9810008.
- [FGOb] M. Faber, J. Greensite, and S. Olejník. First evidence for center dominance in  $SU(3)$  lattice gauge theory. hep-lat/9911006.
- [FGO99] M. Faber, J. Greensite, and S. Olejník. Asymptotic scaling, Casimir scaling, and center vortices. *Nucl. Phys. Proc. Suppl.* 73:572–574, 1999.
- [FHK93] J. Fingberg, U. M. Heller, and F. Karsch. Scaling and asymptotic scaling in the  $SU(2)$  gauge theory. *Nucl. Phys. B* 392:493–517, 1993.
- [FHP81] P. Forgács, Z. Horváth, and L. Palla. Exact, fractionally charged self-dual solution. *Phys. Rev. Lett.* 46:392–394, 1981.
- [FHP82] P. Forgács, Z. Horváth, and L. Palla. One can have noninteger topological charge. *Z. Phys. C* 12:359–360, 1982.

- [GA] A. González-Arroyo. Yang–Mills fields on the torus. Part I: Classical theory. hep-th/9807108.
- [Gil74] R. Gilmore. *Lie Groups, Lie Algebras, and Some of Their Applications*. John Wiley & Sons, New York, 1974.
- [GP96] R. Gambini and J. Pullin. *Loops, Knots, Gauge Theories and Quantum Gravity*. Cambridge University Press, Cambridge, 1996.
- [Gri78] V. N. Gribov. Quantization of non-abelian gauge theories. *Nucl. Phys.* B139:1–19, 1978.
- [Gro88] H. Grosse. *Models in Statistical Physics and Quantum Field Theory*. Springer-Verlag, Berlin, 1988.
- [GS87] M. Gökeler and T. Schücker. *Differential Geometry, Gauge Theories, and Gravity*. Cambridge University Press, Cambridge, 1987.
- [ID89] C. Itzykson and J.-M. Drouffe. *Statistical Field Theory Vols. 1,2*. Cambridge University Press, Cambridge, 1989.
- [IZ80] C. Itzykson and J.-B. Zuber. *Quantum Field Theory*. McGraw-Hill, New York, 1980.
- [Jon74] D. R. T. Jones. Two-loop diagrams in Yang–Mills theory. *Nucl. Phys.* B75:531–538, 1974.
- [KL84] F. Karsch and C. B. Lang.  $SU(2)$  string tension from large Wilson loops. *Phys. Lett.* 138B:176–180, 1984.
- [KPS81] J. Kuti, J. Polónyi, and K. Szlachányi. Monte Carlo study of  $SU(2)$  gauge theory at finite temperature. *Phys. Lett.* 98B:199–204, 1981.
- [KS75] J. Kogut and L. Susskind. Hamiltonian formulation of Wilson’s lattice gauge theory. *Phys. Rev.* D11:395–408, 1975.
- [KT99] T. G. Kovacs and E. T. Tomboulis. On  $P$ -vortices and the Gribov problem. *Phys. Lett.* B463:104–108, 1999.
- [LRT98] K. Langfeld, H. Reinhardt, and O. Tennert. Confinement and scaling of the vortex vacuum of  $SU(2)$  lattice gauge theory. *Phys. Lett.* B419:317–321, 1998.
- [LTER99] K. Langfeld, O. Tennert, M. Engelhardt, and H. Reinhardt. Center vortices of Yang–Mills theory at finite temperatures. *Phys. Lett.* B452:301–309, 1999.

- [M81] G. Münster. High-temperature expansions for the free energy of vortices and the string tension in lattice gauge theories. *Nucl. Phys. B*180 [FS2]:23–60, 1981.
- [Man76] S. Mandelstam. Vortices and quark confinement in non-abelian gauge theories. *Phys. Rept.* 23:245–249, 1976.
- [MM92] K. B. Marathe and G. Martucci. *The Mathematical Foundations of Gauge Theories*. North Holland, Amsterdam, 1992.
- [MM94] I. Montvay and G. Münster. *Quantum Fields on a Lattice*. Cambridge University Press, Cambridge, 1994.
- [MO81] G. Marchesini and E. Onofri. An elementary derivation of Wilson’s and Polyakov’s confinement tests from the Hamiltonian formulation. *Nuovo Cim.* 65A:298–310, 1981.
- [MP79] G. Mack and V. B. Petkova. Comparison of lattice gauge theories with gauge groups  $Z_2$  and  $SU(2)$ . *Ann. Phys.* 123:442–467, 1979.
- [MP80] G. Mack and V. B. Petkova. Sufficient condition for confinement of static quarks by a vortex condensation mechanism. *Ann. Phys.* 125:117–134, 1980.
- [MP82a] G. Mack and V. B. Petkova.  $Z_2$  monopoles in the standard  $SU(2)$  lattice gauge theory model. *Z. Phys. C* 12:177–184, 1982.
- [MP82b] G. Mack and E. Pietarinen. Monopoles, vortices and confinement. *Nucl. Phys. B*205[FS5]:141–167, 1982.
- [MPR91] E. Marinari, C. Parrinello, and R. Ricci. Evidence for the existence of Gribov copies in Landau gauge lattice QCD. *Nucl. Phys. B*362:487–497, 1991.
- [MS81a] L. McLerran and B. Svetitsky. A Monte Carlo study of  $SU(2)$  Yang–Mills theory at finite temperature. *Phys. Lett.* 98B:195–198, 1981.
- [MS81b] L. McLerran and B. Svetitsky. Quark liberation at high temperature: a Monte Carlo study of  $SU(2)$  gauge theory. *Phys. Rev.* D24:450–460, 1981.
- [Mut98] T. Muta. *Foundations of Quantum Chromodynamics*. World Scientific, Singapore, 2nd edition, 1998.
- [Nab97] G. L. Naber. *Topology, Geometry, and Gauge Fields*. Springer-Verlag, New York, 1997.

- [Nak90] M. Nakahara. *Geometry, Topology and Physics*. IOP, Bristol, 1990.
- [O'R86] L. O'Raiheartaigh. *Group Structure of Gauge Theories*. Cambridge University Press, Cambridge, 1986.
- [Pok87] S. Pokorski. *Gauge Field Theories*. Cambridge University Press, Cambridge, 1987.
- [Pol78] A. M. Polyakov. Thermal properties of gauge fields and quark liberation. *Phys. Lett.* 72B:477–480, 1978.
- [Rot97] H. J. Rothe. *Lattice Gauge Theories — An Introduction*. World Scientific, Singapore, 2nd edition, 1997.
- [Rue99] D. Ruelle. *Statistical Mechanics: Rigorous Results*. World Scientific, Singapore, 3rd edition, 1999.
- [Sed82] S. Sedlacek. A direct method for minimizing the Yang–Mills functional over four-manifolds. *Commun. Math. Phys.* 86:515–527, 1982.
- [Sei78] E. Seiler. Upper bound on the color-confining potential. *Phys. Rev.* D18:482–483, 1978.
- [Sha84] B. Sharpe. Gribov copies and the Faddeev–Popov formula in lattice gauge theories. *J. Math. Phys.* 25:3324–3330, 1984.
- [Shu88] E. V. Shuryak. *The QCD Vacuum, Hadrons and the Superdense Matter*. World Scientific, Singapore, 1988.
- [Sin78] J. M. Singer. Some remarks on the Gribov ambiguity. *Commun. Math. Phys.* 60:7–12, 1978.
- [Spa66] E. H. Spanier. *Algebraic Topology*. Springer-Verlag, New York, 1966.
- [Sus79] L. Susskind. Lattice models of quark confinement at high temperature. *Phys. Rev.* D20:2610–2618, 1979.
- [SY82] B. Simon and L. G. Yaffe. Rigorous perimeter law upper bound on Wilson loops. *Phys. Lett.* 115B:145–147, 1982.
- [Sym83a] K. Symanzik. Continuum limit and improved action in lattice theories. I. Principles and  $\phi^4$  theory. *Nucl. Phys.* B226:187–204, 1983.
- [Sym83b] K. Symanzik. Continuum limit and improved action in lattice theories. II.  $O(N)$  non-linear sigma model in perturbation theory. *Nucl. Phys.* B226:205–227, 1983.
- [Ten] O. Tennert. unpublished.

- [tH78] G. 't Hooft. On the phase transition towards permanent quark confinement. *Nucl. Phys.* B138:1–25, 1978.
- [tH79] G. 't Hooft. A property of electric and magnetic flux in non-abelian gauge theories. *Nucl. Phys.* B513:141–160, 1979.
- [tH81] G. 't Hooft. Topology of the gauge condition and new confinement phases in non-abelian gauge theories. *Nucl. Phys.* B190[FS3]:455–478, 1981.
- [tH82] G. 't Hooft. The topological mechanism for permanent quark confinement in a non-abelian gauge theory. *Phys. Scripta* 25:133–142, 1982.
- [Tom81] E. Tomboulis. 't Hooft loop in  $SU(2)$  lattice gauge theories. *Phys. Rev.* D23:2371–2383, 1981.
- [TVZ80] O. V. Tarasov, A. A. Vladimirov, and A. Yu. Zharkov. The Gell–Mann function of QCD in the three-loop approximation. *Phys. Lett.* 93B:429–432, 1980.
- [Weg71] F. J. Wegner. Duality in generalized Ising models and phase transitions without local order parameter. *J. Math. Phys.* 12:2259–2272, 1971.
- [Wil74] K. G. Wilson. Confinement of quarks. *Phys. Rev.* D10:2445–2459, 1974.
- [WY75a] T. T. Wu and C. N. Yang. Concept of nonintegrable phase factors and global formulation of gauge fields. *Phys. Rev.* D12:3845–3857, 1975.
- [WY75b] T. T. Wu and C. N. Yang. Some remarks about unquantized non-abelian gauge fields. *Phys. Rev.* D12:3843–3844, 1975.
- [Yaf80] L. G. Yaffe. Confinement in  $SU(N)$  lattice gauge theories. *Phys. Rev.* D21:1574–1590, 1980.



# Curriculum Vitae

**Name:** Oliver Tennert

**Geboren:** 30.12.1969 in Stuttgart

**Familienstand:** ledig

**Anschrift:** Derendinger Str. 87  
72072 Tübingen

**Schulausbildung:** **1976–1980:** Grundschule in Stuttgart-Bad Cannstatt  
**1981–1989:** Abitur am Gottlieb–Daimler–Gymnasium in Stuttgart-Bad Cannstatt, Gesamtnote 1,8

**Berufsausbildung:** **1989–1991:** Ausbildung zum Bankkaufmann bei der Landesgirokasse Stuttgart mit Zusatzprüfung zum Finanzassistenten, Gesamtnote 2,0

**Studium:** **Oktober 1991 – Februar 1997:** Studium der Physik an der Universität Tübingen, Abschluß Diplom mit Gesamtnote “sehr gut”  
**Oktober 1995 – Februar 1997:** Diplomarbeit bei Professor Dr. Hugo Reinhardt: “*Quark-Confinement und chirale Symmetrie in Random-Colour-Quark-Modellen*”  
**seit März 1997:** Anfertigung der Dissertation “*Vortex Condensation and Confinement in Centre-Projected Lattice Yang–Mills Theory*” bei Professor Dr. Hugo Reinhardt

**Zivildienst:** **Januar 1993 – März 1994:** Zivildienst im Jugendhaus Fellbach

**Akademische Lehrer:** Alkofer, Bödi, Dittrich, Fischer, Gönnenwein, Großer, E. Haug, Huisken, Kasper, Kaul, Kaup, Kramer, Lichte, Mauder, Müther, Pfister, Reinhardt, Schwenk, Wagner, Weigel.